

Charles University
Faculty of Social Sciences
Institute of Economic Studies



MASTER'S THESIS

**Measuring high-frequency phase shifts
between stock markets**

Author: Bc. Jakub Cieslar

Supervisor: Mgr. Lukáš Vácha, Ph.D.

Academic Year: 2018/2019

Declaration of Authorship

The author hereby declares that he compiled this thesis independently, using only the listed resources and literature, and the thesis has not been used to obtain a different or the same degree.

The author grants to Charles University permission to reproduce and to distribute copies of this thesis document in whole or in part.

Prague, January 2, 2019

Signature

Acknowledgments

I would like to express my gratitude towards my supervisor Mgr. Lukáš Vácha for both providing me with such an interesting topic and for his support in developing the methods used in the thesis. I would also like to thank my family for their support that allowed me to complete the thesis in its current form. Access to computing and storage facilities owned by parties and projects contributing to the National Grid Infrastructure MetaCentrum provided under the programme "Projects of Large Research, Development, and Innovations Infrastructures" (CESNET LM2015042), is greatly appreciated.

Abstract

This thesis investigates frequency-related phase relationships among returns of five major 5-minute European stock market indexes and compares relative phases on high frequencies, with focus on dynamics between developed and developing stock markets from 2008 to 2015 using. Using continuous and discrete wavelet transform we find significant phase relationships among the considered indexes, particularly we spot very strong relationship between the developed ones with no significant phase difference on any investigated frequency. Furthermore we observe significant lag of developing markets behind developed ones, particularly on horizons between 20 and 80 minutes. We also observe that the relationships is fading throughout the examined period, with increased variance of the relative phases and diminishing significance of some phase differences. The results indicate that either less developed markets are becoming more effective or it can be a sign of decreasing inter-dependencies (e.g. lower common trends). This thesis contributes to the literature by examining noisy financial time series on highest frequencies and shows relevance of the method on simulated signals with high degree of noise.

JEL Classification C14, C15, C65, G14

Keywords Stock market comovement, phase difference, wavelet analysis, spectral analysis, causality

Author's e-mail cieslarj@gmail.com

Supervisor's e-mail vachal@utia.cas.cz

Abstrakt

Práce zkoumá frekvenčně závislé vztahy ve fázích pětiminutových zisků indexů pěti velkých Evropských trhů a porovnává jejich relativní fáze na vysokých frekvencích s zaměřením na vývoj mezi rozvíjejícími se a rozvinutými akciovými trhy v letech 2008 až 2015. Pomocí vlnkové analýzy nacházíme signifikantní vztahy mezi fázemi akciových indexů, zejména pak silný vztah mezi fázemi FTSE a DAX a signifikantní zpoždění indexů méně rozvinutých evropských trhů, především na frekvencích mezi 20 a 80 minutami. Pozorujeme taktéž snižující se stabilitu těchto vztahů v průběhu zkoumaného horizontu a v některých případech i mizící signifikanci. To může naznačovat jak postupné zefektivňování méně vyspělých trhů tak snižování závislostí mezi evropskými trhy (například v podobě snižujících se společných trendů). Přidanou hodnotou práce je mimo jiné analýza silně zašumněných signálů na nejvyšších frekvencích a demonstrace použitelnosti metod pomocí analýzy umělých signálů.

Klasifikace JEL

C14, C15, C65, G14

Klíčová slova

Společný pohyb akciových trhů, vlnková analýza, spektrální analýza, kauzalita, fázový posun

E-mail autora

cieslarj@gmail.com

E-mail vedoucího práce

vachal@utia.cas.cz

Contents

List of Tables	viii
List of Figures	ix
Acronyms	xii
Thesis Proposal	xiii
1 Introduction	1
2 Related Works	3
2.1 Studies on co-movement and interdependence of financial markets	3
2.2 Spectral methods and comovements on stock markets	5
2.3 Financial time series and phase shifts	8
3 Data description	10
3.1 Missing data	14
4 Methodology	15
4.1 Brief introduction to wavelets	15
4.1.1 Formal requirements	16
4.2 Continuous wavelet transform	17
4.2.1 The transform	17
4.2.2 Wavelet cross-spectrum	18
4.2.3 Wavelet coherency	18
4.2.4 Cone of Influence	20
4.2.5 Morlet wavelet	20
4.2.6 Wavelet phase	21
4.2.7 Discrete wavelet transform	21
4.2.8 Wavelet correlation	23

4.3	Continuous wavelet transform and Phase difference	24
4.3.1	Shannon entropy test	25
4.3.2	Phase bootstrap	26
4.3.3	Computation of CWT with discrete input signal	27
4.3.4	Phase differences of artificial signals	27
4.3.5	Phase synchronization without smoothing	35
4.4	MODWT and Granger Causality	38
4.5	Tools used to carry out the analysis	40
5	Empirical results	41
5.1	Evidence from CWT and wavelet correlation	41
5.1.1	FTSE 100 and DAX	41
5.1.2	PX	43
5.1.3	BUX	46
5.1.4	WIG	49
5.2	Granger causality	51
5.3	Non-smoothed phase synchronization	54
6	Conclusion	58
	Bibliography	66
A	MODWT figures	I

List of Tables

3.1	Correlation Matrix of Stock Indices	12
3.2	Descriptive statistics of the 5-minute returns data	12
4.1	Relative phase confidence intervals and entropies of Red Noise series	32
5.1	Mean phases and Shannon Entropies over years, FTSE 100 and DAX	43
5.2	Phase differences with confidence intervals and entropies for PX and DAX	45
5.3	Mean phases and Shannon Entropies over years, PX and FTSE 100	47
5.4	Mean phases and Shannon Entropies over years, BUX and DAX	48
5.5	Mean phases and Shannon Entropies over years, BUX and FTSE 100	49
5.6	Mean phases and Shannon Entropies over years, WIG and DAX	50
5.7	Mean phases and Shannon Entropies over years, WIG and FTSE 100	50
5.8	Granger causality of the original series	52
5.9	Granger causality of transformed indexes	53

List of Figures

3.1	Values of stock market indices 2008-2015	11
3.2	Log-returns of stock market indices 2008-2015	13
4.1	Borders of Squared Coherence for 2 Red noise signals	20
4.2	Signals $a(t)$ and $b(t)$, on the top without noise	28
4.3	Wavelet phase difference of $a(t)$ and $b(t)$	29
4.4	Wavelet spectra and phase of $a(t)$ and $b(t)$	30
4.5	Wavelet phase difference of $c(t)$ and $d(t)$	30
4.6	Wavelet spectra and phase of $c(t)$ and $d(t)$	31
4.7	Red Noise series phase difference with time-window 50	33
4.8	Red Noise series phase difference with smoothing time-window 400	34
4.9	Red Noise phase histograms	35
4.10	Phase differences of signals $c(t)$ and $d(t)$, smoothing time-window 50	36
4.11	Phase differences of signals $c(t)$ and $d(t)$, smoothing time-window 400	37
4.12	Phase difference histograms of signals $c(t)$ and $d(t)$	38
4.13	95 th quantile of PSIs of White-noise and Red-noise artificial signals	39
5.1	Evolution of MODWT correlation across scales of FTSE and DAX	43
5.2	Evolution of MODWT correlation across scales of PX and DAX	45
5.3	Evolution of MODWT correlation over years of PX and FTSE 100	47
5.4	Evolution of MODWT correlation across scales of BUX and DAX	48
5.5	Evolution of MODWT correlation across scales of BUX and FTSE	49
5.6	Evolution of MODWT correlation across scales between WIG and DAX (six figures on left) and FTSE 100 (six on right) . . .	51
5.7	MODWT of DAX in January 2008, top series is the original . . .	52

5.8	Time-evolution of Phase synchronization index of FTSE100 and DAX	54
5.9	Time-evolution of Phase synchronization index of PX and DAX Red dashed line denotes 95 th quantile of Red Noise pairs' PSI	54
5.10	Time-evolution of Phase synchronization index of PX and FTSE100	55
5.11	Time-evolution of Phase synchronization index of BUX and DAX	55
5.12	Time-evolution of Phase synchronization index of BUX and FTSE100	55
5.13	Time-evolution of Phase synchronization index of WIG and DAX	56
5.14	Time-evolution of Phase synchronization index of WIG and FTSE100	56
A.1	Images of CWT analysis on FTSE 100 and DAX	II
A.2	Evolution of phase difference of FTSE 100 and DAX	III
A.2	Evolution of phase difference of FTSE 100 and DAX	IV
A.2	Evolution of phase difference of FTSE 100 and DAX	V
A.2	Evolution of phase difference of FTSE 100 and DAX	VI
A.3	Images of CWT analysis on PX and DAX	VII
A.4	Evolution of phase difference of PX and DAX	VIII
A.4	Evolution of phase difference of PX and DAX	IX
A.4	Evolution of phase difference of PX and DAX	X
A.4	Evolution of phase difference of PX and DAX	XI
A.5	Images of CWT analysis on PX and FTSE 100	XII
A.6	Evolution of phase difference of PX and FTSE500	XIII
A.6	Evolution of phase difference of PX and FTSE500	XIV
A.6	Evolution of phase difference of PX and FTSE500	XV
A.6	Evolution of phase difference of PX and FTSE500	XVI
A.7	Images of CWT analysis on BUX and DAX	XVII
A.8	Images of CWT analysis on BUX and FTSE 100	XVIII
A.9	Evolution of phase difference of BUX and DAX	XIX
A.9	Evolution of phase difference of BUX and DAX	XX
A.9	Evolution of phase difference of BUX and DAX	XXI
A.9	Evolution of phase difference of BUX and DAX	XXII
A.10	Evolution of phase difference of BUX and FTSE500	XXIII
A.10	Evolution of phase difference of BUX and FTSE500	XXIV
A.10	Evolution of phase difference of BUX and FTSE500	XXV
A.10	Evolution of phase difference of BUX and FTSE500	XXVI
A.11	Images of CWT analysis on WIG and DAX	XXVII
A.12	Images of CWT analysis on WIG and FTSE 100	XXVII

A.13 Evolution of phase difference of WIG and DAX	XXVIII
A.13 Evolution of phase difference of WIG and DAX	XXIX
A.14 Evolution of phase difference of WIG and FTSE500	XXX
A.14 Evolution of phase difference of WIG and FTSE500	XXXI

Acronyms

BUX Budapest Stock Exchange Index

DAX Deutschland Aktienindex

CEE Central and East Europe

CWT Continuous Wavelet Transform]

DWT Discrete Wavelet Transform

FTSE 100 Financial Times Stock Exchange 100

GARCH Generalized auto-regressive conditional correlation

MODWT Maximum Overlap Discrete Wavelet Transform

SE Stock Exchange

VaR Value at risk

Master's Thesis Proposal



Author	Bc. Jakub Cieslar
Supervisor	Mgr. Lukáš Vácha, Ph.D.
Proposed topic	Measuring high-frequency phase shifts between stock markets

Motivation

Information about relationships between stock markets around the world is vital for portfolio management and diversification. Important part of literature has tried to unveil it. Probably the first work finding statistically significant relationship was paper by Fischer & Palasvirta (1990), who found interdependence between several stock markets with U.S. Stock market being the global leader – for example a lag of 48 days of Canadian stock market after U.S. Market. Many others (e.g. Candelon *et al.* (2005), Loh (2013)) have investigated correlations between stock markets. Interesting findings were presented by Graham *et al.* (2012), who examined relationships between emerging markets and U.S. Market, finding evidence of co-movements only for part of the selected countries and consistent over time only for frequencies larger than a year. Above mentioned works have one thing in common – they all explore these relationships on lower frequencies of at most 1 day.

Égert & Kočenda (2007) examine high frequency (5—minutes) data of western and CEE stock exchanges and look for long term and short term relationships between the indexes. They find no evidence of cointegration (long-term) but signs of some short term spillover effects in both returns and volatility.

Wu *et al.* (2006) examined phase difference between NASDAQ and DJIA on inter-day data using Hilbert-Huang method. They find that some big events (9/11 attacks) had in phase reaction, at other periods the two indexes were out-of-phase, with changing relationship over time. For example during 2001 and 2002 DJIA was ahead in phase to NASDAQ, implying that DJIA had greater effect on NASDAQ than vice versa.

Baruník & Vácha (2013) used wavelet methods to explore correlations and contagion of the 2008 crisis across CEE markets. Using high-frequency data they find

correlations mainly on lower frequencies. They also report a little evidence of correlations on high frequencies and find it only on longer horizons. Yet the data-set used ends in 2009 and the causality on different scales is not explored in this work.

This work aims to build on existing literature (abovementioned stock index related papers and other papers using useful wavelet methods) and investigate existence and nature of the shift (lead-lag relationship) between stock indexes with focus on czech stock market.

Hypotheses

1. Market indexes are correlated and in phase on higher frequency level among developed countries
2. Less developed market indexes (such as Czech or Hungarian) exhibit phase-shift after classical indexes
3. There is Granger causality from developed to developing stock exchanges at some frequency which is increasing over time (lag is diminishing)

Methodology

Data I will use for this thesis will be PX, BUX, DAX, FTSE and maybe other indexes and will be obtained from Charles university database. Then high-frequency price data will be converted to 5-minutes data — such high frequency should open the possibility to explore all shifts in the data.

To test the hypotheses, I will use spectral methods, mainly wavelets. For the start, we will follow methodology used by Cazelles *et al.* (2008) and Torrence & Webster (1999), which give us good information about dependence structure of examined markets in time-frequency domain. Later, we may extend our methods to general frequency domain with moving windows. Wavelets, unlike Fourier analysis, offer possibility to analyse time series both in time and frequency domains. This will allow observation of time-evolution of the frequency relationships. Anchor method is going to be wavelet phase coherency that measures how out-of-phase is one signal (time-series) compared to another on different scales.

Following Reboredo *et al.* (2017), I will use Granger (1969) causality test (linear and non-linear) to further explore the dependencies in the time series. After transforming the series using discrete wavelet transform (which will decompose the series into different time-scales with shortest being in 10-minutes frequency (capturing 5-minute moves)), it will be possible to learn more about the causality between the indexes. That should also help to investigate if the difference is diminishing — the causality is expected to shift across scales and parts of the data sample.

Other methods will be added during the work to increase robustness of the results. There is a possibility to use above-mentioned Hilbert-Huang method and many others. Possible extension added throughout the work might be observing influence of the volatility (and other features of the indexes, such as asymmetricity of responses dependent on the sign of the returns) on the results.

Expected Contribution

This work will assess the question of possible phase difference between stock markets with different level of development. Wavelet analysis brings slightly different approach than classical econometrics since it works in time-frequency domain and thus allows for exploring causality and shifts not only on the entire series, but also on its different scales (frequencies). That will allow for understanding the relationship more deeply and might serve as tool to exploit the interdependencies between the markets.

Since the thesis is expected to bring new information about stock indexes it might be useful for both portfolio analysts and policy makers.

Regarding portfolio analysis, if the hypotheses will be confirmed, results will be usable to improve forecasting efficiency of models for speculators (short term traders). Wavelet analysis offer possibility of forecasting different scales separately (i.e. different horizons). Revealed connections between stock markets in some of these scales can then be exploited in the forecasting which mostly outperform simpler forecasting (as shown by Schlüter & Deuschle (2010)). Also this thesis should bring new information in risk-management since time-frequency methods show commovement in indexes in different horizons (Rua & Nunes (2009)).

Preliminary Literature

BARUNÍK, Jozef, and Lukáš VÁCHA. "Contagion among Central and Eastern European Stock Markets during the Financial Crisis." *Czech Journal of Economics and Finance (Finance a uver)* 63.5 (2013): 443-453.

CANDELON, Bertrand; HECQ, Alain; VERSCHOOR, Willem FC. Measuring common cyclical features during financial turmoil: Evidence of interdependence not contagion. *Journal of International Money and Finance*, 2005, 24.8: 1317-1334.

CAZELLES, Bernard, et al. Wavelet analysis of ecological time series. *Oecologia*, 2008, 156.2: 287-304.

ÉGERT, Balázs; KOČENDA, Evžen. Interdependence between Eastern and Western European stock markets: Evidence from intraday data. *Economic Systems*, 2007, 31.2: 184-203.

FISCHER, Klaus P.; PALASVIRTA, A. P. High road to a global marketplace: the

international transmission of stock market fluctuations. *Financial Review*, 1990, 25.3: 371-394.

GRAHAM, Michael; KIVIAHO, Jarno; NIKKINEN, Jussi. Integration of 22 emerging stock markets: A three-dimensional analysis. *Global Finance Journal*, 2012, 23.1: 34-47.

LOH, Lixia. Co-movement of Asia-Pacific with European and US stock market returns: A cross-time-frequency analysis. *Research in International Business and Finance*, 2013, 29: 1-13.

REBOREDO, Juan C.; RIVERA-CASTRO, Miguel A.; UGOLINI, Andrea. Wavelet-based test of co-movement and causality between oil and renewable energy stock prices. *Energy Economics*, 2017, 61: 241-252.

RUA, António; NUNES, Luís C. International comovement of stock market returns: A wavelet analysis. *Journal of Empirical Finance*, 2009, 16.4: 632-639.

SCHLÜTER, Stephan; DEUSCHLE, Carola. Using wavelets for time series forecasting: Does it pay off?. *IWQW discussion paper series*, 2010.

TORRENCE, Christopher; WEBSTER, Peter J. Interdecadal changes in the ENSO-monsoon system. *Journal of Climate*, 1999, 12.8: 2679-2690.

WU, Ming-Chya, et al. Phase distribution and phase correlation of financial time series. *Physical Review E*, 2006, 73.1: 016118.

Author

Supervisor

Chapter 1

Introduction

The study of stock markets' dynamics is present since the beginning of 20th century. Later, co-movement of stock market indices came under study to reveal possibilities of international diversification (e.g. Ansoff (1957), Grubel (1968), Makridakis & Wheelwright (1974)). These possibilities were important both for firms for whom diversification of activities could easily decrease overall risk as well as for investors, who could benefit from the same.

These analysis subsequently turned into co-movement analysis of the market indices, employing every suitable method (including parametric and non-parametric methods, spectral inference). Up until 1990, as far as the author is aware, showed lower co-movements and thus higher potential benefit of diversification and risk management.

In later periods researchers observed increasing correlation among indices. Using spectral methods, researchers could analyze co-movements of markets in different horizons and firstly found evidence of increasing long-term co-movements implying decreased opportunity to diversify in the long run but significant evidence of those opportunities for short term investors. With time the higher co-movement spread over to higher frequencies and after 2006 financial crisis major indices became highly correlated (but left open the opportunity to diversify into emerging markets). Some works even found co-movements among markets be that high that presence of inter-day arbitrage were rare.

One commonality of most previous works is that they employ daily, weekly or even monthly data. Of the exceptions this study notes Égert & Kočenda (2007) that use intra-day data to examine co-movements and volatility and returns spillover effects (but without employing horizon-specific methods) and Vacha & Barunik (2012) who look into interdependence of European indices

around crisis in 2008, both using 5-minutes data.

This thesis is building upon existing literature to examine co-movements using spectral methods, with particular focus on lead-lag relationships and phase similarities, methods used mainly in other fields (Cazelles *et al.* (2008)) but increasingly popular in analysis of financial times series as well (Loh (2013), Roesch *et al.* (2014) and others).

We examine the phase similarities and causality from two developed stock market indices (FTSE 100 and DAX), presumably European market leaders with well documented high correlation, coherency and phase, to "developing" stock market indices (BUX, PX, WIG). We focus on answering three questions:

- Are FTSE 100 and DAX highly correlated and in phase?
- Do developing markets exhibit phase-shift after developed markets that is decreasing in time?
- Is there significant Granger causality from developed to developing markets that shift among frequencies (from lower to higher) in time?

We contribute to existing literature in several ways. We examine relative phases on highest frequencies, where the tendencies are not uncoverable by methods which have enough power for lower ones, on data which, as far as the author is aware, were not examined by other researchers. Furthermore we demonstrate that such alteration does not change the significance of observed lags in phase. We also employ more methods and cross-valuate the results with all parts of wavelet analysis to seek the explanation of the results.

This thesis is organized as follows. Chapter 2 provides broader overview of literature on stock market co-movements and end with financial time series phase analysis. Chapter 3 describes the data used in the analysis. Chapter 4 introduces wavelets (both continuous and discrete) and related methods used in this thesis. Chapter 5 presents the results of all parts of the analysis and Chapter 6 provides conclusion and outlook for possible extensions.

Chapter 2

Related Works

Vast amount of academic papers have examined relationships between stock markets of all sorts. The matters of interest are, among others, cross-correlations, co-movements or lead-lag relationship between them. This chapter aims to bring brief overview of literature that deal with these questions. It begins with examination of how academics studied co-movements of financial markets, then look into works that applied spectral methods to explore them and finally summarize works which apart from examining co-movements specifically look into phase differences between financial time-series using wavelets.

2.1 Studies on co-movement and interdependence of financial markets

Interdependence and inter-connectedness on financial markets have been examined thoroughly for its importance in risk management and asset allocation. Grubel (1968) stressed out benefits of cross-country diversification and was one of the first who empirically shown the potential welfare gains of international diversification on ex post returns of worlds major stock exchanges. To confirm the claim, Makridakis & Wheelwright (1974) found no stable linear relationship among stock exchanges, which could have implied that potential of diversification was easily exploitable. Over time, the relationships between related (geographically, ideologically) stock markets increased significantly. Due to increase inter-connectedness Brooks & Del Negro (2005) analyze the benefits of diversification within and out of Europe and conclude (in perspective of a Dutch investor) that diversifying out of Europe brings twice the risk reduction than diversifying only in Europe.

King *et al.* (1990) investigates monthly data on 16 markets to determine factors influencing conditional volatility and co-variances finding that only little of the co-variation between stock markets is due to observable variables and find evidence to support the hypotheses that correlation is linked to volatility. King & Wadhvani (1990) found empirical evidence that due to investor reaction on price movements in other markets increase in the volatility leads to increased magnitude of contagion on 1987 Black Monday. Longin & Solnik (1995) investigated the correlation among major SE and found positive trend in the conditional correlation in the period 1960-1990 with periods of increased conditional volatility accompanied by increased correlation (but Longin & Solnik (2001) point out that all tests assume multivariate normal distribution, which might not be the case, at least for both bull and bear market). Partially on the contrary, Forbes & Rigobon (2002) investigated the contagion accounting for possible heteroskedasticity and found little or no evidence of increasing correlations during crisis (1987, 1994 and 1997) - moreover they suggest that there is strong interdependence among economies at all states of the world (it is important to note that Forbes & Rigobon (2002) used narrow definition of contagion and thus they do not directly claim that there was not any form of contagion). Syllignakis & Kouretas (2011) used DCC-MGARCH¹ model on weekly data to examine if there are increasing correlations between CEE countries indices and US, Russia and Germany and found increased co-variances between them in times of crises (pointing to increasing contagion).

Lin *et al.* (1994) found significant influence of information incorporated in New York (Tokio) SE during trading hours on setting opening prices in Tokio's (NY's) (i.e. daytime returns of one exchange influence overnight returns of the other (bi-directional relationship)). Karolyi & Stulz (1996) then investigate source of U.S. Japan stock return correlation and find only large shocks to stock indexes to have stable effect on the correlation (unlike industry shocks or macroeconomic announcements).

Johnson & Soenen (2003) using Geweke-Granger measure found high level of the same day market responses among countries in America (on daily data) implying high integration and market efficiency and suggested that there are only rare cross-market adjustments that do not take place on the same day (i.e. cross-market arbitrage opportunities were scarce beyond 24 hours horizon).

Brooks & Del Negro (2004) looked into the source of co-movements among national stock markets and suggested that contemporary increase in co-movements

¹Dynamic Conditional Correlation Multivariate GARCH

is not permanent but rather temporary due to stock market bubble which suggest that after the bubble bursts international diversification still can be effective tool to reduce portfolio risk. Candelon *et al.* (2008) extend the Harding & Pagan (2006) model to measure changes in stock market cycle synchronization in Asia and found an increase in synchronization among these stock markets in time.

Égert & Kočenda (2007) apply wide range of methods (VAR, cointegration test, Granger causality) to investigate comovements among 3 major CEE stock market indices (BUX, WIG, PX) and their relationships with 3 Western European markets (DAX, FTSE 100, CAC) and find no robust cointegration among the stock index pairs. Additionally, they find returns spillover effects among both pairs of markets and from Western Europe to CEE as well as volatility spillover effect in almost all directions (implying that even developing markets can influence Western European markets suggesting that CEE markets can be considered a separate asset class and that should be taken into account for risk measurement). They also find interaction of BUX with both PX and WIG, but not among the two itself.

Gjika & Horvath (2013) examine Central European stock markets using asymmetric DDC-mGARCH model and found that correlation among them has increased in time both in between the Central European markets and with other Euro area markets resulting in very high correlation similar to the correlation of US and Canadian markets. They also suggest that CE stock markets have asymmetric conditional variance and recommend use of flexible models when analyzing them to avoid drawing inappropriate conclusions.

2.2 Spectral methods and comovements on stock markets

Spectral methods have increased in popularity in last decades. Amount of literature applying these methods in signal processing (Fourier Transform, Continuous and discrete wavelet transform and others) is growing rapidly and it is gaining reputation in financial time-series as well since it provides ability to analyze series from investment horizon perspective, it can be used as noise-filtering technique or ability to extract both amplitude and phase of a series (for example using complex wavelets).

Fischer & Palasvirta (1990) have utilized the advantages of spectral methods (Fourier Transform) and examined relatively high-frequency data (daily) on 22 stock exchanges and found coherence in index price movements, several (phase) lead-lag relationships with U.S. being the world price leader (e.g. Canadian market was 0.2π (2-pi period) behind in phase after U.S. market on 420 day frequency)) - where U.S. being the leader could imply either that U.S. price changes affect all the other prices or the existence of single pricing to which U.S. stocks responded the fastest. They also found evidence of possible existence of single pricing mechanism for several combinations of the examined markets. The lead-lag relationship could result, if forecasted correctly, in finding arbitrage opportunities among markets.

Smith (2001) showed that after 1987 crisis, the phase lead-lag relationship among Pacific Rim were significantly smaller and increase in mean coherence (which can be interpreted as increased interdependence) can lead to lower potential benefit of international diversification.

Rua & Nunes (2009) revisit the examination of stock exchange co-movements using wavelet analysis using three-dimensional approach. They apply this approach to assess the risk reduction from diversification thanks to the possibility of assessing different investment horizons (scales, frequencies) and co-movement changes in time simultaneously. They found that on low frequencies the degree of co-movement is relatively high implying that the benefits of international diversification over long term may be less important (at least relatively to the benefit for the short-term investor). They also demonstrate the impact of revealed co-movements on comparing VaR of international portfolio with and without accounting for the co-movements (i.e. omitting co-movements results in severe underestimation of VaR across all frequencies with increasing magnitude). Similarly, Dajcman *et al.* (2012) use MODWT to examine correlations between CEE and other major markets and find the correlations to vary in both time and scale and PX and BUX being highly correlated with developed markets. Graham *et al.* (2012) analyze co-movements of 22 emerging markets and US market using wavelet coherency (on 2001-2010 weekly data) and they find strong co-movements on relatively lower frequencies with change after 2006, where they observe statistically significant coherence even at higher frequencies for some period (with longer periods located also on the monthly scale in some of the markets). They expect that observed changes after 2006 are due to shock from the global financial crisis.

Graham & Nikkinen (2011) focus their wavelet coherency analysis on study of co-movement of Finish stocks with other stock markets and extend previous works² by examining not only (weekly) stock market returns co-movements but also volatility co-movements. Apart from finding high co-movement between Finland and both developed and developing markets on low frequencies, they have observed increase in co-movements on relatively higher frequencies with time, especially after 2006 and towards the end of the data set - they attribute that to the substantial financial and economical deregulation that took place since 2006. For volatility, however, observed co-movements are relatively low in general and mainly observed in separate time-scale windows.

Gallegati (2008) apply discrete wavelet transform (in particular MODWT) on 45 years of monthly data on DJIA index and Industrial production index for US to measure if industrial firms lead the real output on scale-by-scale basis and find strongest evidence of leading the real output on lower frequencies (with periods of 8 months and larger - in accord with economic theory suggesting that institutional investors with larger investment horizons link their investments with macroeconomic variables). They reveal the lags computing the correlation of the growth rate with DJIA returns in windows of 24 months for each scale and observation. In & Kim (2006) use MODWT to examine lead-lag relationship³ between S&P 500 index and S&P 500 futures index daily data using 8 levels of wavelets and find bi-directional Granger causality between stocks and futures on all scales and very large correlation (above 0.92 for all scales).⁴

Vacha & Barunik (2012) examine co-movements and contagion among CEE and DAX around the 2008 crisis using wavelet methods on 5-minute data. They find the highest interdependence between PX and WIG but also find both time and frequency changing nature of the relationships. Important feature is that they find significant correlation not only on low frequencies, but also on high frequencies (e.g. 80 minutes wavelet correlation between DAX and BUX to be 0.6 after fall of Lehman Brothers). Ranta (2013) studied contagion among major world stock markets and defined contagion as changes in time on low scales (higher frequency) without changes on higher scales and they found clear evidence of such a contagion. For example, DAX and FTSE started to have very high coherency after several shocks and have significant coherency of 0.8 around the end of data set (2009) even on the highest frequency (8 days). They

²previous works that analyzed data using wavelet coherency

³their work also document how hedge ratio changes with wavelet scale - investment horizon

⁴overall results point to efficiency between the markets and absence of arbitrage opportunity between them

accompany the continuous wavelet analysis with MODWT and found wavelet correlations between majority of the examined series to reach 0.9 on 2 to 4 days averages.

Aloui & Hkiri (2014) used wavelet coherency to investigate daily co-movement of markets in Gulf Cooperation Council countries and found that for several pairs the co-movements started to be significant after 2006 even at the lowest frequencies. In general they found increasing co-movements with time towards the higher frequencies, especially after external shocks, such as after the sub-prime financial crisis.

2.3 Financial time series and phase shifts

Information transmission in network of markets (three Western equity indices) was studied by Roesch *et al.* (2014) who, using propagation values for all three indices based on work of Schmidbauer *et al.* (2013), aimed to capture relative importance of the market in the network at certain point in time ⁵ and using the wavelet phase difference⁶ found that DJIA was in "anti-phase" to other two while FTSE 100 and Euro Stoxx are in phase to each other (evidence found only on lower frequencies, on higher is the energy of propagation relatively low and the relative phase was not examined), even though range of frequencies with significant phase similarity has shrunk.

Madaleno & Pinho (2012) examine several of the largest stock market indices using CWT and find high coherency on low frequencies (in some pairs increasing in time) but also identify larger periods of coherence in higher frequencies (4-64 days) after 2006 (with exception of DJIA-FTSE where it was present earlier) and identify lead-lag relationships using phase difference (for example they find DJIA to lead Bovespa in 32-64 days horizon and reverse leadership in 128-256 days) but in general changing phase positioning between pairs of indices. Similarly, Albulescu *et al.* (2015) used CWT to examine the contagion among FTSE 100, DAX 30 and CAC 40 futures on daily returns and find long term co-movements to be present over entire sample and in short term strong co-movements over selected windows in the data. They also use wavelet phase difference and find that DAX and CAC are following the FTSE in the long

⁵For example there is a peak in the values for DJIA around 13th October 1989 after failed deal with parent company of United Airlines since it that news had global impact

⁶Referred to as Cross Wavelet Power Spectra Phase

term and for some periods also in the short and mid-term (this can be evidence of slightly different lead-lag relationships in spot and futures markets).

Weekly comovements between Asian stock markets and U.S. and European stock markets we examined by Loh (2013). He found both time and scale variation in the comovements with increasingly important comovements on short scales (high frequencies) after 2006 (similarly as papers on other combinations of integrated markets). Apart from wavelet coherency analysis they report wavelet phase differences, finding, for example, that European and Australian markets were in phase for most periods and scales with several periods of lead or lag on most scales with changing relationship even within a selected scale (thus no overall leadership within a time-horizon could be reported). Europe and Australia combination is particularly interesting since towards the end of the data-set, they exhibit phase similarity and significant coherency across all scales.

Reboredo *et al.* (2017) examined relationships between oil and renewable energy stock using wavelet coherence, phase difference and Granger causality (both linear and non-linear) and imply that unveiled relationships can be used in two ways - absence of causality and relative independence on higher frequencies imply that oil can be used as a hedge for renewable energies while linear causality in interdependence on higher frequencies imply possibility to use one to improve forecast of the another. While cross wavelet phase difference do not indicate homogeneity in the processes as the computed phase difference change very frequently across time and scales, they also computed wavelet coherence phase difference, where they found that oil does not lead the prices of renewable energies (they are in phase) apart from short time periods on some and apart from the lowest frequency examined (512 days) where oil was consistently leading renewable energies.

Chapter 3

Data description

Data used in this thesis are on five of the major European stock indices - Financial Times Stock Exchange 100 (FTSE 100), which is computed from weighted prices of 100 largest companies (with largest market capitalization) that are listed on London stock exchange,¹ Deutschland Aktienindex (DAX) which is stock index based in Frankfurt Bourse and is comprised of 30 largest companies listed in Frankfurt,² Index PX which is computed from prices of 25 companies with largest market capitalization in Czech Republic,³ Budapest Stock Exchange Index (BUX) computed from price changes on up to 25 blue chip Hungarian companies and Warsaw stock exchange index (WIG) constituting of 151 companies.⁴ Data available start for all five indexes on 2nd January 2008 and for the first four span to 30th December 2015, for WIG it is until end of 2011.

Historical values can be found in figure 3.1. In the sub-figures it is easy to observe the impact of the recent global financial crisis where all of the indices plummet and the impact of European Debt crisis in 2010.

Table 3.1 shows correlation matrix of the indices. We can see (as expected) very high correlation coefficients of pairs FTSE 100 — DAX (0.8), medium correlation coefficient between WIG and both FTSE 100 and DAX and moderate correlations between the rest of indices. Correlation between PX and BUX is lower than their respective correlations with FTSE and DAX, however their correlation with WIG is higher than with the developed indices. However this issue can be explained by the fact that the observed period for WIG is

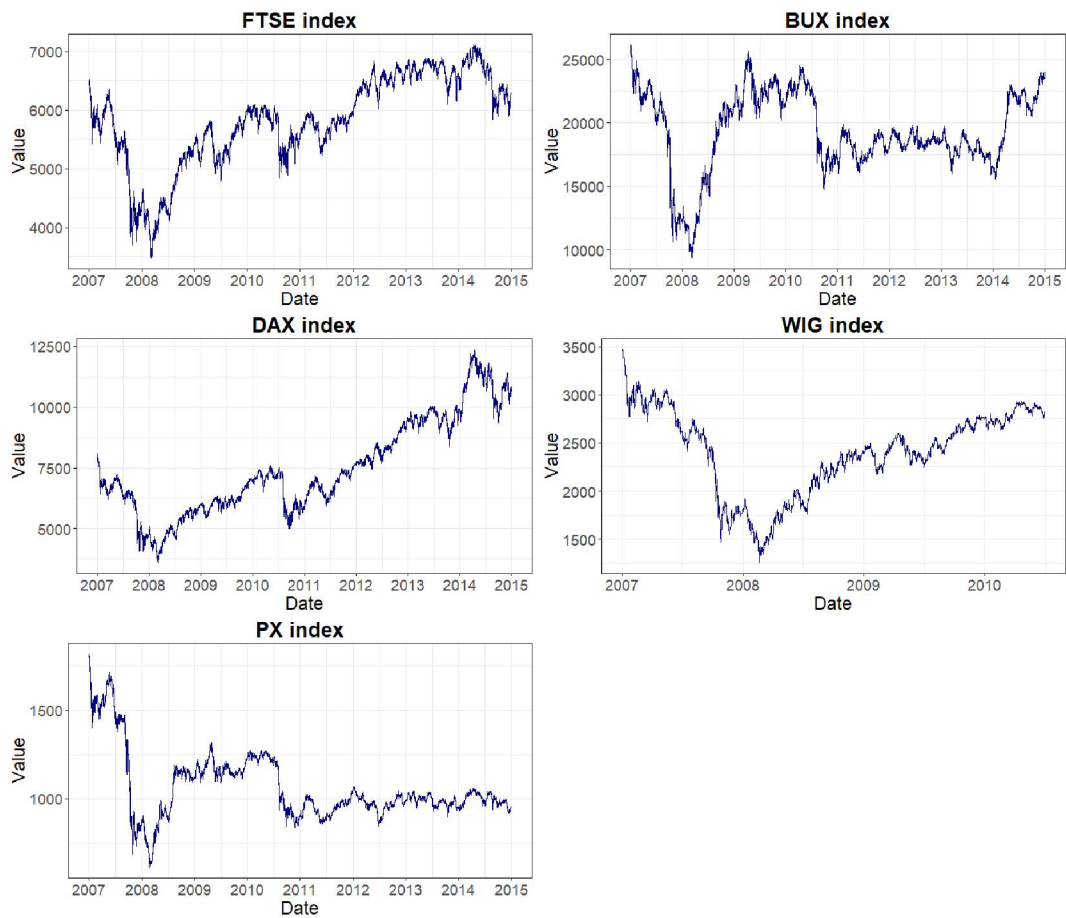
¹more on which companies can be found on www.londonstockexchange.com

²more on <http://en.boerse-frankfurt.de/index/constituents/DAX#Constituents>

³how the index is computed and all constituents can be found on <https://www.pse.cz/indexy/popis-indexu/index-px/>

⁴more can be found on https://www.gpw.pl/opis_indeksu_WIG_en

Figure 3.1: Values of stock market indices 2008-2015



shorter than for the other indexes and contains global financial crisis which might skew the coefficients upward.

Table 3.1: Correlation Matrix of Stock Indices

	FTSE	DAX	PX	BUX	WIG
FTSE	1	0.791	0.279	0.250	0.408
DAX	0.791	1	0.272	0.257	0.402
PX	0.279	0.272	1	0.211	0.291
BUX	0.250	0.257	0.211	1	0.250
WIG	0.408	0.402	0.291	0.250	1

Next, continuously compounded returns (log-returns) are computed. Using data sampled in 5 minute frequency, returns are computed as follows:

$$R_t = \log\left(\frac{P_t}{P_{t-1}}\right) \quad (3.1)$$

Figure 3.2 displays the 5-minute returns for all 5 series.

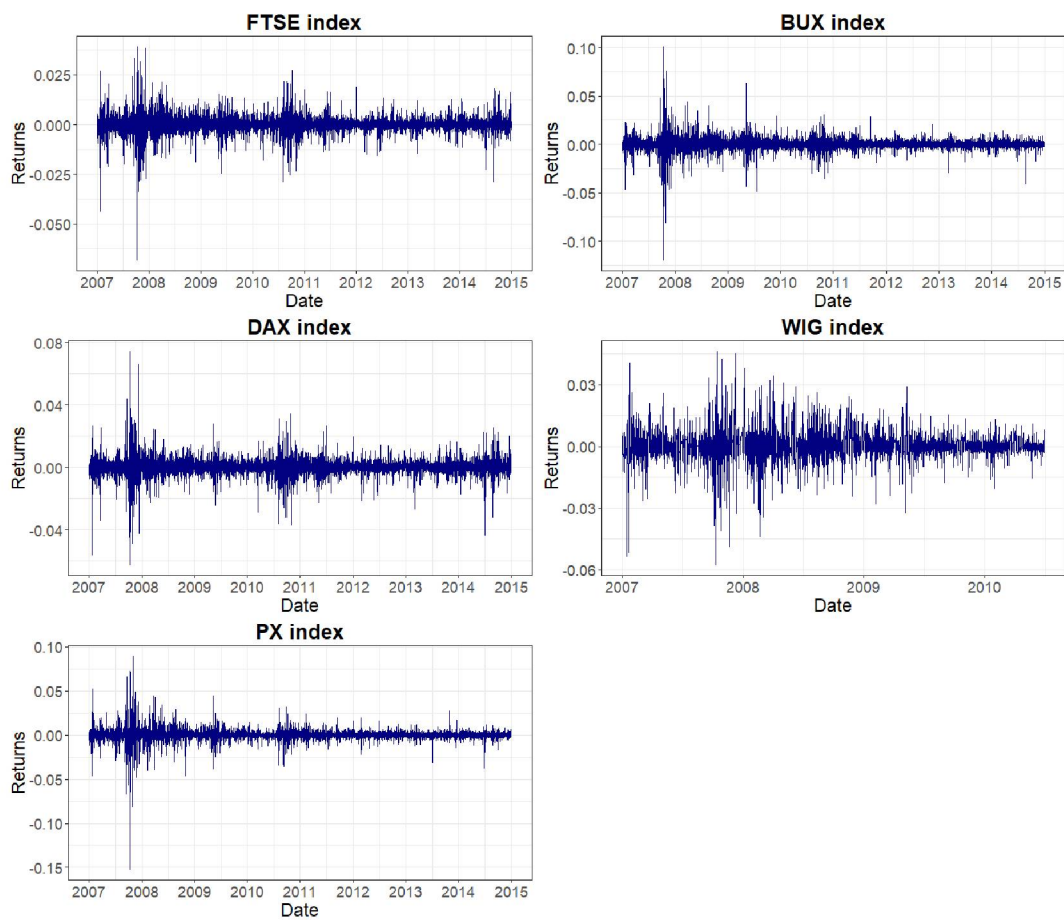
Table 3.2 summarizes the descriptive statistics of the 5-minute returns data for all 5 stock markets. We can see that the number of observations do differ due to different length of the trading hours and different national holidays as well as different time-zones (for FTSE 100). To deal with this issue we use only data that are available for all stock indices (analysis with WIG is carried out separately on shorter data set due to shorter period available) and we omit the first and last observations to address the problem of overnight returns (which would appear is some data-sets but not in all due to the first condition).

Table 3.2: Descriptive statistics of the 5-minute returns data

	FTSE 100	DAX	BUX	PX	WIG
Mean	-1.4e-07	1.4e-06	-4.7e-07	-4e-06	-3e-06
Std. dev.	0.0012	0.0015	0.0017	0.0015	0.002
Skewness	-0.74	-0.26	-0.75	-5	-0.54
Kurtosis	130	14	380	1110	95
Min	-0.068	-0.063	-0.12	-0.15	-0.058
Max	0.039	0.074	0.1	0.09	0.046
N	2.1e+05	2.1e+05	1.8e+05	1.6e+05	7e+04

We can see from both table 3.2 and both figures that best mean performance has DAX (positive 0.0000016 5-minute returns), while relatively the worst per-

Figure 3.2: Log-returns of stock market indices 2008-2015



formed PX followed by WIG - but WIG data may not be directly comparable with statistics for other indices since it includes both crisis but not the other half of the observations. Most stable was FTSE 100 (with standard deviation 0.0012), highest changes we on average observed in Poland (same applies as with the mean). Maximal return is observed on Hungarian index (10%), highest fall on Czech (15%). High skewness and very high kurtosis imply asymmetric (on PX) and much fatter tails than with normal distribution. Interestingly, recalculating both parameters excluding first year the skewness of PX returns falls close to zero (-0.077) implying that significantly "fatter" left tail occurred mostly around the financial crisis.

3.1 Missing data

Due to both use of Spot data and presence of less liquid markets (PX, WIG), data on some days contain missing values. It can be either because the market price did not change over the minute, or that the market was open for shorter period of time. To address mostly the first issue, on certain days missing values were replaced by previous values. Those days had to satisfy two conditions:

- number of 1-minute observations had to be at least 300
- first and last trading hour had to be at least 6 hours apart

This ensure that "strange"⁵ days were not used for the analysis but valid days were completed.

⁵for example days where there were only a single hour of observations

Chapter 4

Methodology

4.1 Brief introduction to wavelets

The wavelet transformation is a time-frequency decomposition that can be in a sense compared to *Fourier transformation*. The basic difference is in the functions that are used for the transformation. While Fourier transformation uses sines and cosines (functions periodic over the whole axis), wavelet transformation uses localized function and thus while Fourier transformation transforms signal from time-domain to the frequency domain, wavelet transformation transforms the signal to the time-frequency plane, where the frequency components are usually called scales. Moreover, wavelets allow for analysis of non-stationary components in stochastic processes(Sifuzzaman *et al.* (2009)). The name of the transformation is derived from central object in the transformation, a function called wavelet. It is a wave-like function, that is centered around some point and its magnitude rather quickly decays to zero (hence it is localized). Basic component of wavelet transformation is then called *mother wavelet*, a standard wavelet with certain properties, usually defined around zero and from whose definition other wavelets are constructed by either moving the center of the mother wavelet (also called translation) and/or by altering the width of the wave-like function (called dilation) or both.

Wavelet can be any function that satisfies certain mathematical properties, but in practice there are some families of functions that are used, for example Haar, Daubechies, Mexican Hat, Morlet or Paul wavelets. Those functions can be either only real valued (Mexican hat) or complex (Morlet wavelet). Their dilations can be either orthogonal to each other, which implies that information extracted on one scale is not present in other scales, or redundant, which is

common for continuous wavelet transform and is more robust to noise (Cazelles *et al.* (2008)).

The wavelet transformation itself takes an input signal and returns it in another form in which some properties can be investigated. It is then done by a convolution of a signal (financial time-series, earth surface profile) with dilated and translated versions of mother wavelet and obtained coefficients are then passed to further analysis. Dilation of the wavelet determines the frequencies of the information that are stored in the coefficient. The computation can be done either over discrete set of dilation parameters (and thus on discrete scales - Discrete Wavelet Transform(DWT)) or smoothly over all possible scales (Continuous Wavelet Transform (CWT)). Simple use of the DWT is for filtration of a signal from high-frequency components (filter out noise) or to different frequency components (different finesse of the information), CWT can be used, for example, for analysis of time-scale variation and for search of coherent structures among the time-frequency plane.

Let us define some mathematical requirements for function to be called (mother) wavelet.

4.1.1 Formal requirements

For a wave-like function to be called wavelet, it must satisfy some mathematical properties (Addison (2017)), firstly, it has to have finite energy:

$$E = \int_{-\infty}^{\infty} |\psi(t)|^2 dt < \infty \quad (4.1)$$

where $\psi(t)$ is chosen wavelet function. It is customary to choose function $\psi(t)$ such that it has unit energy; $\int_{-\infty}^{\infty} |\psi(t)|^2 dt = 1$. Secondly, it must satisfy *Admissibility condition*:

$$C_g = \int_0^{\infty} \frac{|\hat{\psi}(f)|^2}{f} df < \infty \quad (4.2)$$

where $\hat{\psi}(f)$ is the Fourier transform of $\psi(t)$:

$$\hat{\psi}(f) = \int_{-\infty}^{\infty} \psi(t) e^{-i(2\pi f)t} dt \quad (4.3)$$

C_g is called Admissibility constant. This constant is then important for inverse wavelet transformation to recover the original signal. The implication of eq. 4.2

is that the wave-like function has to have zero mean (it has no zero-frequency component). $\psi(t)$ is then called mother wavelet.

4.2 Continuous wavelet transform

4.2.1 The transform

We define a translated and dilated version of the mother wavelet:

$$\psi_{\tau,s}(t) = \psi\left(\frac{t-\tau}{s}\right) \quad (4.4)$$

where τ is a translation parameter (i.e. moves the center of wavelet along the time axis) and s is a scaling parameter (i.e. makes the wavelet function wider or narrower).

Wavelet transform of a signal x is then defined as(Addison (2017)):

$$W_x(s, \tau) = w(s) \int_{-\infty}^{\infty} x(t) \overline{\psi_{\tau,s}(t)} dt \quad (4.5)$$

It is convenient to set function ($w(s)$) to $1/\sqrt{s}$ to ensure that the wavelets have the same energy at all scales and where the bar over the wavelet function means complex conjugate of the function (for real valued wavelets it is equal to the original function). $W(s, \tau)$ then represents the extracted information or contribution of the particular scale at given point in time τ to the signal. The integral is then computed over all scales and time points and from one-dimensional signal yields two-dimensional transformed signal. The original signal (series) can then be obtained by computing the inverse wavelet transform:

$$x(t) = \frac{1}{C_g} \int_{-\infty}^{\infty} \int_0^{\infty} \frac{1}{s^2} W_x(s, \tau) x(t) \psi_{\tau,s}(t) d\tau ds \quad (4.6)$$

To examine local power, the wavelet power of signal x is defined as:

$$W_{x,x}(\tau, s) = W_x(\tau, s) * \overline{W_x(\tau, s)} \quad (4.7)$$

$W_{x,x}(\tau, s)$ can be understood as local variance of a signal at scale s and time τ .

We can compute the contribution to energy of any scale to the total energy by:

$$E_x(s) = \frac{1}{C_g} \int_{-\infty}^{\infty} W_{x,x}(\tau, s) ds \quad (4.8)$$

4.2.2 Wavelet cross-spectrum

To analyze common properties of two signals we can compute their wavelet cross-spectrum:

$$W_{x,y}(\tau, s) = W_x(\tau, s) * \overline{W_y(\tau, s)} \quad (4.9)$$

which shows the areas where the signal have both high power and can be understood as analogy to local co-variance of signals x and y . Regarding two Gaussian white noise signals, its expected value at every point is the same as the signal variance (Roesch *et al.* (2014)). Then for cross coefficients to be well interpreted, it is better to standardize the signals - therefore the returns data were normalized so their mean is equal to 0 and variance equal to 1.

The cross wavelet power is simply $|W_{x,y}(\tau, s)|$.

To investigate which values are significantly different from random Red noise, cross-spectrum distribution is needed. Torrence & Compo (1998) note that theoretical wavelet cross-spectrum of two normalized series with Fourier spectra P_k^x and P_k^y should have distribution (for complex wavelets):

$$|W_{x,y}(\tau, s)| \Rightarrow \frac{Z_2(p)}{2} 2\sqrt{P_k^x P_k^y} \quad (4.10)$$

with $Z_2(95\% \approx 4)^1$. Significant areas with 95% confidence are enclosed by black contours.

4.2.3 Wavelet coherency

Cross wavelet transformation is useful to find areas of high common power, however it can be useful to investigate normalized coefficients that account for magnitude of local powers. Such coefficients are called Wavelet squared coherency. Torrence & Compo (1998) defined it as:

$$R^2(\tau, s) = \frac{|\langle s^{-1} W_{x,y}(\tau, s)^2 \rangle|}{\langle s^{-1} |W_x(\tau, s)|^2 \rangle \langle s^{-1} |W_y(\tau, s)|^2 \rangle} \quad (4.11)$$

¹For precise definition of $Z(\cdot)$, see Torrence & Compo (1998), p. 76

where both in nominator and denominator there are applied smoothing operators $\langle \cdot \rangle$ which stand for smoothing the wavelet power and cross-power in both time and frequency domain. We can choose from a variety of smoothing functions. In this thesis Bartlett window was chosen which is defined as:

$$B - H(a) = 1 - \left| \frac{a - (N - 1)/2}{(N - 1)/2} \right|$$

where N stands for the length of the smoothing window. Such window has triangular shape and the process can be understood as taking weighted average of the coefficients with linearly decreasing weights from the centre. The convolution is done simultaneously in both domains by convolution of the coefficients with two-dimensional version of the filter $(B - H(a)) \times (B - H(a))'$, where $'$ stands for transposition of a vector and \times is matrix multiplication.

Wavelet coherence can by definition attain values from 0 to 1 and thus it can be understood as a spectral counterpart to a local measure of correlation coefficient. Values close to 1 then indicate high level of local co-movement. To assess statistical significance of the wavelet coherence it is feasible to find which values are significantly different from zero, i.e. choose a null hypotheses H_0 under which the coefficients are not statistically significant against random noise. Yet wavelet coherence does not have any theoretical distribution and Monte Carlo method have to be used to determine empirical confidence intervals. Torrence & Compo (1998), Torrence & Webster (1999), Cazelles *et al.* (2008) and others suggest the use of surrogate series to assess significance of wavelet cross-spectrum and wavelet coherence. Such series can be simple white noise, red noise (AR(1) series), random series with the similar spectrum or bootstrap of the series. Here we choose to use simple bootstrap to assess statistical significance. The surrogate series are constructed by taking the original series and bootstrap from it with identical probabilities. H_0 is then such that the cross-spectrum and coherence of the inspected series are not statistically different from random signal (5% significance level). Figure 4.1 shows 90th, 95th and 99th percentile of wavelet squared coherence for two Red noise series with AR(1) coefficient 0.25, based on 1000 Monte-Carlo simulations. Similar simulation was run with White noise series, showing equal results that differ at third decimal place which might be a consequence of lower amount of simulations.

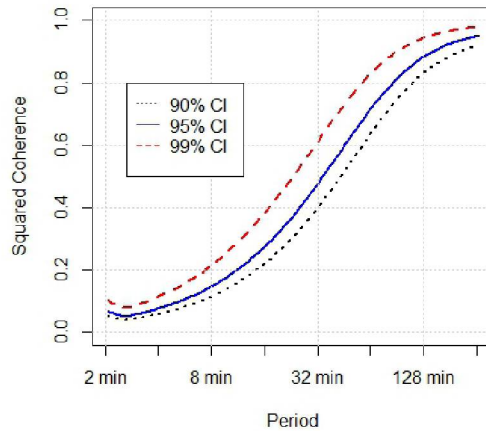


Figure 4.1: Borders of Squared Coherence for 2 Red noise signals

4.2.4 Cone of Influence

The signals that are observed in practice are finite. Its implication is that closer to the edges of the signal (problematic proximity depends on size of the scale) there are no values past the edge on which the calculation should be done and therefore we need to calculate the coefficient on some data. There are several ways how to deal with this issue, such as zero-padding (placing zeroes on both sides of the signal to fill for missing values) or mirroring the series. In this thesis, zero-padding was used on the edges of the data spans. It follows that the coefficients computed using zeroes do not have to represent real coefficients well and thus should not be interpreted. If subsets were investigated, longer series was used and then cut to the desired length. Implication of this approach is that there are no edge-effects in the middle subsets and almost no edge-effect on higher frequencies at the beginning and end of the data-set.

4.2.5 Morlet wavelet

In choosing of an appropriate wavelet function, we have to decide which properties we want to investigate. Since we are interested mainly in phases, only complex wavelets should be considered. Morlet wavelet is deemed to be very well localized in scales (Cazelles *et al.* (2008)) (at least compared to Paul wavelet (Torrence & Compo (1998))), which is a property that is desirable in analysis of the phase differences.

Morlet wavelet consists of a complex wave enclosed within a Gaussian envelope

and is defined as:

$$\psi(t) = \pi^{-1/4}(e^{i2\pi f_0 t} - e^{-(2\pi f_0)^2/2})e^{-\frac{t^2}{2}} \quad (4.12)$$

where f_0 is called central frequency of the wavelet. In practice, the second term in the brackets is not used and the wavelet then simplifies to:

$$\psi(t) = \pi^{-1/4}(e^{i2\pi f_0 t})e^{-\frac{t^2}{2}} \quad (4.13)$$

and with $\omega = 2\pi f$, its Fourier transform is $\hat{\psi}(\omega) = e^{(\omega-\omega_0)^2/2}$ (Ahuja *et al.* (2005)). We can directly see that the zero-frequency component is not zero, but for ω_0 larger than five the zero-frequency component is very small and it produces minimal error (Addison (2017)). Furthermore, the cone of influence for the Morlet wavelet is defined as $\sqrt{2}s$, with s standing for scale. Coefficients further away from the edges are only minimally influenced by the edge-effects. The Morlet wavelet is a complex wavelet, which allows to investigate not only both the local variance and co-variance but also phase and phase difference. Moreover, the Fourier wavelength of the Morlet wavelet is $\lambda = \frac{4\pi}{w_0 + \sqrt{(2+w_0^2)}}$ (Torrence & Compo (1998), thus with $w_0 = 6$ we have $\lambda \approx 1.03$. This means that the scales are almost proportional to the inverse of the frequency which greatly simplifies the interpretation.

4.2.6 Wavelet phase

Wavelet analysis with the use of complex wavelets offer apart from the cross-spectrum and coherency analysis also analysis of phase. For Morlet wavelet, measure of local phase of a signal x is defined as (Torrence & Compo (1998)):

$$\phi_x(\tau, s) = \tan^{-1} \left(\frac{\text{Im}(W_x(\tau, s))}{\text{Re}(W_x(\tau, s))} \right) \quad (4.14)$$

4.2.7 Discrete wavelet transform

Discrete wavelet transform can be defined similarly to the CWT with the difference that only discrete translation and dilation coefficients τ and s are considered. Feasible way to sample the translation parameters is using the shortest considered time steps (1 observation), while for the the scaling parameters can be linked to time steps by using powers of 2 (also called dyadic grid scaling (Addison (2017))). The wavelets and the transform of continuous signal x then

become:

$$\psi_{m,n}(t) = \frac{1}{\sqrt{2^m}} \psi\left(\frac{t - n2^m}{2^m}\right) \quad (4.15)$$

$$W(m, n) = \int_{-\infty}^{\infty} x(t) \psi_{m,n}(t) dt \quad (4.16)$$

where m and n are all integers referring to the scaling and dilation parameters. If the wavelets form an orthonormal basis, simple reconstruction of the signal by sum of all the coefficients is possible and the variance of the signal is preserved in the transformation. To limit the number of scales in the transformation, scaling function can be introduced. Its translated and dilated versions are defined the same as wavelets. The difference is however in the property of its base version (i.e. with parameters m and n both 0) in the sense that it integrates to 1:

$$\int_{-\infty}^{\infty} \phi(t) dt = 1 \quad (4.17)$$

Approximation coefficients at scale m and location n are then defined as:

$$S(m, n) = \int_{-\infty}^{\infty} x(t) \phi_{m,n}(t) dt \quad (4.18)$$

where $S(m, n)$ is then an approximation of the signal at scale m . They have such properties that we can write signal $x(t)$ in a form:

$$x(t) = x_{m_0}(t) + \sum_{m=-\infty}^{m_0} d_m(t) \quad (4.19)$$

where m_0 is arbitrarily chosen highest detail scale, $x_{m_0}(t) = \sum_{n=-\infty}^{\infty} S(m_0, n) \phi_{m_0,n}(t)$ and $d_m(t) = \sum_{n=-\infty}^{\infty} W(m, n) \phi_{m,n}(t)$, first part being called scaling coefficients and second detail coefficients. It can be shown from scaling coefficient on scale J we can compute detail coefficients and scale coefficient on scale $J-1$ (and vice versa).²

When dealing with discrete signal, if the signal has length N being an integer power of 2, we can decompose the signal to J levels of detail coefficients and a scaling coefficient with n being limited by the length of a signal ($N = 2^J$)

²for more detailed information on the definition of father wavelet, wavelet frames, the computation of scaling and detail coefficients and other computations linked to introduced form of definition of DWT, see Addison (2017), p. 65-87. It is also possible to only define DWT on discrete signal in a form of discrete filters (see e.g. Gençay *et al.* (2001)

using multi-resolution algorithm (also know as fast wavelet transform) when we compute one level of detail coefficients at a time from scaling coefficients until we obtain all J levels of details that we want to investigate (we do not have to compute all possible levels). Detail coefficients of level $m \in J$ then contains information from frequency band $f \in \langle 1/2^{m+1}, 1/2^m \rangle$ - i.e. lowest scale $m=1$ represents periods between 2 and 4 observations. We can see that each step can be understood as applying high-pass filter on remainder of the signal.

Unfortunately, DWT is not circular shift invariant (if signal is shifted by 1 observation the coefficients are different, not just shifted by 1) and financial time-series seldom have the length of 2^N . To overcome that problem, *maximum overlap discrete wavelet transform* can be introduced. Moreover, Gençay *et al.* (2001) provide a summary of feasible properties of MODWT, among which the most important is that MODWT can be performed on sample of any length, amount of the coefficients (in time-domain) is the same as the signal length and it is associated with so-called zero-phase filtering. Important consequence is well alignment of time-features in the coefficients. Additionally, MODWT is asymptotically more efficient variance estimator then DWT. It can be shown that MODWT coefficients preserve the variance of the signal, i.e. $\|x^2\| = \sum_{m=1}^J \sum_{n=1}^N \|W(m, n)\|^2 + \sum_{n=1}^N \|S(J, n)\|^2$.

4.2.8 Wavelet correlation

We estimate variance and covariance of analyzed signals at different frequency bands using the MODWT. It can be used as a time-averaged complement to the localized correlation coefficients provided by CWT.³ Following Baruník *et al.* (2016) and Vacha & Baruník (2012), we use wavelet base estimator of correlation of signals x and y on scale j ($j = 2^m$) as:

$$\hat{\rho}_{x,y}(j) = \frac{\hat{Cov}(W_x(m, n), W_y(m, n))}{\sqrt{\hat{Var}(W_x(m, n))\hat{Var}(W_y(m, n))}} \quad (4.20)$$

where $\hat{Cov}(W_x, W_y)$ and $\hat{Var}(W_i)$ are wavelet based covariance and variance estimators, defined as (covariance of signal with itself is variance):

$$\hat{Cov}_{x,y}(j) = \frac{1}{k_m} \sum_{n=L_m-1}^{N-1} W_x(m, n)W_y(m, n) \quad (4.21)$$

³even though smoothing of the coefficient itself does, in a sense, time-averaging

where L_m is the length of the wavelet filter as scale m^4 and $k_m = N - L_m + 1 > 0$. Under the assumption that analyzed processes are stochastic auto-regressive processes of order d (d is the largest lag in the process) and $L_m > 2d$, MODWT correlation estimator at scale m is asymptotically normally distributed around the true value with large sample variance $N_m^{-1}R_m$,⁵ i.e.:

$$\hat{\rho}_{x,y}(j) \sim \mathcal{N}(\rho_{x,y}(j), N_m^{-1}R_m) \quad (4.22)$$

4.3 Continuous wavelet transform and Phase difference

Apart from computing individual phases of each signal we can also compute phase difference or signals x and y . The computation is the same as for the individual phases but we use the cross-transform instead and the relative phase difference (smoothed) is then simply defined as (Torrence & Compo (1998)):

$$\phi_{x,y}(\tau, s) = \tan^{-1} \left(\frac{\text{Im}(\langle W_{x,y}(\tau, s) \rangle)}{\text{Re}(\langle W_{x,y}(\tau, s) \rangle)} \right) \quad (4.23)$$

with $\text{Im}(\cdot)$ and $\text{Re}(\cdot)$ standing for imaginary and real parts of the wavelet cross spectrum. Note that the smoothing in time and scale is done before taking real or imaginary part and thus has to be done only once. Phase is then defined on $(-\pi, \pi)$. If the difference lies on the interval $(-\pi, -\pi/2)$ or $(0, \pi/2)$ the first series is leading the second, otherwise the second is leading (Roesch *et al.* (2014), Hanus & Vácha (2018)). The phase differences are evaluated on sets of scales due to correlation of wavelet coefficients on adjacent scales. Note that several papers (for example Hanus & Vácha (2018)) suggest to divide the cross-wavelet transform at each scale by that scale before the smoothing is done, yet both approaches lead to qualitatively equal results.

If one signal lags behind the other, it has to hold that $\phi(X) - \phi(Y) = \text{constant} \neq 0$ (Cazelles & Stone (2003)). When dealing with a noisy time-series, the relative phase position tend to change, either overall or on certain scales. But if two series tend to have some phase relationship (tend to be phase-locked), there

⁴discrete wavelets such as Daubechies or Symlet wavelets are defined with a finite number of vanishing moments (equivalent of the Gaussian envelope of Morlet wavelet), i.e. they become 0 after some distance from the center. We than say that the length of the wavelet filter on scale 1 is then the number of vanishing moments of the wavelet time 2^m

⁵for precise definition of R_m , see Whitcher *et al.* (1999)

should be some non-zero preferred value. To deal with the circularity, i.e. that $-\pi$ and π are next to each other, when computing mean of the phase shifts we follow Addison (2018)⁶ and introduce circular mean phase shift of signals x and y as follows:

$$CMPD(x, y) = \tan^{-1} \left(\frac{\langle \sin(\phi_{x,y}(\tau, s)) \rangle}{\langle \cos(\phi_{x,y}(\tau, s)) \rangle} \right) \quad (4.24)$$

where $\langle \cdot \rangle$ stand for averaging in time. This measure is used for calculation the raw mean phase difference and also for its confidence intervals described below. There are unfortunately no theoretical distributions available for phase difference of two signals and thus approach employing Monte Carlo methods is needed. We examine some possible approaches and use them to assess our results.

To examine the significance of the existence of the preferred value, normalized Shannon entropy (SE) can be used to determine significance of the peak. Following Hanus & Vácha (2018) the confidence intervals of the mean phase difference were determined with a bootstrap approach.

4.3.1 Shannon entropy test

If two noisy signals are not in any way phase synchronized, their phase differences should follow uniform distribution (i.e. their mutual phase position can be at any point with equal probability), while if the distribution is peaked, it points to tendency to be synchronized. Useful measure that can quantify how different is the phase difference distribution from uniform distribution can then be Normalized Shannon entropy (P. Tass & Freund (1998)) that quantifies the localization of an information. Index of Shannon entropy of distribution $\psi_{x,y}(t)$ is defined as

$$S = - \sum_{k=1}^{N_h} p_k \log p_k \quad (4.25)$$

⁶Addison uses different measure for phase difference when using such circular mean, however it does not affect usability of this measure (even though it decreases the scale of the difference between it and classic mean). Measures proposed by Addison (so-called non-smoothed phase differences) were tested on the artificial (noisy) signals and did not provide correct identification of the phase differences. This leads researcher to the conclusion that those measures are not fit to examine phase-positions of very noisy data on higher frequencies.

p_k is a relative frequency of observation in bin k of a frequency histogram with N_h being the number of bins. Normalized Shannon entropy is then

$$Q = \frac{S_{max} - S}{S_{max}} \quad (4.26)$$

with $S_{max} = \ln N$. Then Q can have values between 0 and 1 with 0 for uniform distribution and 1 for Dirac like distribution, i.e. full phase synchronization. Two independent signals should have phase difference distribution uniform, but to avoid miss-interpretation of the coefficient due to randomness, significantly different value from uniform distribution is then determined by computing the index for 1000 white-noise and red-noise series and the observed Q is evaluated against noise entropies to obtain probability of the signals to be phase-correlated due to randomness.

It is important to note that for two series to be phase-locked over time their phase difference distribution should be unimodal - have one peak. Two (or several) peaked distribution can mean that the phase sharply shifted in certain period or that the relative phase switches between 2 or more states. Thus inspection of the phase in time is needed. Another issue is that the insignificance against random noise indicates that there is no interesting (or observable) relationship between the processes. Conversely if we find significant values it suggest that the is phase relationship present. In the same time, the relative size of the Shannon entropy statistic can be understood as a measure of stability of the phase-difference. Lower values indicate lower stability,⁷ while high values suggest that there is a single phase lock.

4.3.2 Phase bootstrap

To establish the empirical confidence intervals we constructed 500 surrogate series by adding 5% white noise to the original ones. Then for each pair of series the phase difference is computed. At each time point and at each band on which phase difference was obtained a 95% confidence interval is computed. If one series is then significantly lagged in phase after the other, the phase should be stable and different from zero. Therefore confidence interval of the mean phase difference are established by taking mean over series consisting of the border of significance at each time point.

⁷White, Red and Fourier noise all seldom have Shannon entropy over 0.15

4.3.3 Computation of CWT with discrete input signal

Financial time-series do not provide us with continuous data and also all integrals can be numerically approximated with only finite accuracy. To address this issue, it is thus feasible to select approximation finesse and use efficient methods for computation of the coefficients. In time domain, the shortest available resolution is used (i.e. 5-minute), in frequency domain we choose to use scales as powers of 2 (set of scales from one power to another is called octave) and in between each power we compute 25 scales exponentially distributed over the sub-interval. Following Torrence & Compo (1998), the wavelet transform in discrete time can be then rewritten as

$$W(\tau, s) = \frac{1}{N} \sqrt{\frac{2\pi s}{\delta t}} \sum_{k_0}^{N-1} \hat{x}_k \hat{\psi}^*(s\omega_k) e^{i\omega_k n \delta t} \quad (4.27)$$

where \hat{x}_k stands for Fourier transform of a signal x , $\hat{\psi}(\cdot)$ is Fourier transform of the wavelet and ω stands for angular frequency which is $\frac{2\pi k}{N\delta t}$ for $k \leq N/2$ and $-\frac{2\pi k}{N\delta t}$ otherwise. The coefficients are then computed employing Fast Fourier Transformation algorithm.

The scale decorrelation length was empirically determined to be 0.6 of an octave for Morlet wavelet (Torrence & Compo (1998)) and it was chosen as a smoothing window in frequency domain. The smoothing window in time represents trade-off between resolution in time-localization and robustness to noise. Various window lengths are used in practice, for example Cazelles *et al.* (2008) use in their MatLab package window of a tenth of time-series length. In this thesis it was chosen to be 400, which means that each coefficient is smoothed by observations distant up to two and a half day with linearly decaying weights. More details are provided in the following section.

4.3.4 Phase differences of artificial signals

To demonstrate the strength of wavelet analysis, this section employs above introduced method on a signals composed of single or multiple sinus waves with added noise and compares them signals generated by White and Red noise processes and to phase-randomized Fourier surrogate of indexes PX and DAX in 2008.

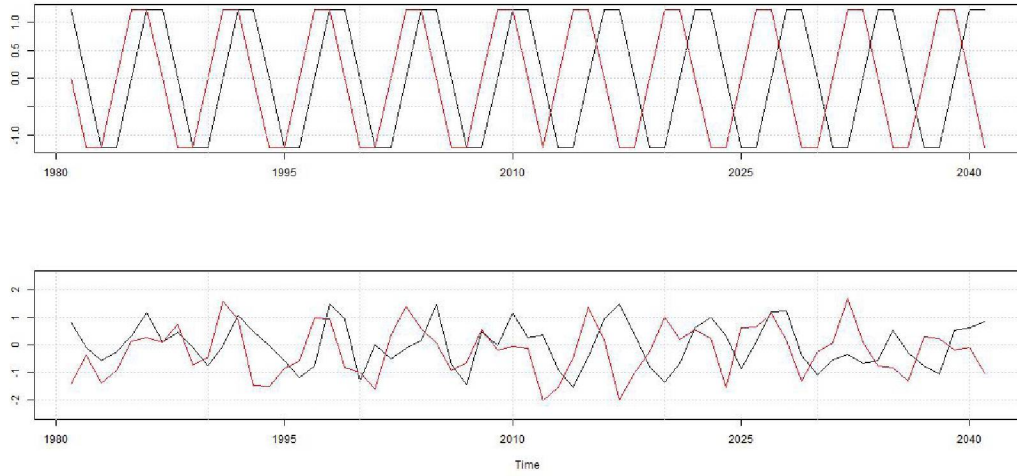


Figure 4.2: Signals $a(t)$ and $b(t)$, on the top without noise

First pair of signals are simple sinuses shifted twice:

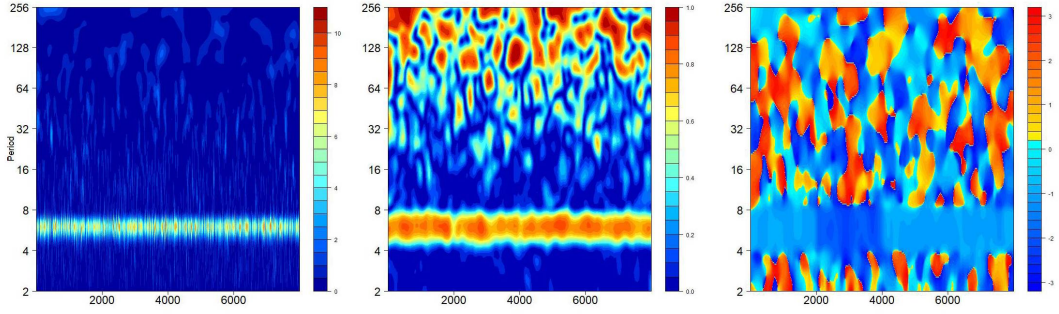
$$a(t) = \sin(2 * \pi * t/6) + \epsilon_a \quad (4.28)$$

$$b(t) = \epsilon_b + \begin{cases} \sin(2 * \pi * (t + 1)/6), & \text{if } t < 2000 \\ \sin(2 * \pi * (t + 1)/6), & \text{if } t \in (2000, 4000) \\ \sin(2 * \pi * (t + 1)/6), & \text{if } t > 4000 \end{cases} \quad (4.29)$$

where ϵ_i is a random normally distributed noise with zero mean and variance equal to the signal without it (e.g. $\epsilon_a \sim N(0, 0.5)$). Figure 4.2 shows the signals around the first shift with and without the noise. We can see that without the noise the signals periodicity and phase are very clear while with the noise, no apparent comovement, phase difference or shift in it are observable.

Figure 4.3 show wavelet Cross-power, squared coherence and phase difference of simple noisy signal $a(t)$ and composite noisy signal $b(t)$. On the y-axis of the first two graphs Cross-power shows that the variation is interesting only at periods around 6. Coherence nicely smooths the relationship and show that the signals are indeed highly coherent across entire existence around period 6 but also show some random coherence on lower frequencies. However in the phase plot, it is easy to see that stable phase is present only on band 4-8, where it starts at -1, then shifts two -2 and reverts back to -1 - indicating changing lag of $a(t)$ behind $b(t)$.

Figure 4.4 shows the evolution of phase difference on three bands (2-4, 4-8 and 16-32). We can see that the phase difference clearly shows the relationship



(a) Wavelet Cross power (b) squared Coherence (c) Wavelet Phase difference

Figure 4.3: Wavelet phase difference of $a(t)$ and $b(t)$

on the band 4-8, while no stable relationship is present for the other bands. Shannon Entropies are 0.1, 0.56 and 0.08, respectively. For the band 4-8 we see a value that never occurred for random noises in our simulation (relatively higher stability) while the values for the other two bands are not statistically different from random.

Second, composite signals $c(t)$ and $d(t)$ consisting of 4 sinus wave were created:

$$x(t) = \sin(2 * \pi * t/3) \quad (4.30)$$

$$y(t) = \sin(2 * \pi * t/6) \quad (4.31)$$

$$z(t) = \sin(2 * \pi * t/24) \quad (4.32)$$

$$w(t) = \sin(2 * \pi * t/48) \quad (4.33)$$

$$c(t) = x(t) + y(t) + z(t) + w(t) + \epsilon_c \quad (4.34)$$

$$d(t) = z(t) + w(t) + \epsilon_d + \begin{cases} 3 * x(t) + y(t + 1), & \text{if } t < 2000 \\ x(t - 1) + y(t + 2), & \text{if } t \in (2000, 4000) \\ x(t - 1) + y(t + 1), & \text{if } t > 4000 \end{cases} \quad (4.35)$$

We can see that the processes are in phase for periods 24 and 48 (lower frequencies), and with changing phase difference on high frequencies (periods 3 and 6). Their wavelet cross-power, coherence and phase are showed in figure 4.5. It is interesting to see the almost vanishing coherence on the highest frequency after signal $d(t)$'s amplitude was lowered to 1 in comparison to 3. The phase difference plot indicates quite stable phase on bands 16-32 and 32-64 and changing phase difference on bands 2-4 and 4-8, where darker blue colours indicate shift onward while shift to red colours on band 2-4 show the lag of $d(t)$ behind $c(t)$. Figure 4.6 investigates few bands of the phase difference. We can see stable

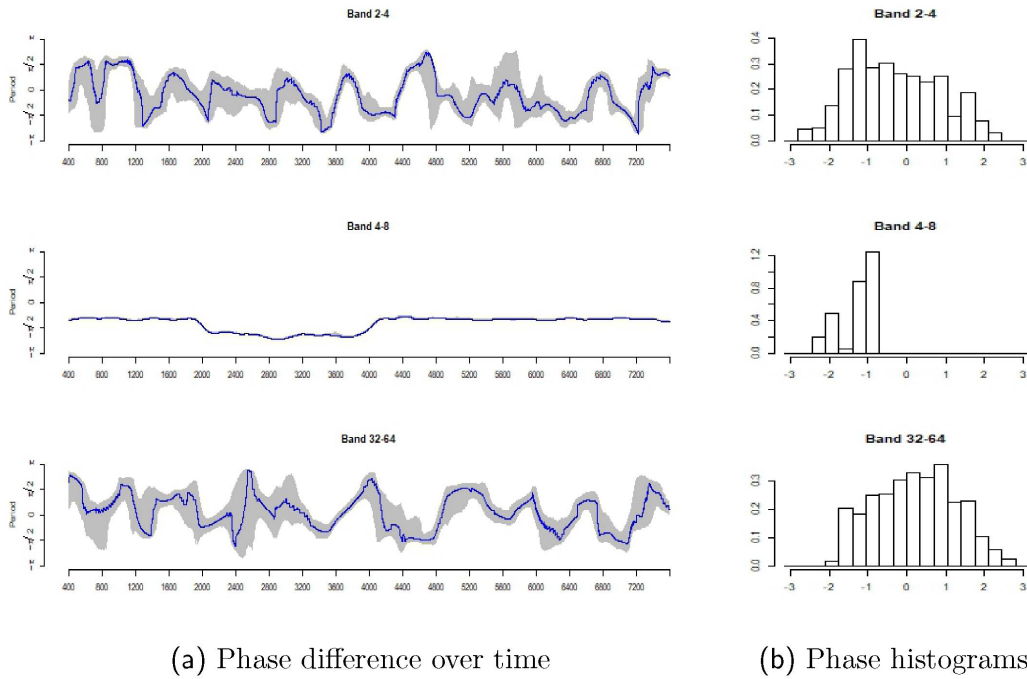


Figure 4.4: Wavelet spectra and phase of $a(t)$ and $b(t)$

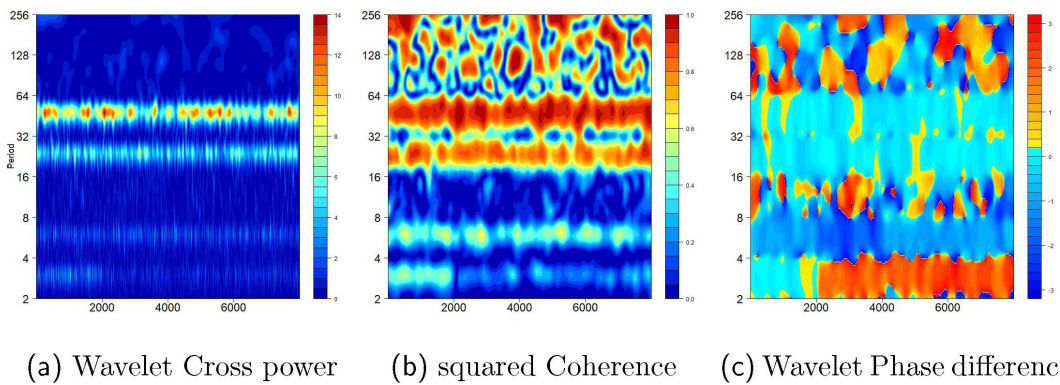
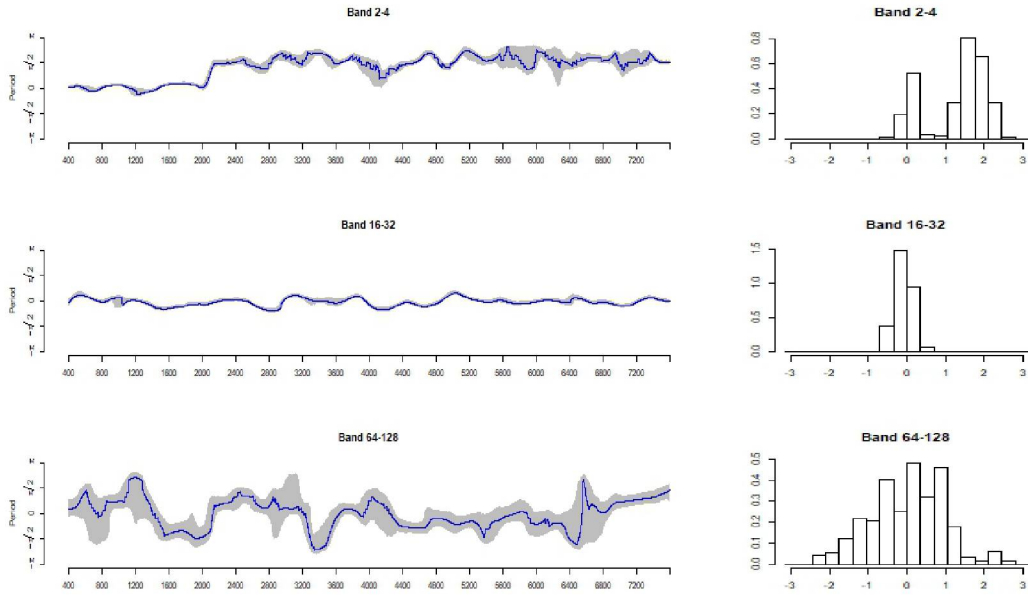


Figure 4.5: Wavelet phase difference of $c(t)$ and $d(t)$



(a) Phase difference over time

(b) Phase histograms

Figure 4.6: Wavelet spectra and phase of $c(t)$ and $d(t)$

phase-lock on band 16-32, 2 clear peaks and shift around point 2000 and band 2-4 and no clear relationship on band 64-128. Shannon entropies from top down are 0.3, 0.5 and 0.15. Latest can be surprising since it is marginally higher than what we get from simulations of all three types of noise. This is due to the smoothing and correlation on adjacent scales as the 0 phase difference from scale 32-64 influenced the result and demonstrates important implication on Shannon entropy test: SE only rejects that the signal is a random noise process (colours white, red and Fourier phase randomized surrogate). But the coefficient remains valid to tell us about the relative stability of the phase difference.

Noises and smoothing window

Changing the size of the smoothing window affects the time-resolution of the phase-difference and thus it is important to use the appropriate length of the window. First, let us have a look at the Red Noise phase difference. Red-noise can be defined as Gilman *et al.* (1963):

$$RN(t) = \alpha * RN(t - 1) + \sqrt{(1 - \alpha^2)} * \epsilon, \epsilon \sim N(0, 1) \quad (4.36)$$

Figures 4.7 and 4.8 show the time-evolution of the wavelet phase difference with the windows set to 50 and 400. It can be seen that regardless of the frequency band, the distribution of the phase difference is dispersed across the whole period. Histograms 4.12 of the phase difference look almost the same across all periods and smoothing windows. White noise exhibit identical properties and the same is valid for phase-randomized Fourier surrogate of the indices (as defined by Cazelles *et al.* (2008)).

Figures 4.10 and 4.11 show the time-evolution of the wavelet phase difference for the composite process $c(t)$ and $d(t)$ with smoothing windows set to be 50 a 400. It can be seen that while for the relatively low frequency band (64-128) the phase-lock can be observed with window 50, the high-frequency components seem like a noise and it is hard to distinguish for example between band 2-4 and 8-16. On the other hand, with window 400 the relationship unveils itself and we can observe, even-though still noisy, the relationships on expected scale while the scale 8-16 remains random. The effects of the smoothing are much larger on the highest frequencies than the lower ones. Reason is fairly straightforward - the wavelets on higher scales work in a broad sense as weighted averages themselves, and thus are smoother by definition and only less space for smoothing remains.

Figures below well illustrate the effect of the smoothing. The phase-relationship between the series remain the same, since we smooth the coefficients from which we calculate the phase difference, not the phases itself. That has direct impact for the bootstrap approach of obtaining the confidence intervals of the *means* of the relative phases - they are quite robust to the changes of smoothing windows. Extreme example is shown in table 4.1 where we compare Red noise processes with 19500 observations smoothed with windows of length 15 and 400 where we do not observe much change in the confidence intervals.

Table 4.1: Relative phase confidence intervals and entropies of Red Noise series

Window length	2-4 scale	Confidence interval	Shannon entropy	4-8 scale	Confidence interval	Shannon entropy	8-16 scale	Confidence interval	Shannon entropy
15	0.04	(-0.8, 0.9)	0.06	0.00	(-0.7, 0.7)	0.07	0.03	(-0.6, 0.6)	0.07
400	0.07	(-0.7, 0.9)	0.09	0.12	(-0.5, 0.8)	0.08	0.15	(-0.5, 0.6)	0.07
Window length	16-32 scale	Confidence interval	Shannon entropy	32-64 scale	Confidence interval	Shannon entropy	64-128 scale	Confidence interval	Shannon entropy
15	0.08	(-0.5, 0.6)	0.08	0.02	(-0.5, 0.6)	0.08	0.24	(-0.3, 0.8)	0.09
400	0.10	(-0.5, 0.6)	0.07	0.10	(-0.4, 0.6)	0.08	0.34	(-0.2, 0.9)	0.10

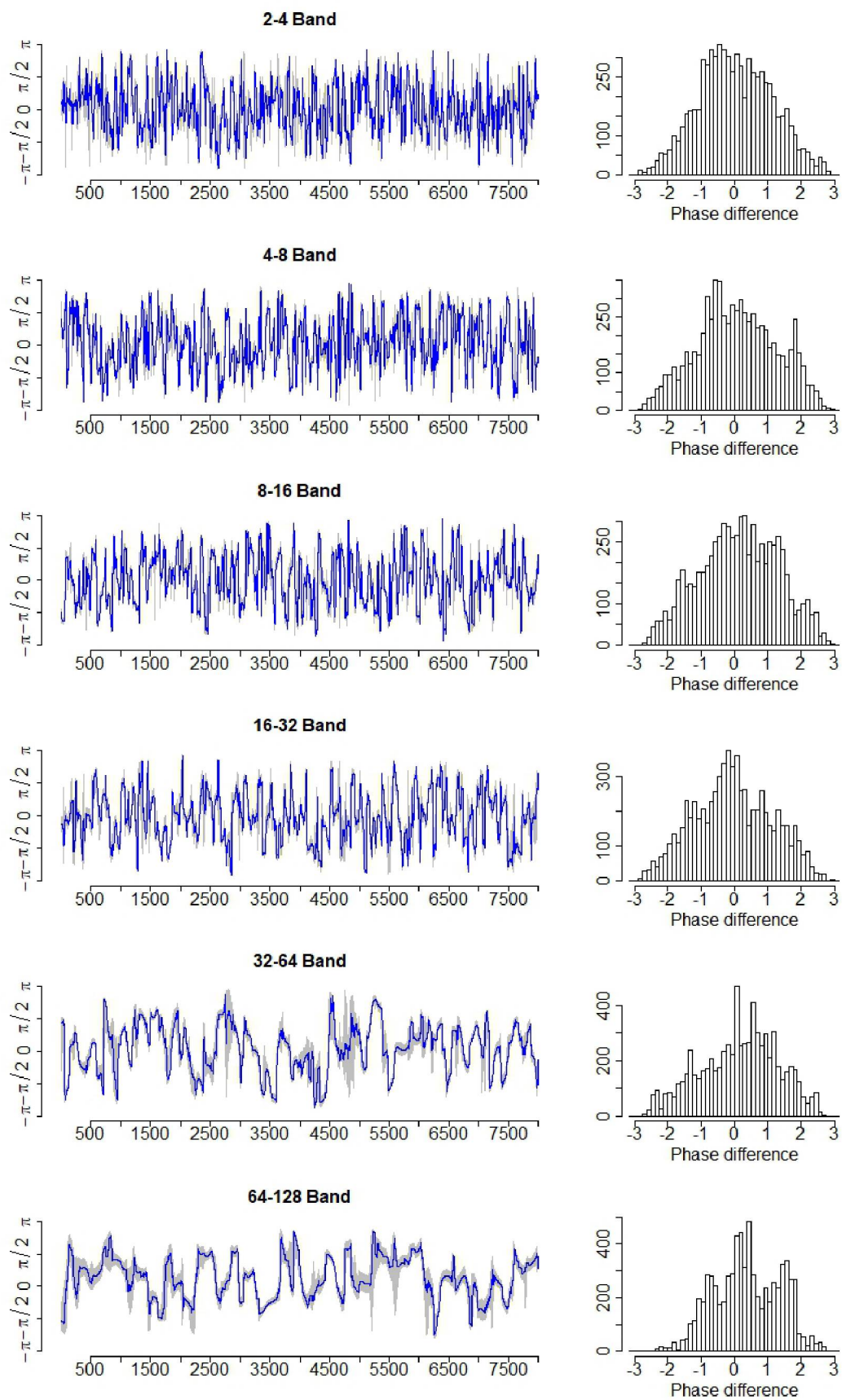


Figure 4.7: Red Noise series phase difference with time-window 50

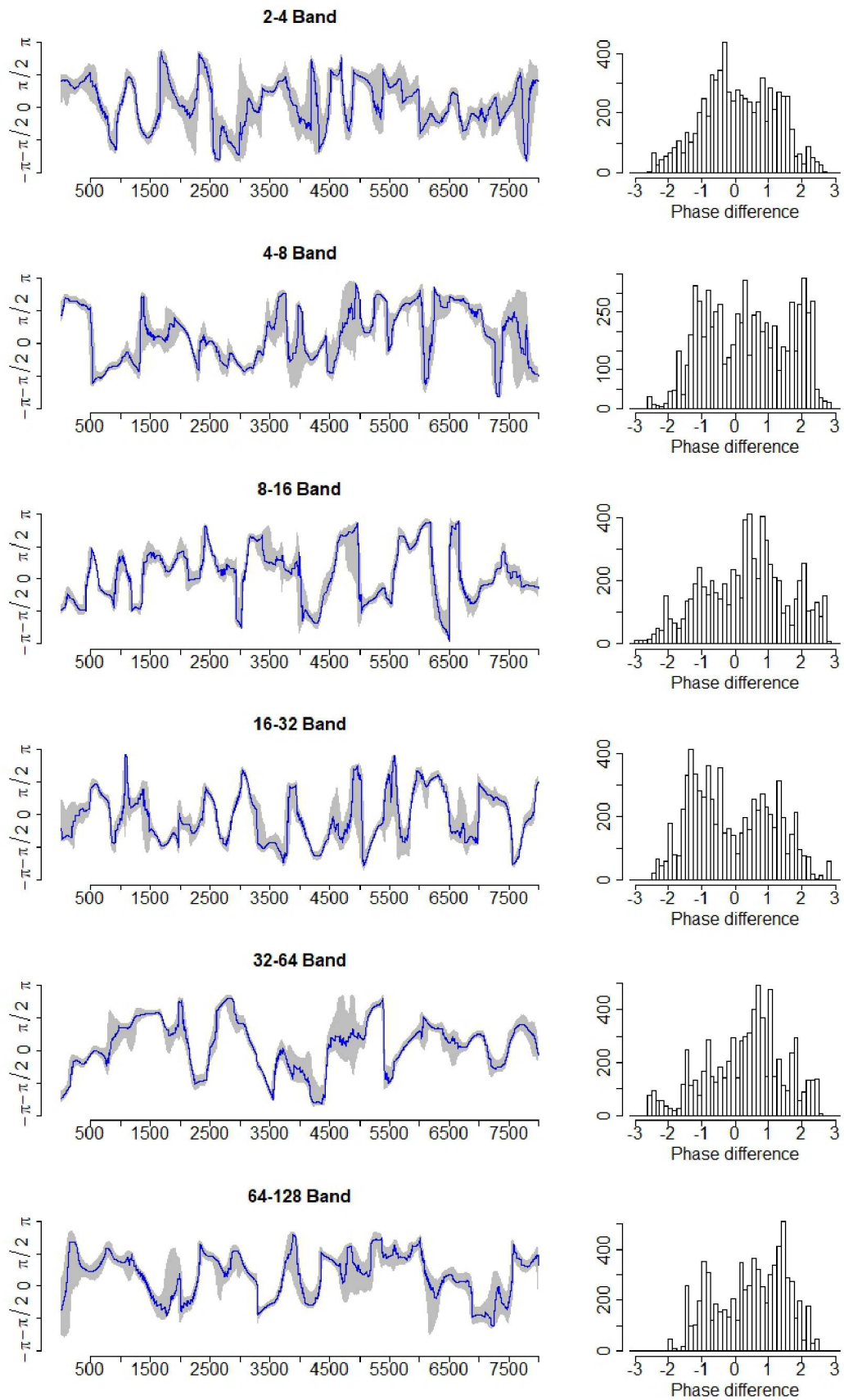


Figure 4.8: Red Noise series phase difference with smoothing time-window 400

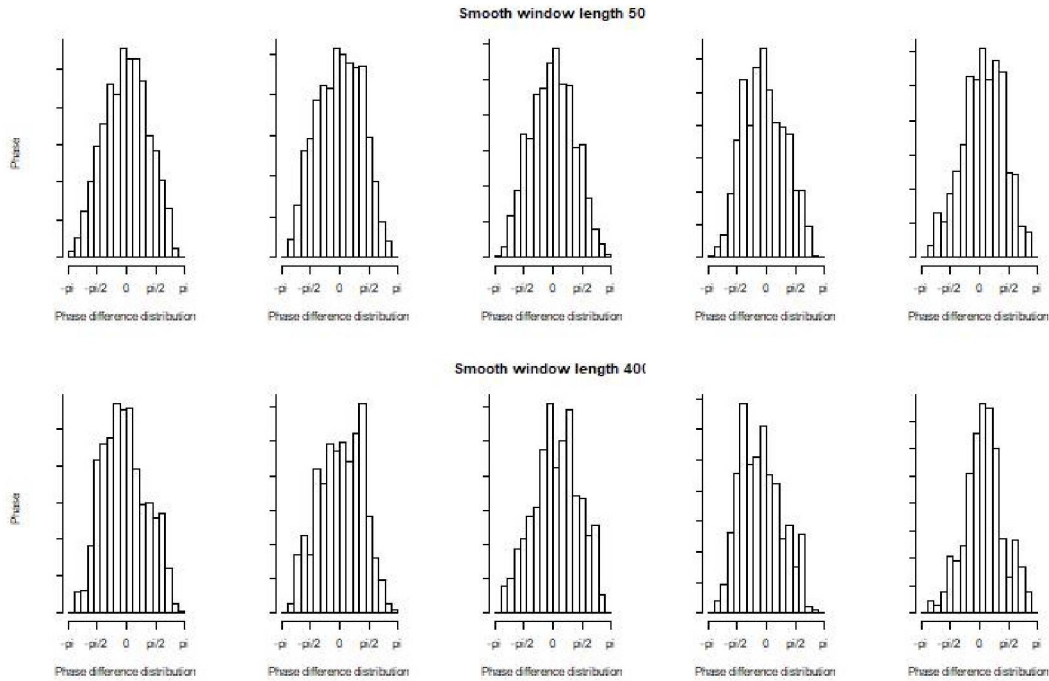


Figure 4.9: Red Noise phase histograms

4.3.5 Phase synchronization without smoothing

In recent paper Addison (2018) points out possibility to examine phase differences on scales without any smoothing of the transform itself. The phase-synchronicity is measured by averaging the "raw" phase difference of the signals x and y defined as

$$\begin{aligned} \delta\phi_{x,y}(\tau, s) &= \delta\phi_x(\tau, s) - \delta\phi_y(\tau, s) = \\ &= \tan^{-1} \left(\frac{\text{Im}(W_x(\tau, s))}{\text{Re}(W_x(\tau, s))} \right) - \tan^{-1} \left(\frac{\text{Im}(W_y(\tau, s))}{\text{Re}(W_y(\tau, s))} \right) \end{aligned} \quad (4.37)$$

This definition is however equivalent to computing the non-smoothed phase of the cross-transform.

Addison (2018) defines so-called *phase synchronization index*, a measure to compare phase-synchronicity of different signals, as:

$$PSI_{x,y}(s) = \langle \sin(\delta\phi_{x,y}(\tau, s)) \rangle^2 + \langle \cos(\delta\phi_{x,y}(\tau, s)) \rangle^2 \quad (4.38)$$

Such measure can have values ranging from 0 to 1, with 0 pointing to full randomness of the series and 1 to perfect synchronization on particular scale similarly to Shannon entropy. Since the measure produces single value for

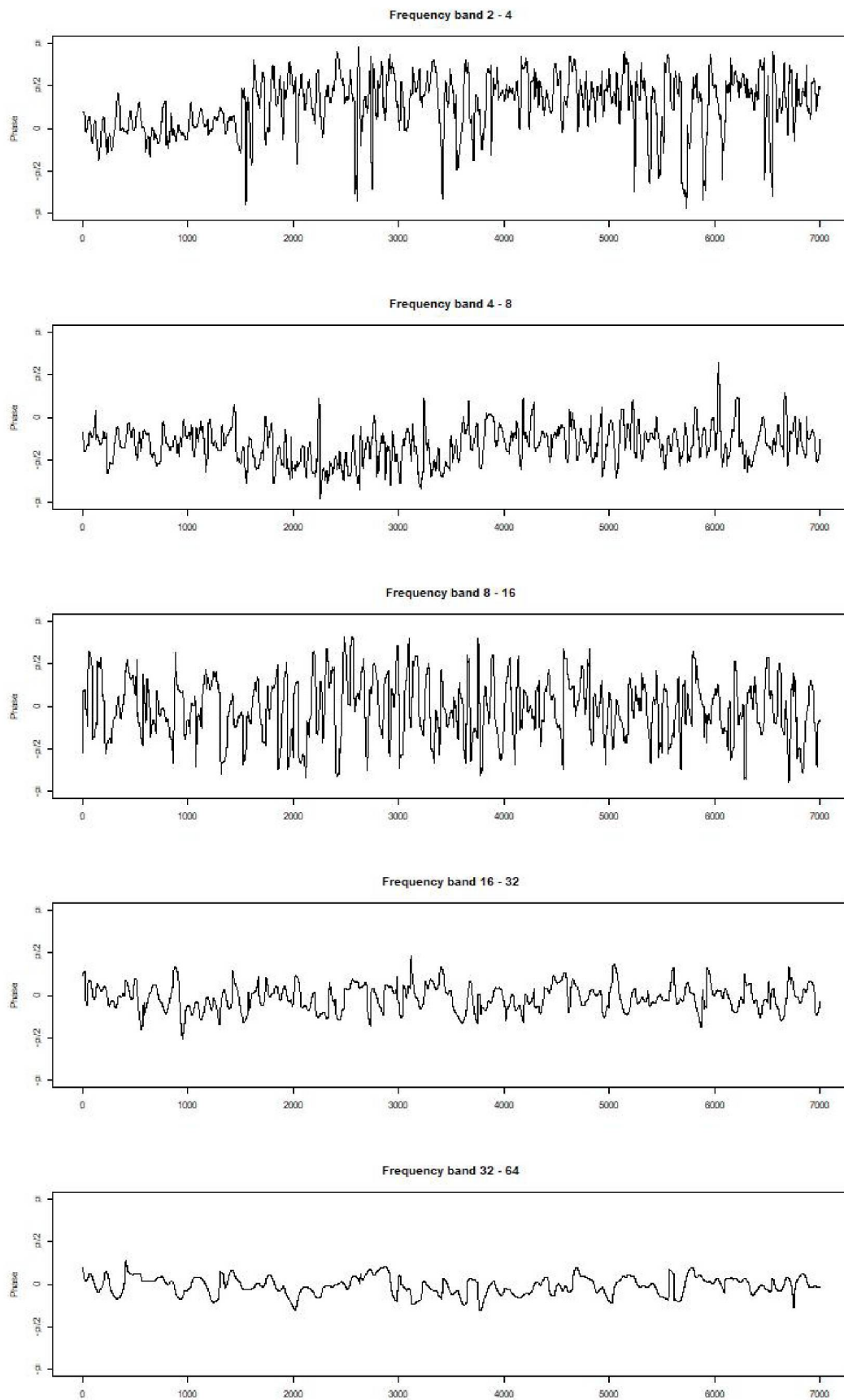


Figure 4.10: Phase differences of signals $c(t)$ and $d(t)$, smoothing time-window 50

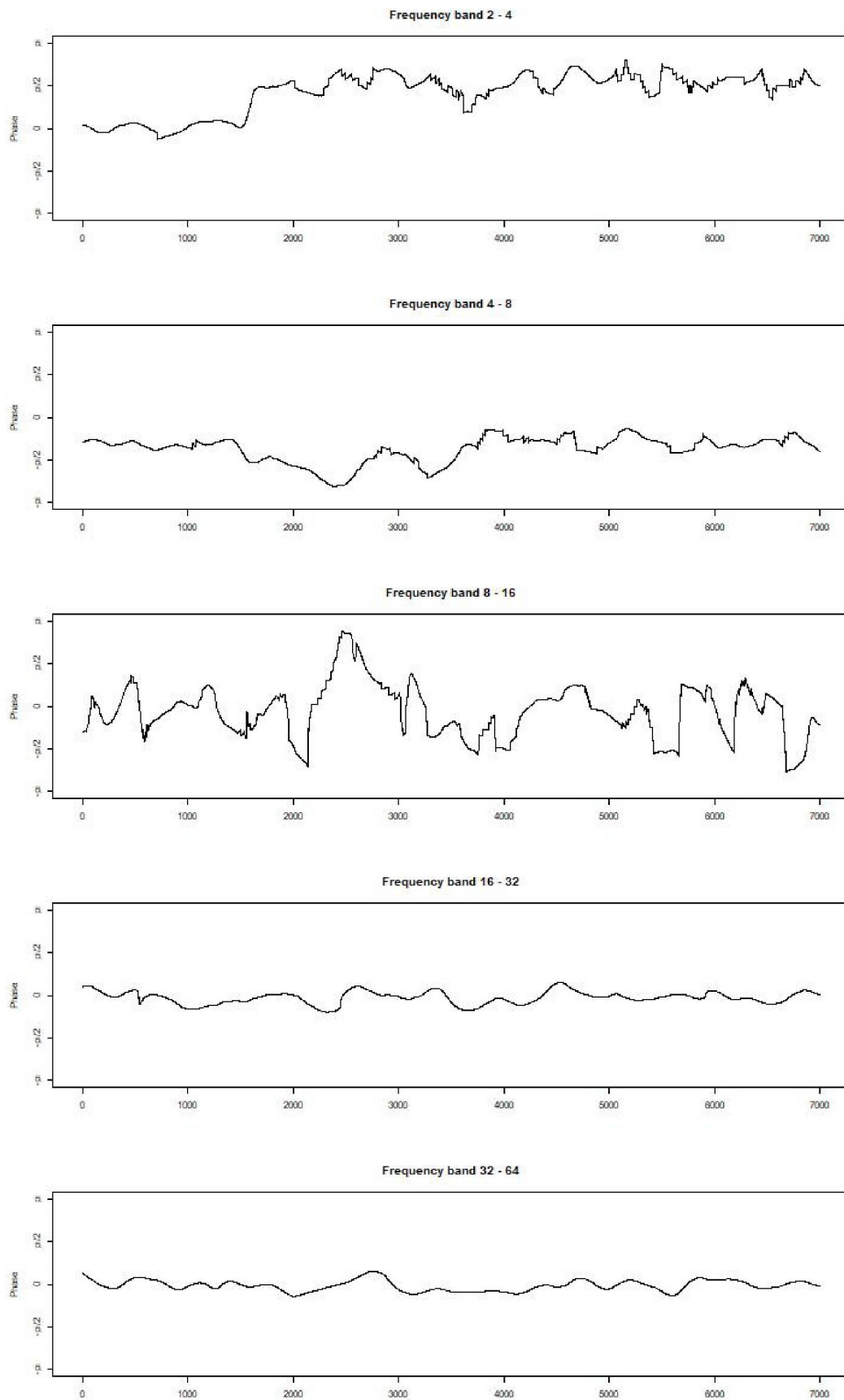


Figure 4.11: Phase differences of signals $c(t)$ and $d(t)$, smoothing time-window 400

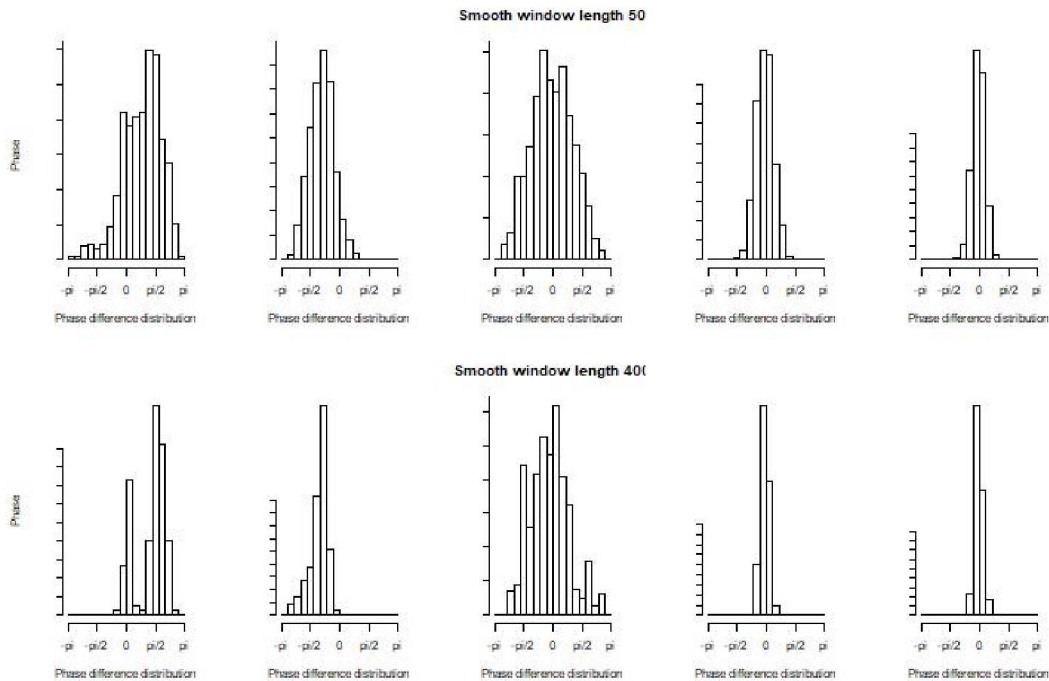


Figure 4.12: Phase difference histograms of signals $c(t)$ and $d(t)$

each scale, it is possible to examine it 'continuously'. It is not clear which synchronization values are significantly larger than 0 and not caused only by finite length of the series. We thus use bootstrap approach on 1000 red-noise signal pairs to establish indication of significance of the synchronicity. Figure 4.13 shows 95th percentile of values of PSIs between 2 random signals (both white-noise and red-noise shown).

We have to point out that the measure is not equivalent to any of the above measures - since here we do not smooth the data nor the transforms which averages out part of the deviations. This can lead to failure to uncover existing relationships that remain masked under noise on particular scale. On the other hand it offers more detailed and less biased information on the synchronicity.

4.4 MODWT and Granger Causality

One well known test of cross-influence between signals (time-series, indexes) is called linear Granger Causality test. It is a spectral test designed to statistically assess if information contained in past realizations of A is useful for prediction of process B after accounting for all the information in process B (i.e. its past values). If such a causality is present on some frequencies it shows slightly

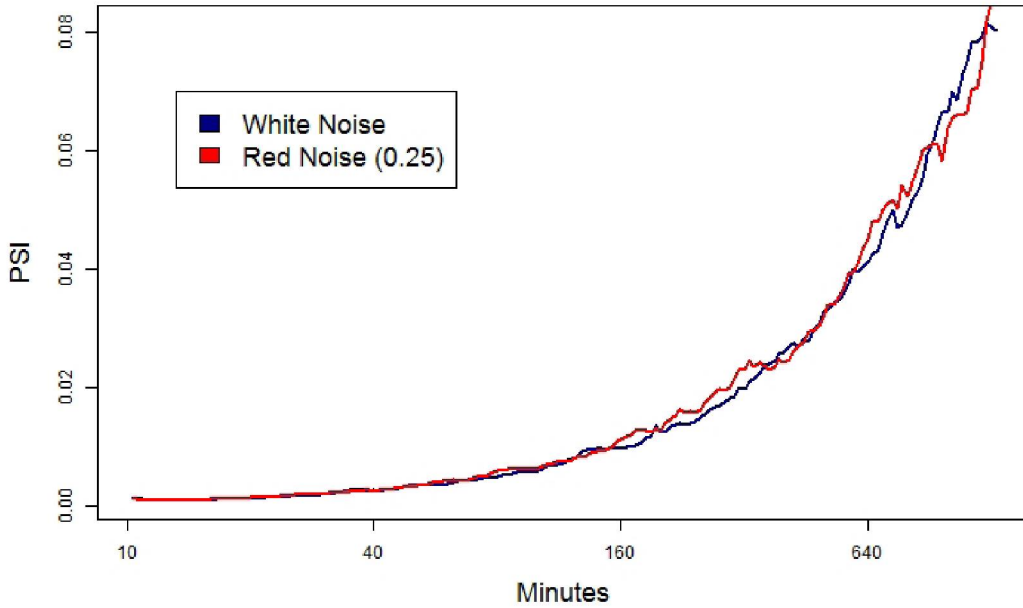


Figure 4.13: 95th quantile of PSIs of White-noise and Red-noise artificial signals

different but stronger picture how the series are following each other (however the presence of bidirectional causality is possible, while instantaneous lead of both series is not). Following Reboredo *et al.* (2017), we introduce VAR model without instantaneous causality as follows:

$$x_t = a_1 + \sum_{i=1}^k \alpha_i x_{t-i} + \sum_{i=1}^k \beta_i y_{t-i} + u_{x,t} \quad (4.39)$$

$$y_t = a_1 + \sum_{i=1}^k \gamma_i x_{t-i} + \sum_{i=1}^k \delta_i y_{t-i} + u_{y,t} \quad (4.40)$$

where $u_{s,t}$ is random term in time t for series s . To select which lags should be used to in VAR model, variety of methods are commonly used in practice - i.e. Aikake's, Hannan-Quinn or Schwarz's Bayesian information criterions or likelihood ratio test. Dziak *et al.* (2012) note that while AIC has quickly decreasing probability of Type I error (under-fitting) with increasing sample size, probability of Type II error remains the same. On the other hand SBIC's probability of both types of error decrease slowly with sample size. Since samples used in this thesis are quite large, SBIC is used for lag selection.

We can set null hypotheses that x does not cause y $H_0^x : \beta_1 = \dots = \beta_k = 0$ and y does not cause x $H_0^y : \gamma_1 = \dots = \gamma_k = 0$. In presence of normally distributed

random terms with constant variance, the test statistic for such a test follows Fisher distribution with $(k, T-2k-1)$ degrees of freedom. However, for the raw series, normality of the error term is a strong and unlikely assumption (even though it is satisfied for sub-series obtained by MODWT). Mantalos *et al.* (2007) show if the underlying processes contain conditional heteroskedasticity, linear Granger causality test tends to over-reject the null hypotheses of no causality and therefore lead to finding causality where none is present. Since the raw data exhibit auto-correlation and conditional heteroskedasticity, following Hafner & Herwartz (2009) we use wild bootstrap to establish empirical p-value of the Granger causality (using 5000 runs⁸).

We then apply this model on a sub-sample of 2008 and 2015 (2011 for WIG) on both original series and the filtered series obtained by inverse MODWT on the scale coefficients allowing for, apart from observing direct causality, also for causality localized on certain frequency band providing possibly both localization of causality and identification of new ones (that could be covert in the process by other information).

4.5 Tools used to carry out the analysis

The analysis is done in R 3.4.0. Several tools of the tools were originally coded in MatLab by other researchers but they were rewritten to R language syntax.⁹ Packages *data.table* (Dowle & Srinivasan (2017)) *waveslim* and *wmtsa* (for MODWT calculation) were used to carry out the analysis.

⁸This number is a result of compromise in which the variance between two model runs on the same data seems negligible for the use-case whilst keeping the computational time reasonable (to cope with dozens of runs)

⁹particularly the wavelet transform itself

Chapter 5

Empirical results

5.1 Evidence from CWT and wavelet correlation

5.1.1 FTSE 100 and DAX

We start the empirical section by comparison of the two indexes that are considered as being developed markets, FTSE 100 and DAX. Figure A.1¹ shows the contour plots of the evolution of wavelet cross-power, wavelet squared coherence and wavelet phase difference of the two time-series, with significant areas being enclosed by solid black lines. On the x-axis we have time domain (each graph standing for 1 year, months as labels), on the y-axis we have frequency domain. To be able to focus on high frequency aspects, only scales of cycles of up to 3 days are depicted (the calculation was done over another octave to control for unwanted effects of smoothing). Thus relatively lower frequencies in this study point to scales of around 1 day. Regarding the wavelet power, we can see that the common high power is usually located to short time-period which as a consequence causes black areas in the plots (since every small area is enclosed by black line). Significant areas indicate high common energy on particular scale in certain points in time. It brings interesting results regarding where and how the significant areas are clustered - we can see a cluster in the end at 2008 and in many other periods and those clusters span over most scales. However, it is hard to observe any time-effects since it does not reflect significant comovements over relatively calmer periods.

On the other hand, wavelet coherence controls for relative energy of underlying processes and shows how well processes co-move with each after energy at that

¹All the figures of CWT to which the text refers are shown in the Appendix A due to their very large number and/or size

time and scale is account for. We can see that that the areas of very high coherence indicate strong link between *DAX* and *FTSE 100*. On frequencies below 80 minutes, the coherence is almost always significant. Surprising is the time-evolution of the coherence that we observe. Over time, the coherence particularly on highest but also on relatively lower frequencies decreases with the usual values falling from around 0.6 to 0.2 (with localized windows of higher significance) - even though it is still significant against random noise. This effect appears to be stronger from second half of the 2012. The reasons behind that are unclear - one possibility could be that the common pricing mechanism that influences the global prices shifts its localization to lower frequencies (beyond those inspected in this work). Lowest six plots of figure A.1 show relative phase difference of the 2 time-series. We can observe mostly only marginally negative or positive values with exceptions on relatively lower frequencies towards the end of the sample. Figure A.2 and table 5.1 together bring more focused evidence on the relative phase. During year 2008 to 2012, we can see that the phase difference fluctuates with very low amplitude around 0 (with small exception for band 64-128 which relates to 320-640 minutes namely in 2008 and 2011). Bootstrap test do not indicate any year of significant non-zero phase. Shannon entropies on high-frequency bands are very high (approximately 4 times higher than highest SE for random noise pairs) suggesting the overall stability of the differences. Interesting is the observed lower stability of the relative phase over the years 2013 to 2015 where particularly on lower frequency bands the phase histograms are flatter. This could be the result of lower coherence of the processes. Figure 5.1 show evolution of wavelet correlation on each scale across years. We can see that correlation has similar values for all the frequency bands are the follow rather similar time-pattern. The correlations, mainly on the highest frequency bands, undergone significant changes and, at least from 2010, they show decreasing correlations with minimum in 2013. This minimum is consistent with stability of the phase difference that is also lowest in 2013. These results are baffling, however possible explanation is that the global pricing mechanism that drives common changes in the series is becoming more stable and moves to lower frequencies and as a consequence leave less energy to higher frequencies. The level of the noise remains the same and even when the series are phase-locked on those frequencies, uncorrelated behavior increasingly dominates the observed relative phase.

In general, the results of CWT and correlations on FTSE 100 and DAX indicate that the two indexes are well phase synchronized and are then either in phase

or in a very small lag one behind the other without any indication which one could be the leader. This points in favor of the first hypotheses of this thesis, however there is no test suited to confirm it.

Year	10-20 minutes	Confidence interval	Shannon entropy	20-40 minutes	Confidence interval	Shannon entropy	40-80 minutes	Confidence interval	Shannon entropy
2008	-0.06	(-0.14, 0.02)	0.72	-0.04	(-0.14, 0.06)	0.70	-0.01	(-0.16, 0.13)	0.61
2009	-0.06	(-0.12, 0.00)	0.73	-0.05	(-0.13, 0.03)	0.72	0.01	(-0.11, 0.13)	0.67
2010	-0.01	(-0.08, 0.04)	0.78	-0.02	(-0.10, 0.05)	0.75	0.00	(-0.10, 0.11)	0.69
2011	-0.00	(-0.08, 0.07)	0.76	-0.02	(-0.13, 0.07)	0.71	-0.02	(-0.17, 0.12)	0.63
2012	0.00	(-0.05, 0.07)	0.76	0.00	(-0.08, 0.08)	0.67	0.03	(-0.10, 0.14)	0.65
2013	-0.01	(-0.08, 0.05)	0.72	-0.02	(-0.11, 0.06)	0.65	-0.02	(-0.16, 0.10)	0.61
2014	-0.01	(-0.08, 0.05)	0.71	-0.01	(-0.10, 0.08)	0.66	-0.01	(-0.14, 0.12)	0.59
2015	0.00	(-0.07, 0.07)	0.68	-0.01	(-0.10, 0.08)	0.64	-0.02	(-0.16, 0.12)	0.54

Year	80-160 minutes	Confidence interval	Shannon entropy	160-320 minutes	Confidence interval	Shannon entropy	320-640 minutes	Confidence interval	Shannon entropy
2008	0.01	(-0.19, 0.23)	0.59	0.02	(-0.27, 0.32)	0.54	0.02	(-0.39, 0.45)	0.44
2009	-0.00	(-0.17, 0.15)	0.62	0.02	(-0.21, 0.26)	0.58	-0.07	(-0.40, 0.26)	0.47
2010	-0.00	(-0.16, 0.15)	0.65	-0.02	(-0.24, 0.21)	0.58	0.01	(-0.29, 0.30)	0.54
2011	-0.03	(-0.26, 0.20)	0.58	0.01	(-0.29, 0.32)	0.51	-0.00	(-0.43, 0.44)	0.43
2012	0.03	(-0.14, 0.22)	0.53	0.02	(-0.23, 0.28)	0.49	0.02	(-0.33, 0.37)	0.45
2013	-0.05	(-0.24, 0.15)	0.50	-0.06	(-0.32, 0.21)	0.42	-0.07	(-0.40, 0.32)	0.39
2014	-0.07	(-0.27, 0.12)	0.51	0.01	(-0.27, 0.29)	0.46	-0.07	(-0.43, 0.27)	0.42
2015	-0.02	(-0.25, 0.19)	0.48	-0.01	(-0.33, 0.28)	0.41	-0.02	(-0.43, 0.39)	0.33

Table 5.1: Mean phases and Shannon Entropies over years, FTSE 100 and DAX

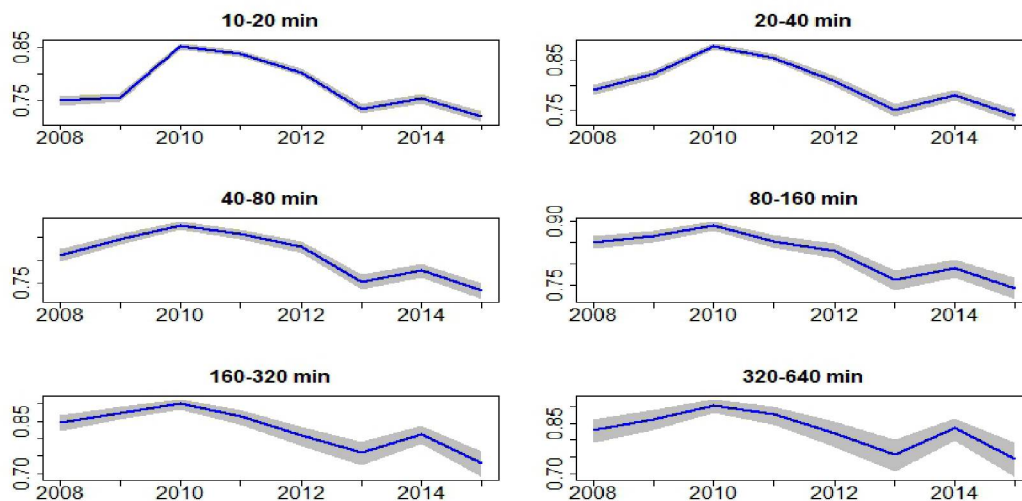


Figure 5.1: Evolution of MODWT correlation across scales of FTSE and DAX

5.1.2 PX

Figure A.3 show the results of the transform on Czech spot index prices PX and DAX. It is interesting to observe similar patterns in wavelet power as between FTSE 100 and DAX. But for example in the first four months of

2009 the areas appear larger on lower frequencies which might indicate higher common reaction to Global financial crisis at that time (*Blue Monday*). The coherence is however much lower. Warmer colors in lower frequencies are almost missing indicating, even though significant, relatively low degree of correlation on highest scales. Nevertheless the time evolution share similar pattern where the coherence even loses significance in majority of time periods.

The graphs of phase difference offer different picture. They imply that the phase difference is negative and PX is lagging behind DAX in earlier years of the observed period and mainly on higher frequencies while in latter we observe wider confidence intervals and higher uncertainty over the phase-difference. This is supported by graphs in figure A.4 and the results showed in table 5.2. On the highest frequency band (frequencies of 10 to 20 minutes standing for the finest information in the data) the mean of the phase is ranging between -0.78 and -0.46 with less negative values toward the end of the sample. With time also the significance falls and the phase difference become more scattered and in 2015 we cannot say on 5% significance level that that PX is still lagging behind DAX. The most volatile phase difference can be observed in 2013 (similarly for all bands) where even though the distribution is peaked and with negative mean resembles the distribution of random noises (Shannon entropy is only 0.16). Similar values we observe on next band where particularly in the first half of the subset CWT indicates highly significant non-zero values with normalized Shannon Entropy from 0.4 to 0.5. Phase difference remains marginally significant to the end of the sample but loses much of its stability (as can be seen on the shape of phase histograms in figure A.4. Identical pattern is present for band of scales from 40-80 minutes. On relatively lower frequencies the results point to a preferred value but with lower stability and mostly insignificantly non-zero values which imply lower phase-correlation and no significant lag of Prague behind Frankfurt. These patterns are supported by the correlation estimates (fig. 5.2). We can see that on high frequencies, the correlation is relatively lower. On band with frequencies of 10-20 minutes we observe correlations around 0.15 with its low of 0.05 in 2013, which corresponds to the almost-noise Shannon entropy. On lower frequencies the correlation increases, though the pattern in the values of Shannon entropy resembles the pattern in correlations. However, the observed correlations serve as contrast to results of Égert & Kočenda (2011) for time period 2003 to 2006, who calculated correlations on high frequency data from PX and DAX of 0.007 while 2 years later we see much higher values on scales shorter than one day.

Year	10-20 minutes	Confidence interval	Shannon entropy	20-40 minutes	Confidence interval	Shannon entropy	40-80 minutes	Confidence interval	Shannon entropy
2008	-0.78	(-1.11, -0.42)	0.28	-0.69	(-0.92, -0.45)	0.45	-0.41	(-0.66, -0.14)	0.40
2009	-0.56	(-0.87, -0.21)	0.26	-0.70	(-0.91, -0.49)	0.36	-0.52	(-0.73, -0.28)	0.39
2010	-0.62	(-0.89, -0.32)	0.29	-0.64	(-0.81, -0.47)	0.47	-0.50	(-0.69, -0.30)	0.43
2011	-0.78	(-1.17, -0.37)	0.27	-0.74	(-0.97, -0.48)	0.42	-0.47	(-0.73, -0.19)	0.40
2012	-0.59	(-0.93, -0.26)	0.28	-0.72	(-0.94, -0.50)	0.39	-0.47	(-0.71, -0.24)	0.38
2013	-0.70	(-1.11, -0.19)	0.16	-0.72	(-1.03, -0.38)	0.28	-0.39	(-0.77, -0.05)	0.24
2014	-0.58	(-0.96, -0.11)	0.16	-0.64	(-1.02, -0.21)	0.24	-0.44	(-0.78, -0.10)	0.27
2015	-0.46	(-0.94, -0.00)	0.21	-0.52	(-0.84, -0.20)	0.25	-0.37	(-0.70, -0.05)	0.26

Year	80-160 minutes	Confidence interval	Shannon entropy	160-320 minutes	Confidence interval	Shannon entropy	320-640 minutes	Confidence interval	Shannon entropy
2008	-0.27	(-0.55, 0.06)	0.41	-0.19	(-0.58, 0.23)	0.33	-0.04	(-0.59, 0.53)	0.28
2009	-0.36	(-0.59, -0.11)	0.40	-0.24	(-0.52, 0.05)	0.35	-0.19	(-0.64, 0.24)	0.29
2010	-0.28	(-0.52, -0.06)	0.42	-0.22	(-0.54, 0.09)	0.33	-0.22	(-0.60, 0.14)	0.31
2011	-0.24	(-0.62, 0.11)	0.35	-0.19	(-0.60, 0.23)	0.28	-0.06	(-0.66, 0.46)	0.26
2012	-0.36	(-0.65, -0.10)	0.41	-0.30	(-0.63, 0.04)	0.30	-0.13	(-0.64, 0.44)	0.24
2013	-0.24	(-0.67, 0.15)	0.25	-0.04	(-0.54, 0.39)	0.19	-0.24	(-0.78, 0.25)	0.18
2014	-0.33	(-0.75, 0.14)	0.26	-0.19	(-0.65, 0.24)	0.24	-0.15	(-0.66, 0.33)	0.24
2015	-0.35	(-0.72, 0.03)	0.26	-0.17	(-0.55, 0.22)	0.26	-0.09	(-0.73, 0.47)	0.22

Table 5.2: Phase differences with confidence intervals and entropies for PX and DAX

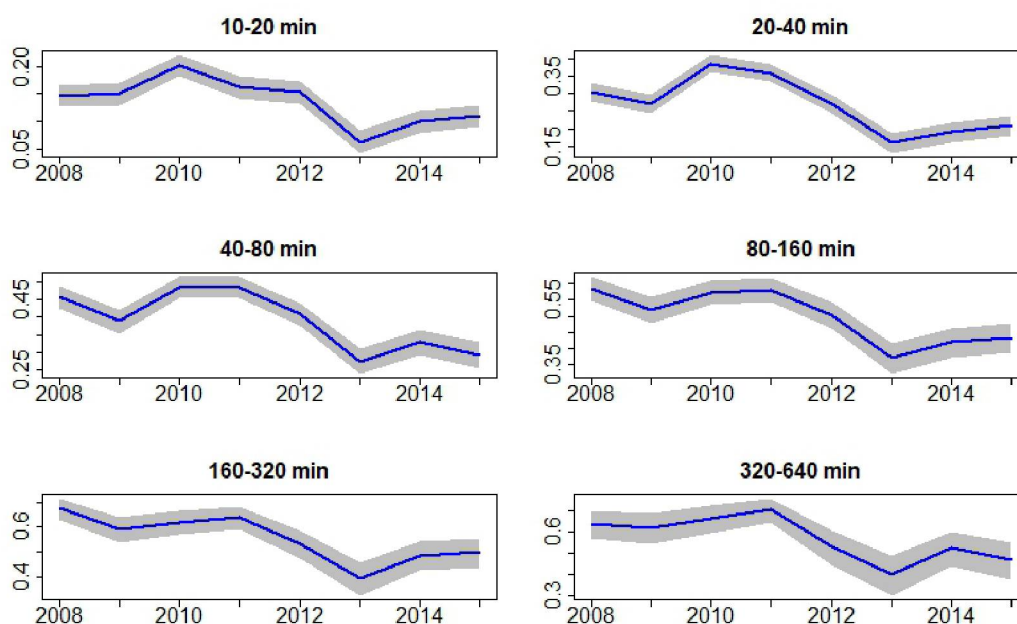


Figure 5.2: Evolution of MODWT correlation across scales of PX and DAX

Figure A.5 depict wavelet transformations of indexes PX and FTSE 100. Wavelet power confirms the occurrences of commonly highly volatile sessions between DAX, FTSE 100 and PX. We can see higher dispersion of power in 2013 and extremely high localized periods in 2011 and 2015 with wavelet cross-power over 100 (average for two white noise processes is 1 with 3 as upper bound of 95% confidence interval). Coherency patterns are highly similar to those be-

tween DAX and PX but show lower degree of coherence mainly in first half of 2011 and from 2013 onward. Phase difference plots indicate that PX lags also behind FTSE 100, mainly between 2008 and 2010. Figure A.6 brings evidence that the phase difference is more unstable than with DAX. This is visible both on the line plots (we can see shorter periods of stability and more periods where the synchronization is not visible) and on the values of Shannon entropy (table 5.3). On highest frequencies the average lag becomes insignificant on 5% level in 2014 and on scales between 40 and 80 minutes it is not significant since 2013. Relatively lower frequencies indicate lower level of phase-lock. The values are insignificantly negative (with several exceptions on scale around 2 hours) and the Shannon Entropy approaches values of random noise. Histogram and line plot for band 64-128 (320 to 640 minutes, around 1 trading day) in figure A.6 (h) show that the preference of 0 among the values is very weak and in many periods it escapes to the edges of the cycle. Surprising are the estimates for correlations (figure 5.3), that are almost identical to those with DAX (only they drop sooner on some bands).

These results are partly in favor of the second thesis hypotheses. We do observe the phase lag of Prague behind developed stock markets on highest frequencies, but while on some frequencies we see significant lag throughout the observed periods, on some of the investigated frequencies the phase differences become statistically insignificantly different from zero.

Nonetheless, due to the lower stability of observed phase differences, we cannot reject the hypotheses that PX tends to lag less throughout the years. For example on the 10-20 minute band the values of mean phase difference are closer to 0 in 2014 and 2015, however as the uncertainty regions expand the true value might be even largely negative than in previous years².

5.1.3 BUX

We continue with comparing BUX with FTSE 100 and DAX. Graphical representation of the continuous wavelet analysis is depicted in figures A.7 and 5.5, respectively. The cross power with both resembles the plots of PX, though the peaks have lower values (for DAX in the whole sample and FTSE 100 in second part of the data set). This observation has impacted the coherency plots. Significant areas are scarcer, even more from 2013 when the mutual coherence values are extremely low. Phase plots seem less stable and the patterns are

²we we need non-overlapping confidence intervals to be able to claim observed difference

Year	10-20 minutes	Confidence interval	Shannon entropy	20-40 minutes	Confidence interval	Shannon entropy	40-80 minutes	Confidence interval	Shannon entropy
2008	-0.64	(-0.92, -0.28)	0.28	-0.64	(-0.88, -0.40)	0.41	-0.43	(-0.67, -0.15)	0.40
2009	-0.51	(-0.82, -0.20)	0.30	-0.66	(-0.86, -0.44)	0.35	-0.55	(-0.78, -0.29)	0.38
2010	-0.63	(-0.91, -0.32)	0.32	-0.63	(-0.79, -0.46)	0.45	-0.50	(-0.70, -0.31)	0.40
2011	-0.66	(-1.09, -0.23)	0.27	-0.67	(-0.92, -0.39)	0.38	-0.47	(-0.74, -0.18)	0.38
2012	-0.55	(-0.90, -0.23)	0.28	-0.78	(-0.99, -0.54)	0.37	-0.51	(-0.76, -0.29)	0.35
2013	-0.54	(-1.04, -0.05)	0.17	-0.71	(-1.10, -0.26)	0.22	-0.39	(-0.81, 0.02)	0.21
2014	-0.47	(-0.97, 0.14)	0.16	-0.55	(-0.96, -0.08)	0.22	-0.36	(-0.79, 0.02)	0.25
2015	-0.34	(-0.81, 0.14)	0.17	-0.47	(-0.85, -0.10)	0.23	-0.33	(-0.73, 0.08)	0.24

Year	80-160 minutes	Confidence interval	Shannon entropy	160-320 minutes	Confidence interval	Shannon entropy	320-640 minutes	Confidence interval	Shannon entropy
2008	-0.32	(-0.60, 0.03)	0.38	-0.27	(-0.63, 0.15)	0.31	-0.13	(-0.66, 0.40)	0.26
2009	-0.38	(-0.62, -0.09)	0.36	-0.27	(-0.58, 0.03)	0.35	-0.10	(-0.58, 0.31)	0.25
2010	-0.27	(-0.51, -0.03)	0.44	-0.24	(-0.54, 0.06)	0.37	-0.28	(-0.64, 0.09)	0.30
2011	-0.26	(-0.64, 0.12)	0.30	-0.22	(-0.61, 0.20)	0.29	-0.04	(-0.58, 0.48)	0.30
2012	-0.43	(-0.73, -0.17)	0.38	-0.40	(-0.77, 0.03)	0.28	-0.11	(-0.69, 0.43)	0.24
2013	-0.30	(-0.69, 0.13)	0.22	-0.06	(-0.59, 0.39)	0.18	-0.18	(-0.76, 0.30)	0.17
2014	-0.23	(-0.74, 0.29)	0.23	-0.17	(-0.72, 0.32)	0.22	-0.12	(-0.63, 0.31)	0.22
2015	-0.28	(-0.69, 0.15)	0.24	-0.23	(-0.66, 0.22)	0.22	0.11	(-0.56, 0.78)	0.16

Table 5.3: Mean phases and Shannon Entropies over years, PX and FTSE 100

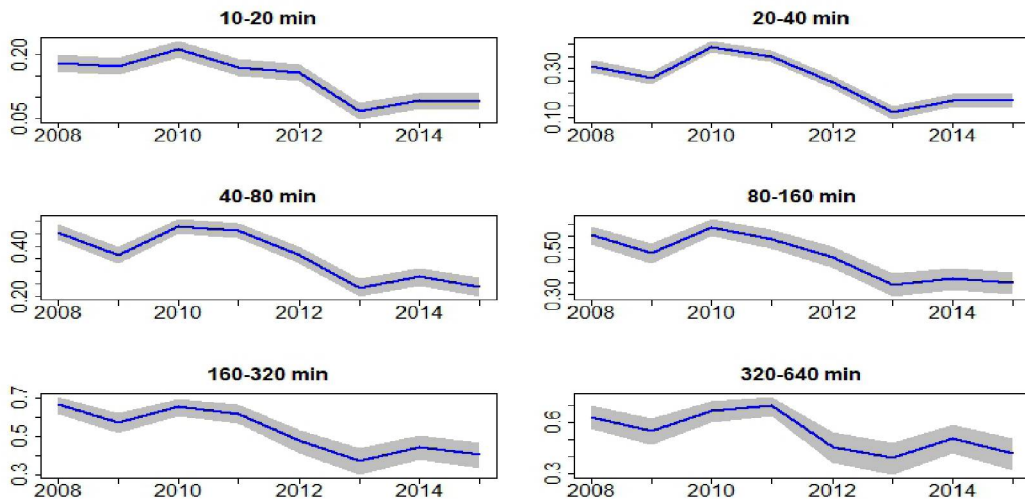


Figure 5.3: Evolution of MODWT correlation over years of PX and FTSE 100

observable on frequencies between 20 and 80 minutes. We can see in tables 5.4 and 5.5 and figures A.9 and A.10 that on relatively lower frequencies we find no significant lag of BUX after either of developed indexes. Conversely, until 2013, on the highest frequencies the lag is significant and, apart from 2008, quite stable. Both the stability and the size of the lag is higher between BUX and DAX than FTSE 100. However on the highest frequency, the Shannon entropies become very low in the second part of the data set (and for 2008) and in case of FTSE 100, the relative phases are not different from random noise on 10-20 minute band. Going through the line plots, it is easy to see that there appear to be no preferred value on the highest frequency band. It

is supported by the wavelet coherency, which approaches zero in these years. The results in terms of the hypotheses are a bit different than in the case of PX. Hungarian index seems to follow both DAX and FTSE in certain years, however the stability is low not only from 2013 but also in 2008. The relationship perishes for highest frequencies and the behavior becomes unrecognizable from random. There is no straight-forward explanation for that. It seems that the pricing mechanism may remain common for parts of the information stored in the prices, but below 20 minute horizon there seems to be no information transmission and loses stability on all high frequencies.

Year	10-20 minutes	Confidence interval	Shannon entropy	20-40 minutes	Confidence interval	Shannon entropy	40-80 minutes	Confidence interval	Shannon entropy
2008	-0.79	(-1.29, -0.17)	0.20	-0.62	(-0.99, -0.24)	0.30	-0.45	(-0.81, -0.04)	0.29
2009	-0.50	(-0.77, -0.25)	0.31	-0.50	(-0.71, -0.32)	0.39	-0.34	(-0.58, -0.13)	0.39
2010	-0.44	(-0.68, -0.19)	0.39	-0.40	(-0.57, -0.21)	0.45	-0.26	(-0.46, -0.02)	0.42
2011	-0.45	(-0.77, -0.10)	0.34	-0.47	(-0.71, -0.18)	0.42	-0.34	(-0.63, -0.04)	0.41
2012	-0.33	(-0.65, -0.01)	0.22	-0.40	(-0.66, -0.17)	0.30	-0.33	(-0.62, -0.05)	0.37
2013	-0.40	(-0.83, 0.13)	0.15	-0.63	(-1.04, -0.14)	0.24	-0.38	(-0.89, 0.13)	0.21
2014	-0.47	(-0.98, 0.04)	0.14	-0.57	(-0.96, -0.20)	0.24	-0.53	(-0.90, -0.06)	0.23
2015	-0.55	(-1.11, 0.13)	0.15	-0.65	(-1.03, -0.21)	0.19	-0.57	(-0.92, -0.14)	0.24

Year	80-160 minutes	Confidence interval	Shannon entropy	160-320 minutes	Confidence interval	Shannon entropy	320-640 minutes	Confidence interval	Shannon entropy
2008	-0.32	(-0.67, 0.01)	0.35	-0.12	(-0.60, 0.30)	0.34	-0.10	(-0.69, 0.48)	0.27
2009	-0.29	(-0.55, -0.00)	0.38	-0.12	(-0.47, 0.21)	0.29	-0.14	(-0.63, 0.34)	0.30
2010	-0.21	(-0.48, 0.06)	0.39	-0.08	(-0.44, 0.28)	0.31	-0.13	(-0.58, 0.30)	0.30
2011	-0.21	(-0.60, 0.17)	0.34	-0.14	(-0.59, 0.29)	0.27	0.00	(-0.61, 0.59)	0.26
2012	-0.34	(-0.64, 0.00)	0.33	-0.07	(-0.52, 0.38)	0.23	-0.03	(-0.57, 0.56)	0.20
2013	-0.24	(-0.69, 0.20)	0.19	0.01	(-0.56, 0.55)	0.15	-0.01	(-0.75, 0.64)	0.14
2014	-0.26	(-0.72, 0.23)	0.20	-0.16	(-0.67, 0.34)	0.16	0.12	(-0.55, 0.86)	0.17
2015	-0.29	(-0.80, 0.20)	0.27	-0.23	(-0.81, 0.32)	0.21	-0.04	(-0.72, 0.61)	0.23

Table 5.4: Mean phases and Shannon Entropies over years, BUX and DAX

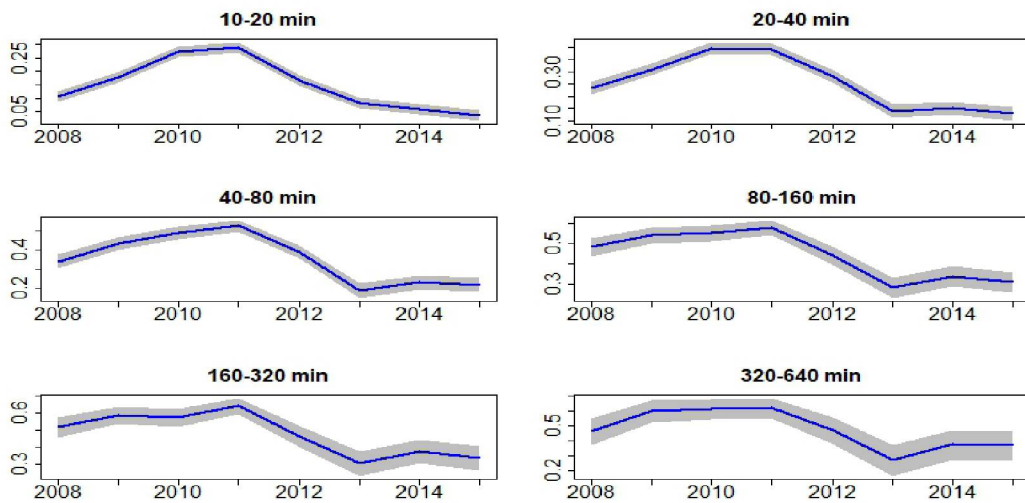


Figure 5.4: Evolution of MODWT correlation across scales of BUX and DAX

Year	10-20 minutes	Confidence interval	Shannon entropy	20-40 minutes	Confidence interval	Shannon entropy	40-80 minutes	Confidence interval	Shannon entropy
2008	-0.60	(-1.13, 0.02)	0.16	-0.56	(-0.96, -0.16)	0.27	-0.39	(-0.77, 0.02)	0.29
2009	-0.40	(-0.68, -0.12)	0.34	-0.42	(-0.65, -0.23)	0.43	-0.32	(-0.60, -0.10)	0.38
2010	-0.47	(-0.73, -0.23)	0.37	-0.40	(-0.55, -0.21)	0.43	-0.28	(-0.52, -0.03)	0.39
2011	-0.45	(-0.78, -0.05)	0.29	-0.45	(-0.68, -0.17)	0.36	-0.29	(-0.59, 0.02)	0.37
2012	-0.38	(-0.70, 0.01)	0.22	-0.42	(-0.66, -0.13)	0.29	-0.41	(-0.68, -0.10)	0.33
2013	-0.31	(-0.83, 0.32)	0.11	-0.51	(-0.96, -0.05)	0.20	-0.26	(-0.77, 0.21)	0.19
2014	-0.32	(-0.91, 0.29)	0.12	-0.61	(-0.98, -0.12)	0.20	-0.45	(-0.95, 0.13)	0.16
2015	-0.58	(-1.15, 0.03)	0.13	-0.65	(-1.04, -0.15)	0.16	-0.54	(-1.00, 0.03)	0.19

Year	80-160 minutes	Confidence interval	Shannon entropy	160-320 minutes	Confidence interval	Shannon entropy	320-640 minutes	Confidence interval	Shannon entropy
2008	-0.31	(-0.67, 0.07)	0.34	-0.19	(-0.64, 0.23)	0.30	-0.15	(-0.71, 0.39)	0.26
2009	-0.25	(-0.55, 0.07)	0.39	-0.13	(-0.50, 0.26)	0.28	-0.04	(-0.55, 0.42)	0.27
2010	-0.20	(-0.50, 0.11)	0.38	-0.03	(-0.39, 0.36)	0.28	-0.21	(-0.63, 0.24)	0.28
2011	-0.16	(-0.57, 0.23)	0.29	-0.18	(-0.61, 0.25)	0.28	0.00	(-0.63, 0.66)	0.19
2012	-0.39	(-0.74, -0.02)	0.29	-0.07	(-0.60, 0.42)	0.24	-0.06	(-0.69, 0.52)	0.22
2013	-0.16	(-0.62, 0.34)	0.19	-0.05	(-0.62, 0.54)	0.16	0.00	(-0.79, 0.70)	0.15
2014	-0.17	(-0.68, 0.29)	0.20	-0.12	(-0.65, 0.38)	0.16	0.05	(-0.64, 0.82)	0.15
2015	-0.26	(-0.76, 0.23)	0.16	-0.19	(-0.78, 0.36)	0.19	-0.00	(-0.72, 0.60)	0.19

Table 5.5: Mean phases and Shannon Entropies over years, BUX and FTSE 100

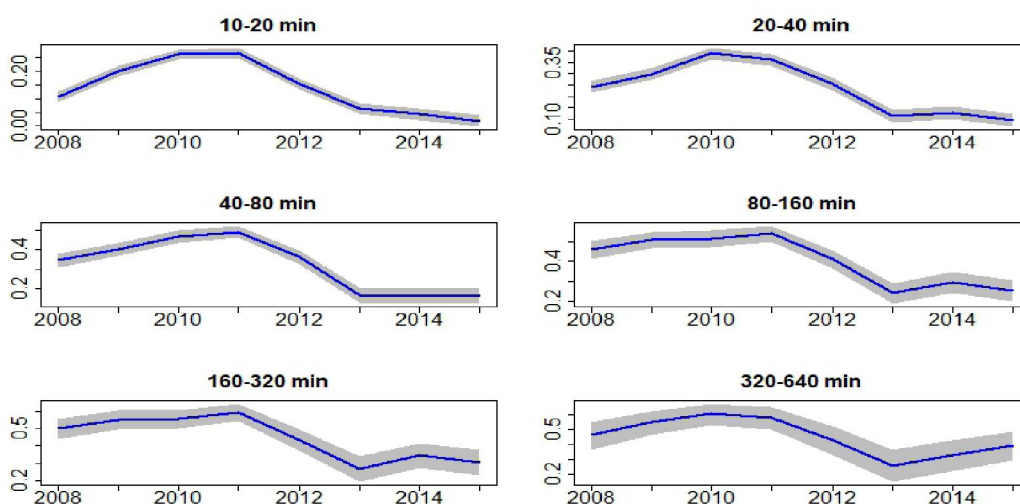


Figure 5.5: Evolution of MODWT correlation across scales of BUX and FTSE

5.1.4 WIG

Finally, we examine index WIG. Figure A.11 shows CWT with DAX, figure A.12 shows analysis with FTSE 100. We can observe similar pattern as with PX, however peaks of common power have lower absolute values and are spread more even over the years. Wavelet coherence analysis show quite stable regions of comovement on frequencies below 80 minutes with warmer tones in 2009 and 2010 and more localized but higher coherency on lower frequencies. Similar break is visible on phase difference plot with lag on frequencies up to 80 minutes and changing behavior on lower ones. Wavelet correlation sheds some

light into the time-pattern, with on average highest correlations in years 2010 and 2011 (peak), but the differences are significant only in certain scale-time combinations (see figure 5.6).

Tables 5.6 and 5.7 with figures A.13 and A.14 provide scale-by scale time inspection of the relative phases. We can see that lag is quite small but significant in horizons of 10-20 minutes and 20-40 minutes, with highest stability in 2009. Highest frequency band very stable relationship particularly with DAX. However we do not see any strong changes in the strength of the lag itself. Surprising is that the entropy is highest in 2011 even when the correlation falls. On the horizon around half an hour it is stable for both pairs. On frequencies of up to 5 hours, they appear to be almost in phase, with stronger stability on the continent, mainly in 2011.

Year	10-20 minutes	Confidence interval	Shannon entropy	20-40 minutes	Confidence interval	Shannon entropy	40-80 minutes	Confidence interval	Shannon entropy
2008	-0.46	(-0.73, -0.16)	0.35	-0.38	(-0.57, -0.19)	0.46	-0.21	(-0.44, 0.01)	0.48
2009	-0.38	(-0.54, -0.22)	0.44	-0.31	(-0.44, -0.19)	0.50	-0.08	(-0.28, 0.10)	0.50
2010	-0.30	(-0.47, -0.13)	0.43	-0.27	(-0.39, -0.13)	0.51	-0.16	(-0.33, 0.03)	0.50
2011	-0.38	(-0.57, -0.23)	0.46	-0.30	(-0.45, -0.15)	0.50	-0.16	(-0.34, 0.00)	0.50
Year	80-160 minutes	Confidence interval	Shannon entropy	160-320 minutes	Confidence interval	Shannon entropy	320-640 minutes	Confidence interval	Shannon entropy
2008	-0.11	(-0.41, 0.17)	0.43	0.01	(-0.37, 0.39)	0.36	-0.12	(-0.69, 0.48)	0.27
2009	-0.05	(-0.28, 0.15)	0.44	-0.01	(-0.37, 0.33)	0.38	-0.04	(-0.48, 0.37)	0.29
2010	-0.09	(-0.32, 0.15)	0.45	-0.08	(-0.38, 0.20)	0.40	-0.08	(-0.48, 0.28)	0.34
2011	-0.05	(-0.29, 0.18)	0.53	-0.08	(-0.39, 0.20)	0.40	-0.07	(-0.56, 0.42)	0.31

Table 5.6: Mean phases and Shannon Entropies over years, WIG and DAX

Year	10-20 minutes	Confidence interval	Shannon entropy	20-40 minutes	Confidence interval	Shannon entropy	40-80 minutes	Confidence interval	Shannon entropy
2008	-0.37	(-0.59, -0.13)	0.39	-0.33	(-0.52, -0.12)	0.50	-0.22	(-0.44, 0.01)	0.47
2009	-0.29	(-0.46, -0.13)	0.43	-0.27	(-0.41, -0.15)	0.53	-0.10	(-0.32, 0.09)	0.45
2010	-0.27	(-0.47, -0.10)	0.41	-0.24	(-0.37, -0.10)	0.50	-0.17	(-0.35, 0.01)	0.48
2011	-0.50	(-0.71, -0.25)	0.35	-0.34	(-0.50, -0.19)	0.48	-0.14	(-0.34, 0.04)	0.47
Year	80-160 minutes	Confidence interval	Shannon entropy	160-320 minutes	Confidence interval	Shannon entropy	320-640 minutes	Confidence interval	Shannon entropy
2008	-0.14	(-0.44, 0.15)	0.37	-0.01	(-0.42, 0.35)	0.31	-0.18	(-0.73, 0.40)	0.25
2009	-0.09	(-0.33, 0.14)	0.42	-0.02	(-0.37, 0.30)	0.40	0.01	(-0.40, 0.43)	0.33
2010	-0.11	(-0.37, 0.12)	0.43	-0.01	(-0.31, 0.28)	0.41	-0.11	(-0.51, 0.28)	0.31
2011	-0.13	(-0.39, 0.16)	0.44	-0.15	(-0.48, 0.19)	0.35	-0.04	(-0.60, 0.43)	0.31

Table 5.7: Mean phases and Shannon Entropies over years, WIG and FTSE 100

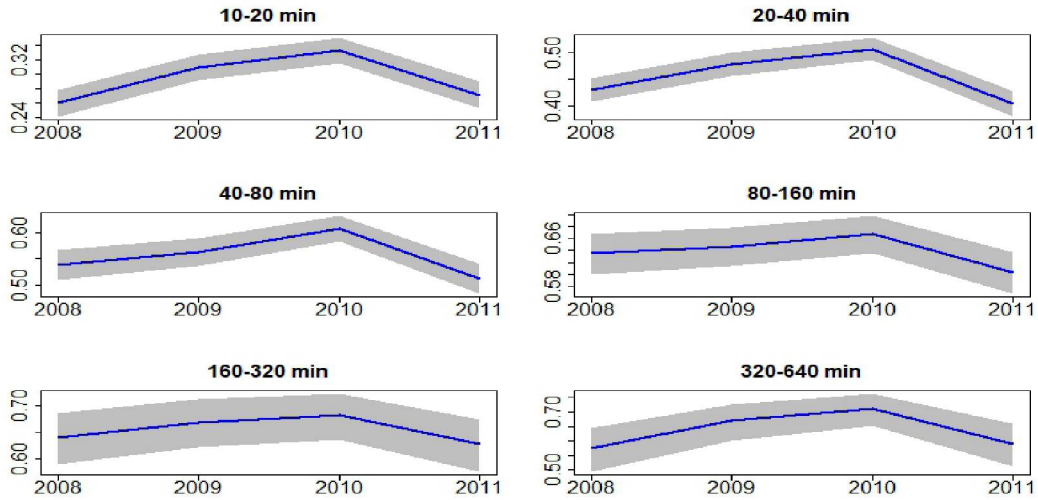


Figure 5.6: Evolution of MODWT correlation across scales between WIG and DAX (six figures on left) and FTSE 100 (six on right)

5.2 Granger causality

First, Granger causalities of the non-decomposed indexes were examined. Table 5.8 shows the Granger causality results. The arrows show the direction of the causality, with right arrow (\implies) indicating that index on the left Granger-causes index on the top and \iff indicates bidirectional causality (indexes significantly influence each other).

We can see that overall that the interaction between the series has lowered between the year 2008 and 2015, which is consistent with the decreasing wavelet correlations. However it is interesting to point out that DAX Granger caused FTSE 100 in 2008³, and both of these indices tend to influence the ones considered less developed. Interesting difference is that DAX and PX used to have bidirectional relationship and it changed to one-directional in 2015. For the rest, the relationships remained the same (FTSE and DAX cause WIG and BUX). Regarding the interactions between the less developed ones (to which this thesis gives lower level of interest) there is a full level of bidirectional causality. It indicates either that the indices are not subject to separate pricing mechanisms and interact with each other on general level or that they are strongly influenced by the same third factor (e.g. DAX index).

Second, all the indices were decomposed using maximum-overlap discrete wavelet transform onto 6 detailed series and trend series. The detail series are thus constructed to contain information that has scales (horizon) of up to 640 minutes

³it is important to note that the p-value for the direction FTSE 100 \implies DAX was 0.066 but we choose not to reject no influence

2008	FTSE 100	DAX	PX	WIG	BUX	2015 ¹	FTSE 100	DAX	PX	WIG	BUX
FTSE 100	—	⇐	⇔	⇐	⇒	FTSE 100	—	None*	⇒*	⇒	⇒
DAX	⇒	—	⇔	⇒	⇒	DAX	None*	—	⇒*	⇒	⇒
PX	⇔	⇔	—	⇔	⇔	PX	⇐*	⇐*	—	⇔	⇔
WIG	⇐	⇐	⇔	—	⇐	WIG	⇐	⇐	⇔	—	⇔
BUX	⇐	⇐	⇔	⇔	—	BUX	⇐	⇐	⇔	⇔	—

¹ 2011 for WIG, ⇒ left cause top, ⇐ top cause left, ⇔ bidirectional causality, * causality changed

Table 5.8: Granger causality of the original series

(roughly corresponding to 2 days). However one of the implications of MODWT redundancy is that the scales (frequencies) are not perfectly separated. Figure 5.7 shows the transformation for DAX in 2008 for January. We can see the nice alignment of the decomposed series and the original one (one on the top, d1 to d6 correspond to detail series and s6 to 6th level of scaling coefficient). Note that most of the variance is present on higher frequencies.

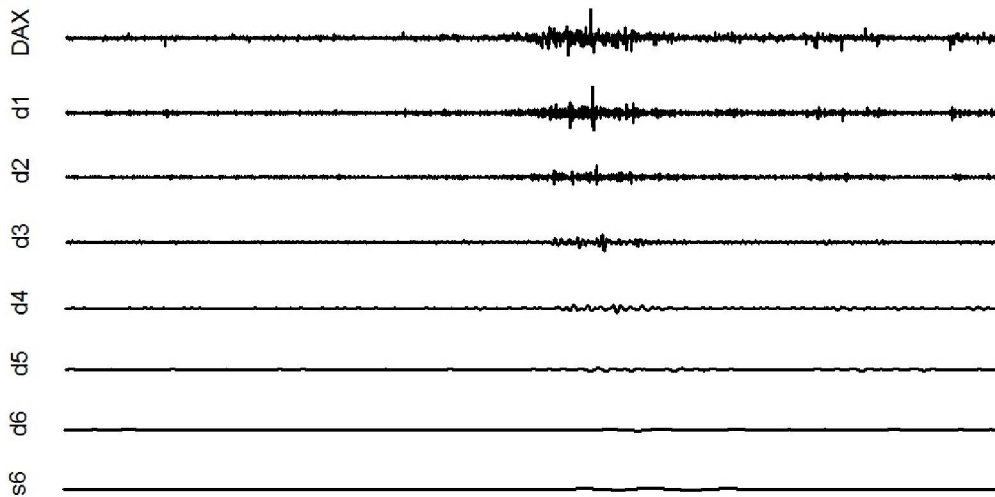


Figure 5.7: MODWT of DAX in January 2008, top series is the original

Table 5.9 displays Granger-causalities of the investigated indexed by their decomposed sub-parts. Results for pair FTSE-DAX are surprising - even though the relationship seemed one-directional without decomposition, apart from 20-40 minute scale they exhibit bidirectional causality. This might be partially caused by the fact that for the raw series, only 1 lag was selected by the criterion, however various larger lags are selected for the decomposed series. Results of the causality are in line with the phase-results - in 2008 the series influence each other and as the phase-differences become more unstable in 2015 also the Granger-causalities perish (at least on the highest frequencies). However, the lack of linear causality does not imply some degree of phase synchronization since it does not address entirely same question.

Index-pair	FTSE — DAX		Index-pair	FTSE — PX		DAX — PX	
Year	2008	2015	Year	2008	2015	2008	2015
Detail level			Detail level				
1	\Leftrightarrow	None*	1	\Rightarrow	\Rightarrow	\Leftrightarrow	\Rightarrow^*
2	None	None	2	\Rightarrow	\Rightarrow	\Rightarrow	\Rightarrow
3	\Leftrightarrow	None*	3	\Leftrightarrow	\Leftrightarrow	\Leftrightarrow	\Leftrightarrow
4	\Leftrightarrow	\Rightarrow^*	4	\Leftrightarrow	\Leftrightarrow	\Leftrightarrow	\Leftrightarrow
5	\Leftrightarrow	\Rightarrow^*	5	\Leftrightarrow	\Leftrightarrow	\Leftrightarrow	\Leftrightarrow
6	\Leftrightarrow	\Leftrightarrow	6	\Leftrightarrow	\Leftrightarrow	\Leftrightarrow	\Rightarrow^*

Index-pair	FTSE — BUX		DAX — BUX		Index-pair	FTSE — WIG		FTSE — WIG	
Year	2008	2015	2008	2015	Year	2008	2015	2008	2015
Detail level					Detail level				
1	\Rightarrow	\Rightarrow	\Rightarrow	\Rightarrow	1	\Rightarrow	\Rightarrow	\Rightarrow	\Leftrightarrow^*
2	\Rightarrow	\Rightarrow	\Rightarrow	\Rightarrow	2	\Rightarrow	\Rightarrow	\Rightarrow	\Rightarrow
3	\Rightarrow	\Rightarrow	\Leftrightarrow	\Rightarrow^*	3	\Rightarrow	\Rightarrow	\Rightarrow	\Leftrightarrow^*
4	\Rightarrow	\Rightarrow	\Rightarrow	\Rightarrow	4	\Leftrightarrow	\Rightarrow^*	\Leftrightarrow	\Leftrightarrow
5	\Rightarrow	\Leftrightarrow^*	\Rightarrow	\Leftrightarrow^*	5	\Leftrightarrow	\Leftrightarrow	\Leftrightarrow	\Leftrightarrow
6	\Leftrightarrow	\Leftrightarrow	\Rightarrow	\Leftrightarrow^*	6	\Leftrightarrow	\Leftrightarrow	\Leftrightarrow	\Leftrightarrow

\Rightarrow left cause right, \Leftarrow right cause left, \Leftrightarrow bidirectional causality, * causality changed

Table 5.9: Granger causality of transformed indexes

In general we observe uni-directional causalities on highest frequencies from developed to developing markets, on lower the dynamics are more diverse. It always holds that developed markets Granger-cause developing (on 95% significance level) although, in many cases, the relationship is bidirectional. This result is however not contradictory to the observed phase-differences. Mostly, bidirectionality is added in the latter period, with exception of DAX-PX on detail 1 and 6 and for DAX-BUX on detail level 3 and WIG-FTSE on detail 4. Bidirectional relationship implies increased expectation of non-significant phase-difference, however it does not have to be the case. In presence of semi-periodic components and with low restriction on size of maximal lag in VAR model⁴, different dynamics can be uncovered.

Results do however suggest possibility of larger-than-expected interactions between Western indexes and Eastern ones.⁵ The other explanation could be that presence of general pricing mechanism to which both are subject affects indexes in different manner and both developed and developing markets can react to different types of information with changing speed.

⁴Model selected optimal lag with maximum set to 50

⁵On the other hand, significant causality does not say anything about the importance of the causality. The effects can still be negligible for any kind of real use (e.g. predictions)

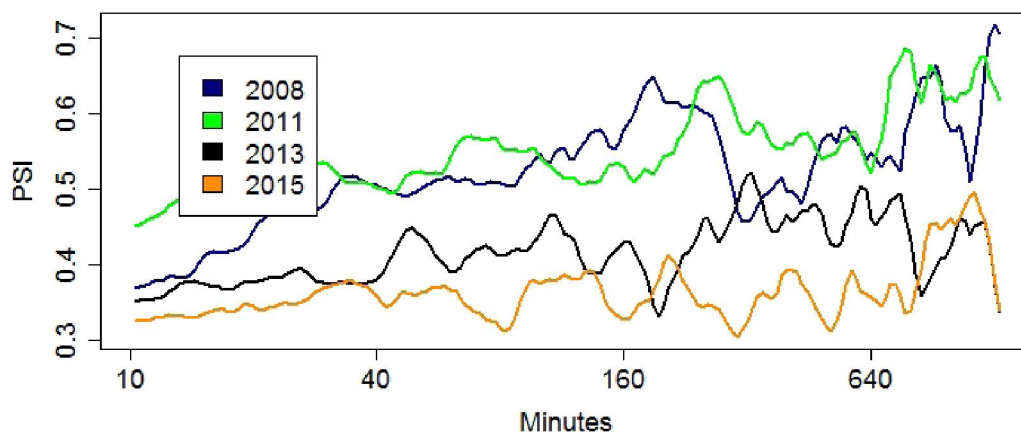


Figure 5.8: Time-evolution of Phase synchronization index of FTSE100 and DAX

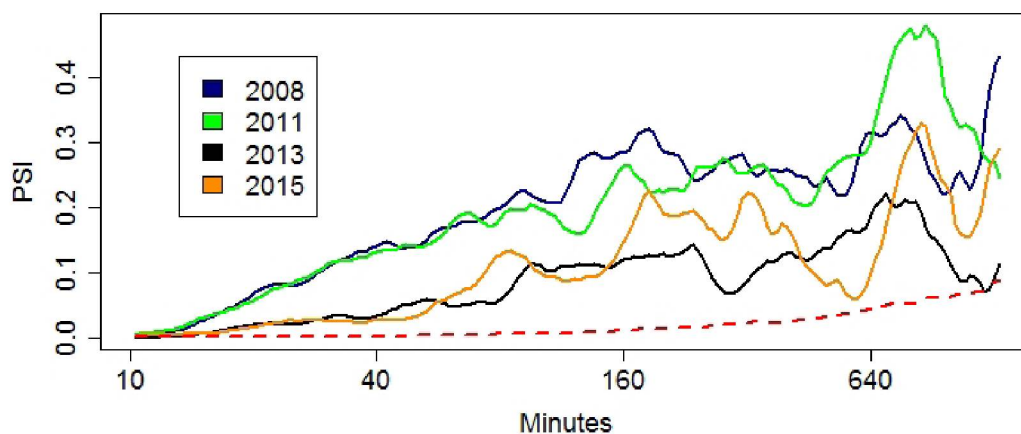


Figure 5.9: Time-evolution of Phase synchronization index of PX and DAX
Red dashed line denotes 95th quantile of Red Noise pairs' PSI

5.3 Non-smoothed phase synchronization

Final part of our examination focused on measuring the stability of the phase synchronicity without any upfront smoothing with the PSI (figures 5.8, 5.9, 5.10, 5.11, 5.12, 5.13 and 5.14). The lines represent years 2008, 2011, 2013 and 2015 (2008, 2009, 2010 and 2011 for WIG) to capture the evolution of the phase synchronization index over time.

We can see that DAX and FTSE 100 exhibit quite high values over all of the measured frequencies, while the developed-developing pairs show much lower values. The common observed pattern is the formation of 2 clusters (for WIG for all years between 2008 and 2011 form 1 cluster), before 2012 and after

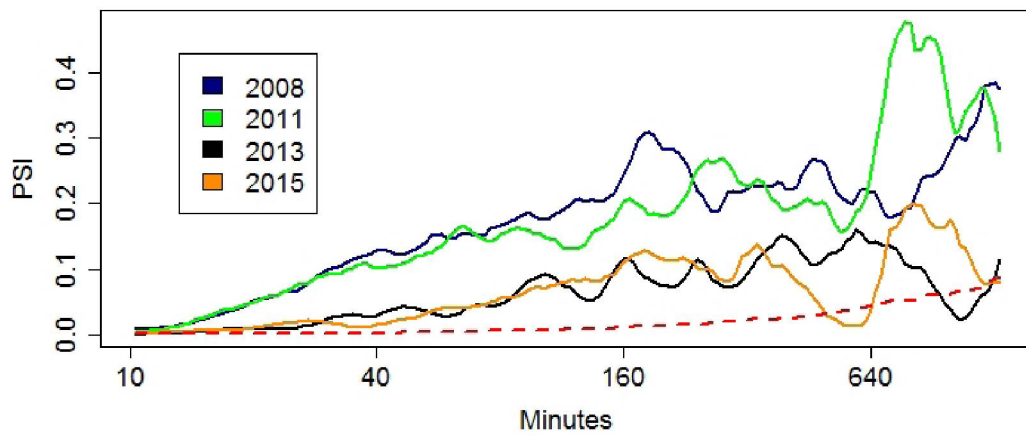


Figure 5.10: Time-evolution of Phase synchronization index of PX and FTSE100

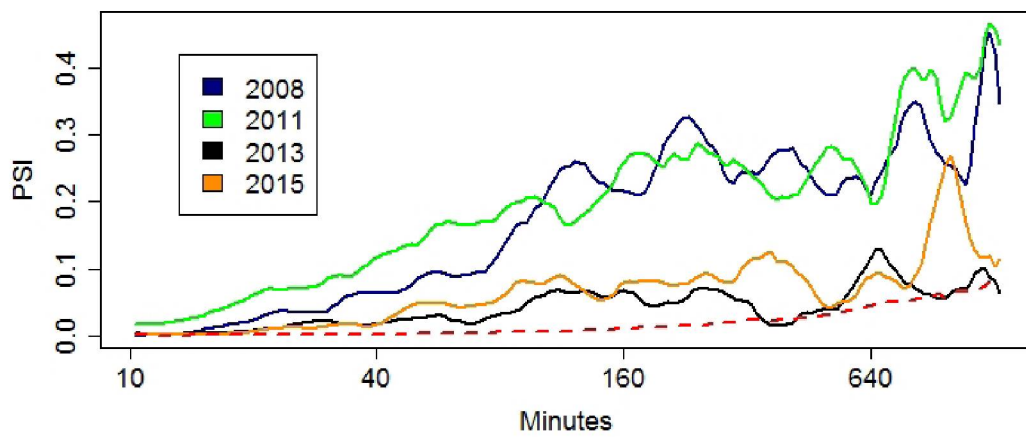


Figure 5.11: Time-evolution of Phase synchronization index of BUX and DAX

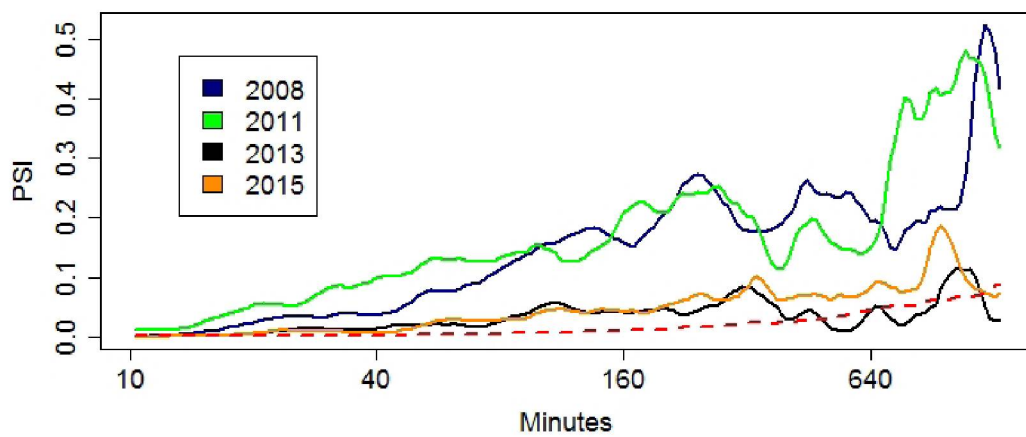


Figure 5.12: Time-evolution of Phase synchronization index of BUX and FTSE100

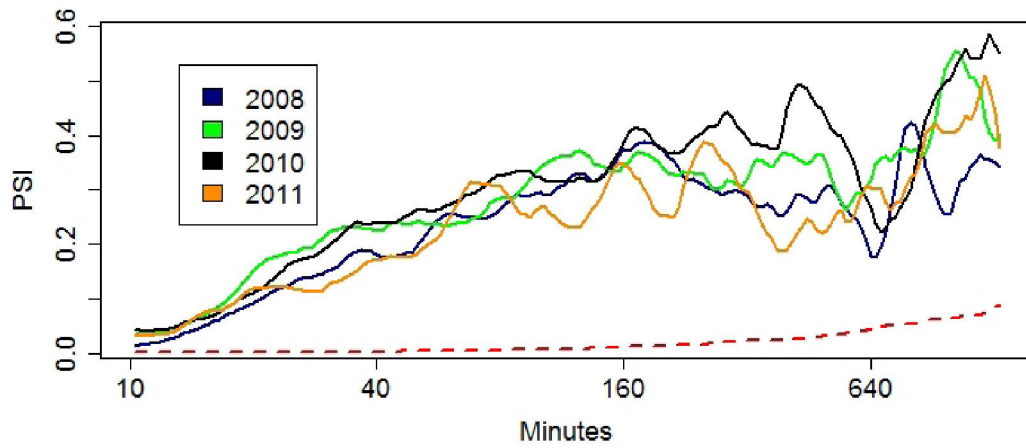


Figure 5.13: Time-evolution of Phase synchronization index of WIG and DAX

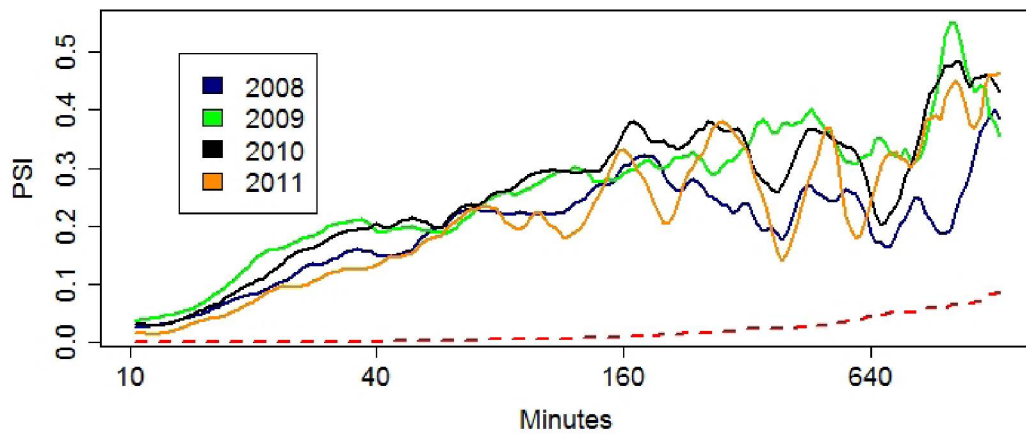


Figure 5.14: Time-evolution of Phase synchronization index of WIG and FTSE100

that - we observe lowering phase synchronization index in the second period. While for PX and both DAX and FTSE we see equal or marginally higher synchronization for 2008 in contrast to 2011 on the highest frequencies (which favors the hypotheses of this thesis), for BUX, at least on the frequencies below 80 minutes, we see the highest-synchronization in 2011. One explanation for this might be that BUX did not react as much to global pricing mechanisms in the beginning of the observed sample, but caught up in the second part of the sample. Interesting are also the values for WIG, they seem to be the largest of all developed-developing pairs, unfortunately there is no straightforward explanation for that.

These results (and mainly the comparisons) have to be considered with caution. We do not have any statistical approach show that the differences are significantly different from each other. On the other hand, it provides another confirmation of the overall results as they are in line with both lower stability of the phase-plots (and thus Shannon entropies) and wider confidence intervals for the mean phases.

Chapter 6

Conclusion

In this thesis, we have built upon existing approaches to investigate time-scale dependencies and phase-relationship patterns using methods of wavelet analysis, not common in economic literature. Center point of the work is the discovery of a suitable method that can work with extremely noisy data such as high-frequency price development patterns. The challenge was both to correctly specify and demonstrate relevance of our approach. Continuous wavelet transform and smoothed phase analysis can depend significantly on the smoothing window that is used, and while in the frequency domain there is natural value for its length, contemporary Economic research uses rather arbitrarily chosen window lengths¹ (e.g. Roesch *et al.* (2014)). We show that with moderately large window (in comparison to the length of the time-series) we are able to uncover information well masked under the random noise. This property comes at a price - it is possibly subject to the variance-bias trade-off which should be investigated on more rigorous basis, possibly with standalone research.

To support our research with a measure of statistical significance, apart from investigation of noisy periodic signals and real series, we have compared our results with various types of random noise (white noise, red noise (AR(1)) or 'Fourier' noise²). This serves as a common benchmark for significance of Shannon entropy test (see e.g. Cazelles & Stone (2003)) or for wavelet cross-power or coherence. However assumption of full randomness between time-series in our data might not be strict enough, and since significance of phase difference cannot be approached analytically, we also add another measure employed by Hanus & Vácha (2018). The underlying assumption is that when

¹Or they do not provide deeper explanation for the chosen filter length

²Random series that maintains basic spectral relationships of the investigated data

two series have consistent phase differences, adding further noise would not weaken this relationship, however when the observed value is only random, we would observe 'diverging' phase difference pattern (and thus large confidence intervals). In chapter 4 we show that the method correctly identifies significant phase differences in artificial signals only on frequency bands on which those difference were put in data-generating process. To provide wider picture in the results, we contrast CWT with MODWT approach to measure linear Granger causality on data decomposed on approximately equivalent bands.

We find, in accordance with the first thesis hypotheses, that there is no significant phase difference between UK's FTSE100 and DAX indexes. We are not aware of any test that rejects non-synchronization of the phase-differences, however the measures we employ point to very close synchronization of the two indexes throughout the period on frequencies at least up to daily (on highest frequencies, the 95% confidence intervals are wide only one 45th of the period). Additionally, the level of stability is much larger than with any other investigated pair (supported by the highest wavelet correlation coefficient). However decreasing correlation and Granger-causality points to disappearing of linear influences in most recent year.

We observe highly significant lag of all PX, BUX and WIG behind both FTSE100 and DAX on the highest frequency bands. It is the strongest in the first half of the sample, but becomes lower and more volatile towards the end of the period. Exact values cannot be quantified, but under assumption that observed values of the lag are the true values then for example PX on 20-40 frequency band (where the stability is the highest) would be lagging behind DAX by approximately 200 seconds in 2008 and 150 seconds in 2015. Situation is similar for this frequency band for all "developed"- "developing" index pairs on this frequency band. On the other frequency bands, we observe lower stability, where for PX we saw stable significant phase differences only to band 40-80 minutes and for PX-FTSE we saw no significant difference on that band in 2013. However throughout the years we observe lowering stability of the differences. While on average they remain non-zero, the relative phases are more volatile and its practical usability decreases.

Lowering stability has unfortunate suggestions for exploitability of the results of this thesis, especially if one would want to use it to improve his trading strategy. Even though phase-lag does not tell any story about how largely the information will be transmitted into the lagged signal, it should provide indication on average direction that is to come. However with lower stability it

might become much harder to create improvement of the strategy that would generate positive expected value. Although this possibility calls for further exploration, trading implication are above the scope of this work.

On the other, hand the results provide very interesting insight on the mutual relationship among the indices. We observe lower synchronicity (in sense of stability of both synchronization and lag) and decreasing lag of developing financial markets, which suggest lowering gap between the developing and developed financial markets and reduction in common trends in price-developments in intra-day markets.

Possible extensions of this thesis could be the inspection of the average high-frequency phase-relationship for each day separately to deal with the problem of breaks in the data (we try to deal with the problem by omitting first and last 5-minute periods of the trading day, however it brings disturbance to the cross-coefficients between the last-of-day and first-of-day returns). Downside of this approach would be very limited investigable frequency bands due to only several observations per day and therefore large edge effects on lower frequencies.

Another suggested extension is the link of phase differences to the trading volumes, where larger liquidity would suggest obvious hypotheses of lower phase-difference between the indexes, unfortunately both are above the scope of the thesis.

Bibliography

- ADDISON, P. S. (2017): *The illustrated wavelet transform handbook: introductory theory and applications in science, engineering, medicine and finance*. CRC press.
- ADDISON, P. S. (2018): “Introduction to redundancy rules: the continuous wavelet transform comes of age.”
- AHUJA, N., S. LERTRATTANAPANICH, & N. BOSE (2005): “Properties determining choice of mother wavelet.” *IEEE Proceedings-Vision, Image and Signal Processing* **152(5)**: pp. 659–664.
- ALBULESCU, C. T., D. GOYEAU, & A. K. TIWARI (2015): “Contagion and dynamic correlation of the main european stock index futures markets: A time-frequency approach.” *Procedia Economics and Finance* **20**: pp. 19–27.
- ALOU, C. & B. HKIRI (2014): “Co-movements of gcc emerging stock markets: New evidence from wavelet coherence analysis.” *Economic Modelling* **36**: pp. 421–431.
- ANSOFF, H. I. (1957): “Strategies for diversification.” *Harvard business review* **35(5)**: pp. 113–124.
- BARUNÍK, J., E. KOČENDA, & L. VÁCHA (2016): “Gold, oil, and stocks: Dynamic correlations.” *International Review of Economics & Finance* **42**: pp. 186–201.
- BARUNÍK, J. & L. VACHA (2013): “Contagion among central and eastern european stock markets during the financial crisis.” *arXiv preprint arXiv:1309.0491* .
- BROOKS, R. & M. DEL NEGRO (2004): “The rise in comovement across national stock markets: market integration or it bubble?” *Journal of Empirical Finance* **11(5)**: pp. 659–680.

- BROOKS, R. & M. DEL NEGRO (2005): “Country versus region effects in international stock returns.” *The Journal of Portfolio Management* **31(4)**: pp. 67–72.
- CANDELON, B., A. HECQ, & W. F. VERSCHOOR (2005): “Measuring common cyclical features during financial turmoil: Evidence of interdependence not contagion.” *Journal of International Money and Finance* **24(8)**: pp. 1317–1334.
- CANDELON, B., J. PIPLACK, & S. STRAETMANS (2008): “On measuring synchronization of bulls and bears: The case of east asia.” *Journal of banking & finance* **32(6)**: pp. 1022–1035.
- CAZELLES, B., M. CHAVEZ, D. BERTEAUX, F. MÉNARD, J. O. VIK, S. JE-NOUVRIER, & N. C. STENSETH (2008): “Wavelet analysis of ecological time series.” *Oecologia* **156(2)**: pp. 287–304.
- CAZELLES, B. & L. STONE (2003): “Detection of imperfect population synchrony in an uncertain world.” *Journal of Animal Ecology* **72(6)**: pp. 953–968.
- DAJCMAN, S., M. FESTIC, & A. KAVKLER (2012): “Comovement between central and eastern european and developed european stock markets: scale based wavelet analysis.” *Actual Probles of Economics* **3**: pp. 375–384.
- DOWLE, M. & A. SRINIVASAN (2017): *data.table: Extension of ‘data.frame’*. R package version 1.10.4-3.
- DZIAK, J. J., D. L. COFFMAN, S. T. LANZA, & R. LI (2012): “Sensitivity and specificity of information criteria.” *The Methodology Center and Department of Statistics, Penn State, The Pennsylvania State University* **16(30)**: p. 140.
- ÉGERT, B. & E. KOČENDA (2007): “Interdependence between eastern and western european stock markets: Evidence from intraday data.” *Economic Systems* **31(2)**: pp. 184–203.
- ÉGERT, B. & E. KOČENDA (2011): “Time-varying synchronization of european stock markets.” *Empirical Economics* **40(2)**: pp. 393–407.
- FISCHER, K. P. & A. PALASVIRTA (1990): “High road to a global marketplace: the international transmission of stock market fluctuations.” *Financial Review* **25(3)**: pp. 371–394.

- FORBES, K. J. & R. RIGOBON (2002): “No contagion, only interdependence: measuring stock market comovements.” *The Journal of Finance* **57(5)**: pp. 2223–2261.
- GALLEGATI, M. (2008): “Wavelet analysis of stock returns and aggregate economic activity.” *Computational Statistics & Data Analysis* **52(6)**: pp. 3061–3074.
- GENÇAY, R., F. SELÇUK, & B. J. WHITCHER (2001): *An introduction to wavelets and other filtering methods in finance and economics*. Elsevier.
- GILMAN, D. L., F. J. FUGLISTER, & J. M. MITCHELL JR (1963): “On the power spectrum of “red noise”.” *Journal of the Atmospheric Sciences* **20(2)**: pp. 182–184.
- GJIKA, D. & R. HORVATH (2013): “Stock market comovements in central europe: Evidence from the asymmetric dcc model.” *Economic Modelling* **33**: pp. 55–64.
- GRAHAM, M., J. KIVIAHO, & J. NIKKINEN (2012): “Integration of 22 emerging stock markets: A three-dimensional analysis.” *Global Finance Journal* **23(1)**: pp. 34–47.
- GRAHAM, M. & J. NIKKINEN (2011): “Co-movement of the finnish and international stock markets: a wavelet analysis.” *The European Journal of Finance* **17(5-6)**: pp. 409–425.
- GRANGER, C. W. (1969): “Investigating causal relations by econometric models and cross-spectral methods.” *Econometrica: Journal of the Econometric Society* pp. 424–438.
- GRUBEL, H. G. (1968): “Internationally diversified portfolios: welfare gains and capital flows.” *The American Economic Review* **58(5)**: pp. 1299–1314.
- HAFNER, C. M. & H. HERWARTZ (2009): “Testing for linear vector autoregressive dynamics under multivariate generalized autoregressive heteroskedasticity.” *Statistica Neerlandica* **63(3)**: pp. 294–323.
- HANUS, L. & L. VÁCHA (2018): “Growth cycle synchronization of the visegrad four and the european union.” *Empirical Economics* pp. 1–17.

- HARDING, D. & A. PAGAN (2006): "Synchronization of cycles." *Journal of Econometrics* **132(1)**: pp. 59–79.
- IN, F. & S. KIM (2006): "The hedge ratio and the empirical relationship between the stock and futures markets: a new approach using wavelet analysis." *The Journal of Business* **79(2)**: pp. 799–820.
- JOHNSON, R. & L. SOENEN (2003): "Economic integration and stock market comovement in the americas." *Journal of Multinational Financial Management* **13(1)**: pp. 85–100.
- KAROLYI, G. A. & R. M. STULZ (1996): "Why do markets move together? an investigation of us-japan stock return comovements." *The Journal of Finance* **51(3)**: pp. 951–986.
- KING, M., E. SENTANA, & S. WADHWANI (1990): "Volatiltiy and links between national stock markets." *Technical report*, National Bureau of Economic Research.
- KING, M. A. & S. WADHWANI (1990): "Transmission of volatility between stock markets." *Review of Financial studies* **3(1)**: pp. 5–33.
- LIN, W.-L., R. F. ENGLE, & T. ITO (1994): "Do bulls and bears move across borders? international transmission of stock returns and volatility." *Review of financial studies* **7(3)**: pp. 507–538.
- LOH, L. (2013): "Co-movement of asia-pacific with european and us stock market returns: A cross-time-frequency analysis." *Research in International Business and Finance* **29**: pp. 1–13.
- LONGIN, F. & B. SOLNIK (1995): "Is the correlation in international equity returns constant: 1960–1990?" *Journal of international money and finance* **14(1)**: pp. 3–26.
- LONGIN, F. & B. SOLNIK (2001): "Extreme correlation of international equity markets." *The journal of finance* **56(2)**: pp. 649–676.
- MADALENO, M. & C. PINHO (2012): "International stock market indices comovements: a new look." *International Journal of Finance & Economics* **17(1)**: pp. 89–102.

- MAKRIDAKIS, S. G. & S. C. WHEELWRIGHT (1974): "An analysis of the inter-relationships among the major world stock exchanges." *Journal of Business Finance & Accounting* **1(2)**: pp. 195–215.
- MANTALOS, P., G. SHUKUR, & P. SJÖLANDER (2007): "The effect of garch (1, 1) on the granger causality test in stable var models." *Journal of Modern Applied Statistical Methods* **6(2)**: p. 12.
- P. TASS, MG Rosenblum, J. W. J. K. A. P. J. V. A. S. & H.-J. FREUND (1998): "Detection of n : m phase locking from noisy data: application to magnetoencephalography." *Phys. Rev. Lett.* **81**: p. 3291.
- RANTA, M. (2013): "Contagion among major world markets: a wavelet approach." *International Journal of Managerial Finance* **9(2)**: pp. 133–149.
- REBOREDO, J. C., M. A. RIVERA-CASTRO, & A. UGOLINI (2017): "Wavelet-based test of co-movement and causality between oil and renewable energy stock prices." *Energy Economics* **61**: pp. 241–252.
- ROESCH, A., H. SCHMIDBAUER, E. ULUCEVIZ *et al.* (2014): "Frequency aspects of information transmission in networks of equity markets." *Technical report*, EcoMod.
- RUA, A. & L. C. NUNES (2009): "International comovement of stock market returns: A wavelet analysis." *Journal of Empirical Finance* **16(4)**: pp. 632–639.
- SCHLÜTER, S. & C. DEUSCHLE (2010): "Using wavelets for time series forecasting: Does it pay off?" *Technical report*, IWQW discussion paper series.
- SCHMIDBAUER, H., A. ROESCH, & E. ULUCEVIZ (2013): "Market connectedness: Spillovers, information flow, and relative market entropy." *Koç University-TÜSİAD Economic Research Forum Working Paper Series 1320*, Istanbul.
- SIFUZZAMAN, M., M. ISLAM, & M. ALI (2009): "Application of wavelet transform and its advantages compared to fourier transform." .
- SMITH, K. L. (2001): "Pre-and post-1987 crash frequency domain analysis among pacific rim equity markets." *Journal of Multinational Financial Management* **11(1)**: pp. 69–87.

- SYLLIGNAKIS, M. N. & G. P. KOURETAS (2011): “Dynamic correlation analysis of financial contagion: Evidence from the central and eastern european markets.” *International Review of Economics & Finance* **20(4)**: pp. 717–732.
- TORRENCE, C. & G. P. COMPO (1998): “A practical guide to wavelet analysis.” *Bulletin of the American Meteorological society* **79(1)**: pp. 61–78.
- TORRENCE, C. & P. J. WEBSTER (1999): “Interdecadal changes in the ENSO-monsoon system.” *Journal of Climate* **12(8)**: pp. 2679–2690.
- VACHA, L. & J. BARUNIK (2012): “Co-movement of energy commodities revisited: Evidence from wavelet coherence analysis.” *Energy Economics* **34(1)**: pp. 241–247.
- WHITCHER, B., P. GUTTORP, & D. PERCIVAL (1999): “Mathematical background for wavelet estimators of cross-covariance and cross-correlation.” .
- WU, M.-C., M.-C. HUANG, H.-C. YU, & T. C. CHIANG (2006): “Phase distribution and phase correlation of financial time series.” *Physical Review E* **73(1)**: p. 016118.

Appendix A

MODWT figures

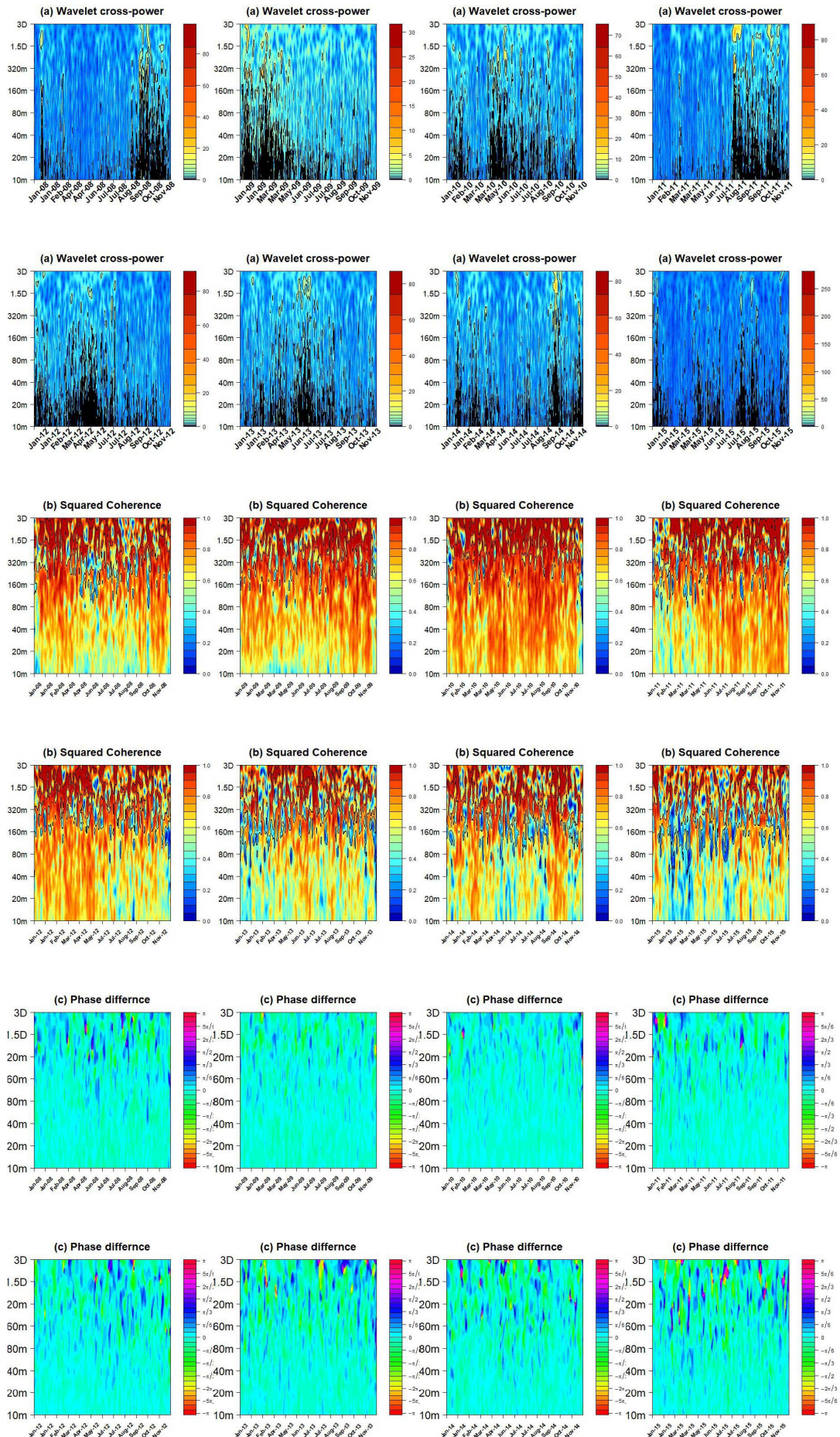
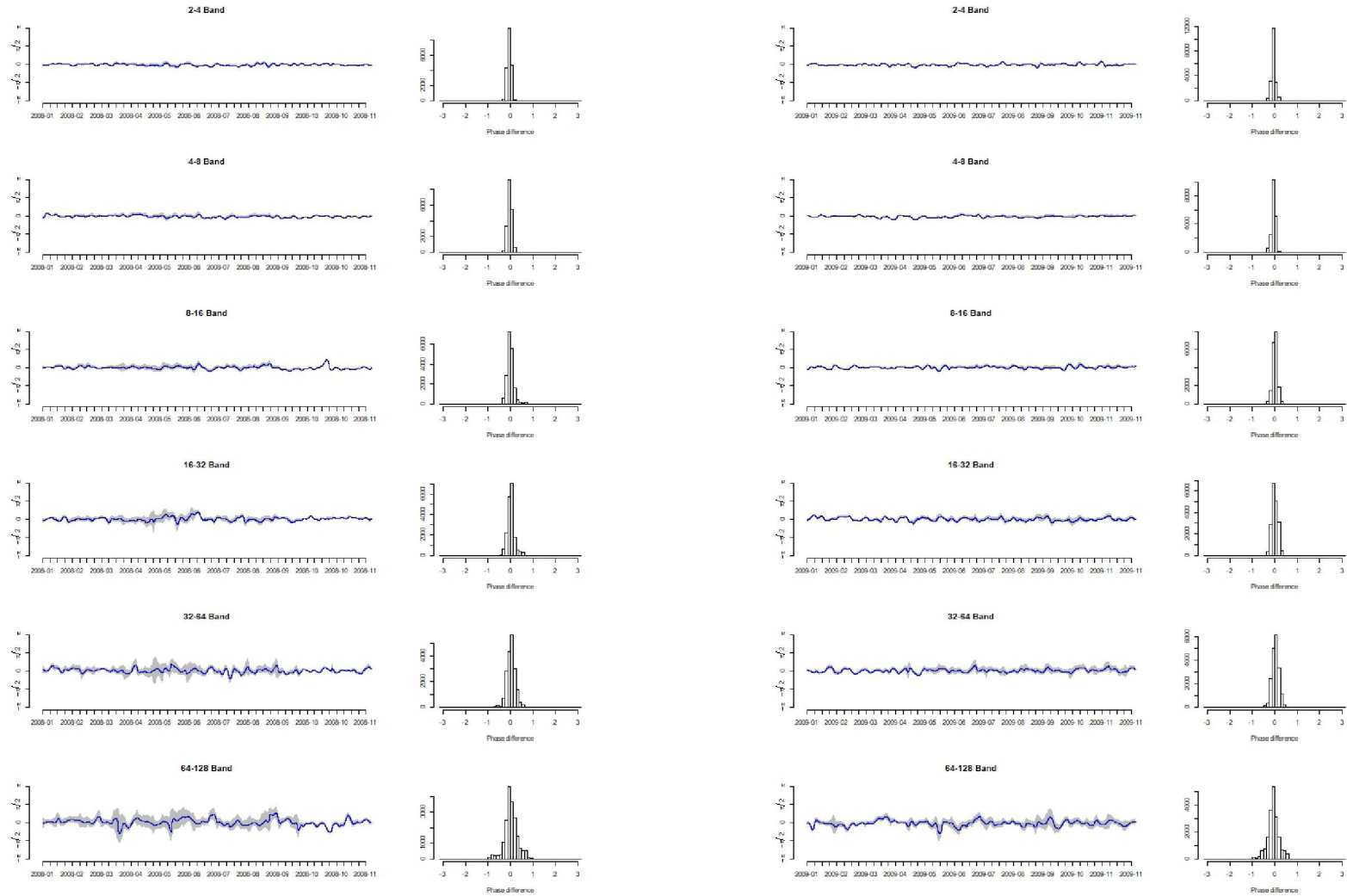


Figure A.1: Images of CWT analysis on FTSE 100 and DAX

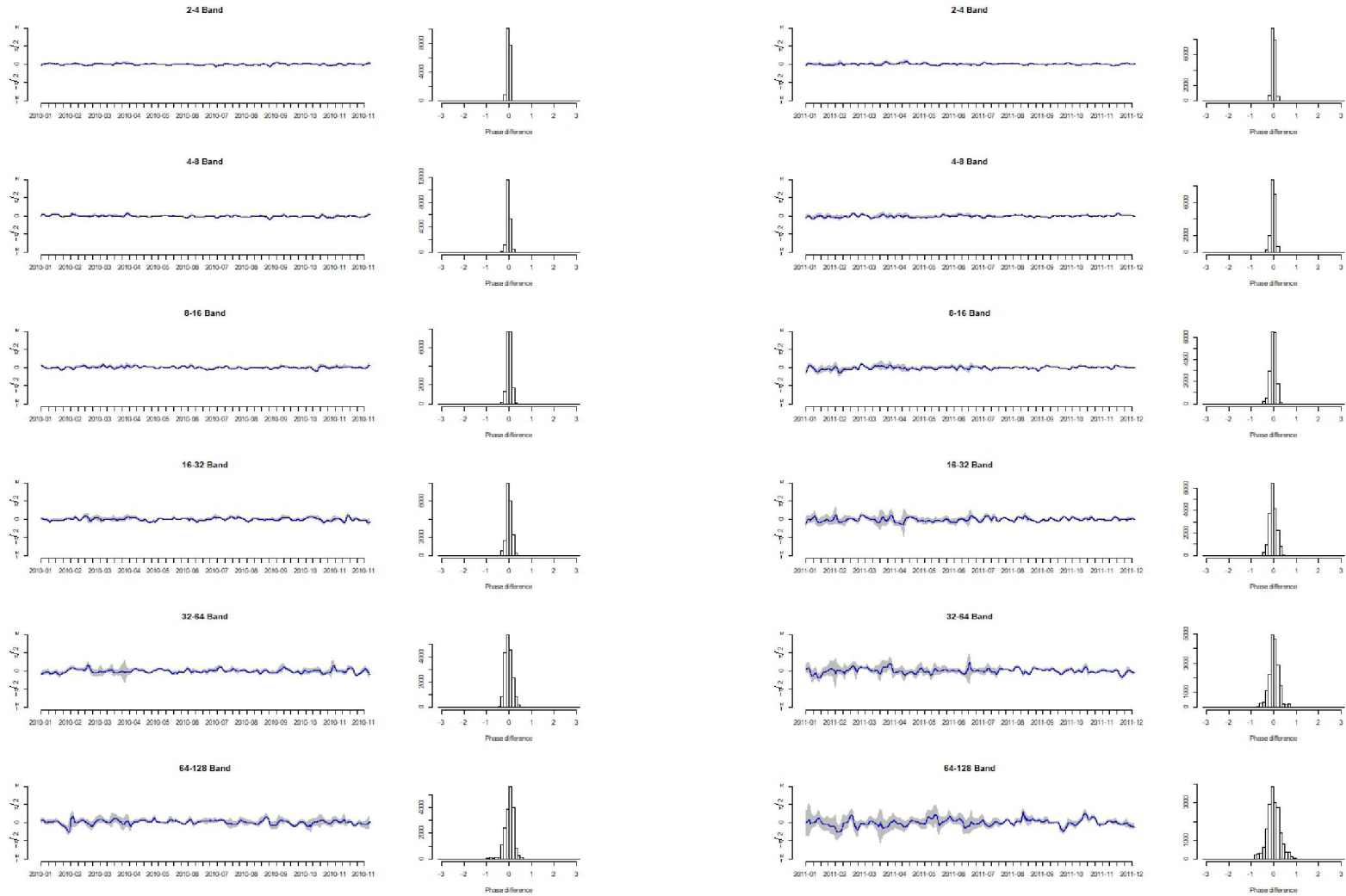
Figure A.2: Evolution of phase difference of FTSE 100 and DAX



(a) year 2008

(b) year 2009

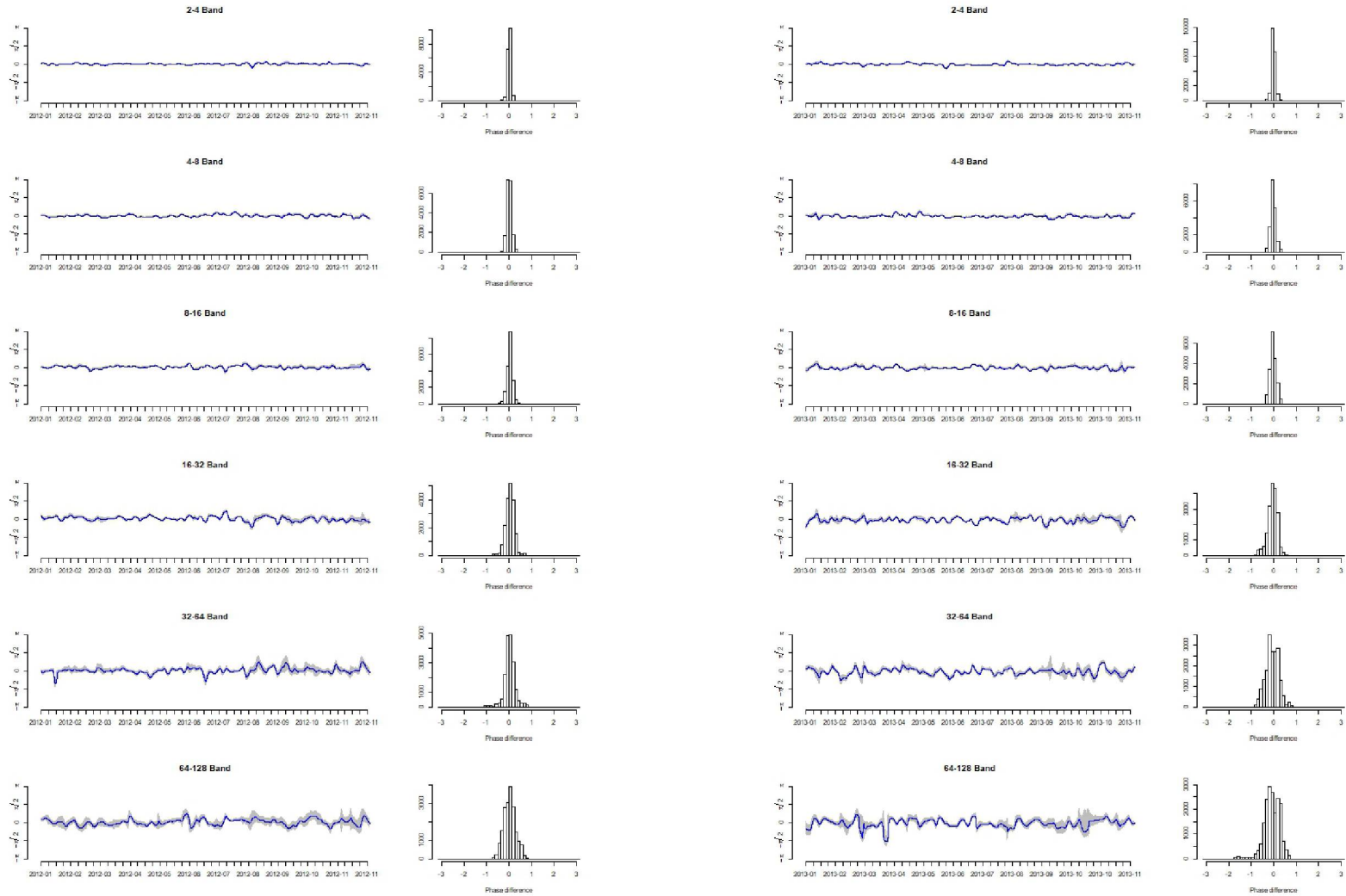
Figure A.2: Evolution of phase difference of FTSE 100 and DAX



(c) year 2010

(d) year 2011

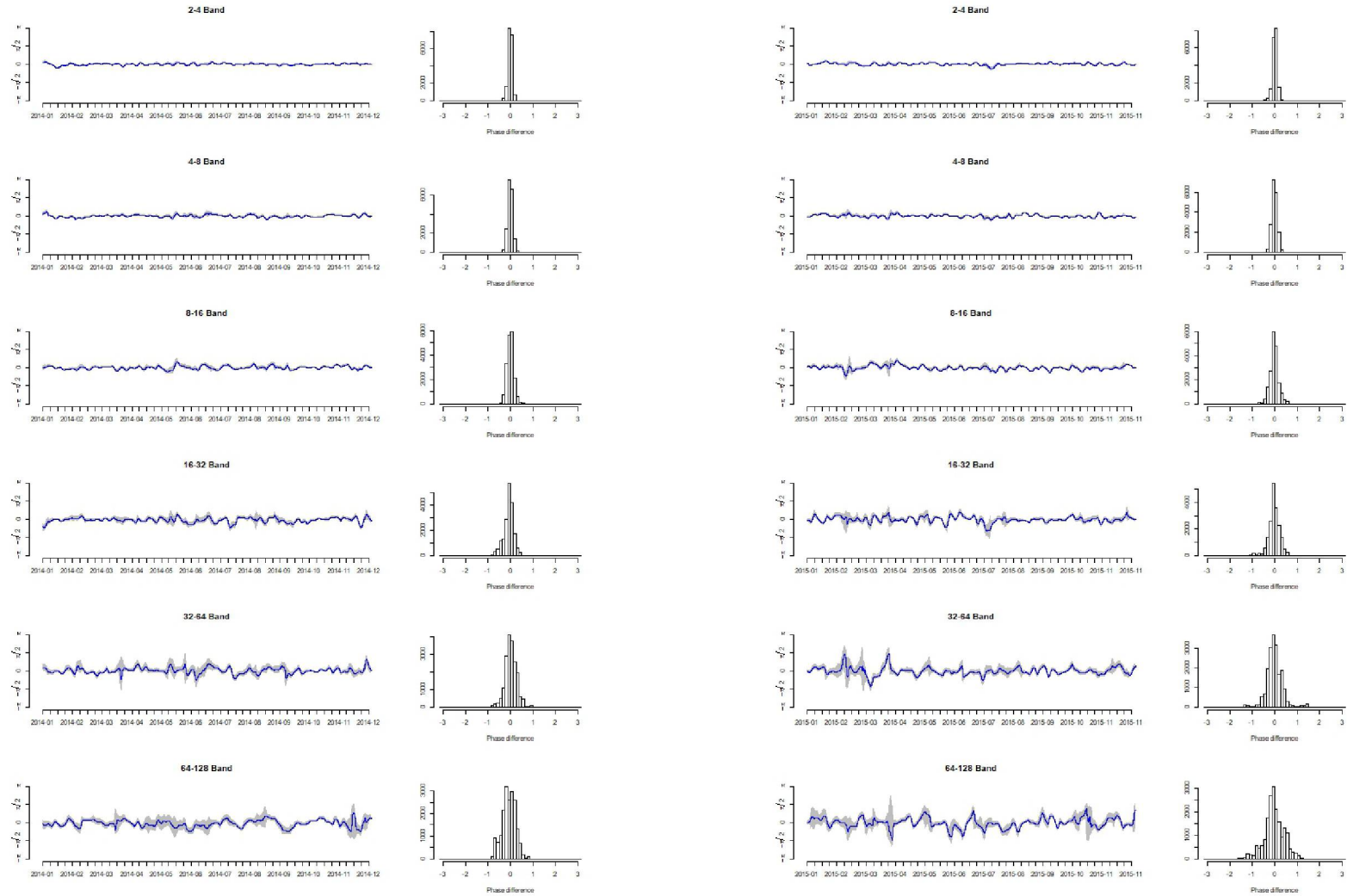
Figure A.2: Evolution of phase difference of FTSE 100 and DAX



(e) year 2012

(f) Evolution of phase differences, 2013

Figure A.2: Evolution of phase difference of FTSE 100 and DAX



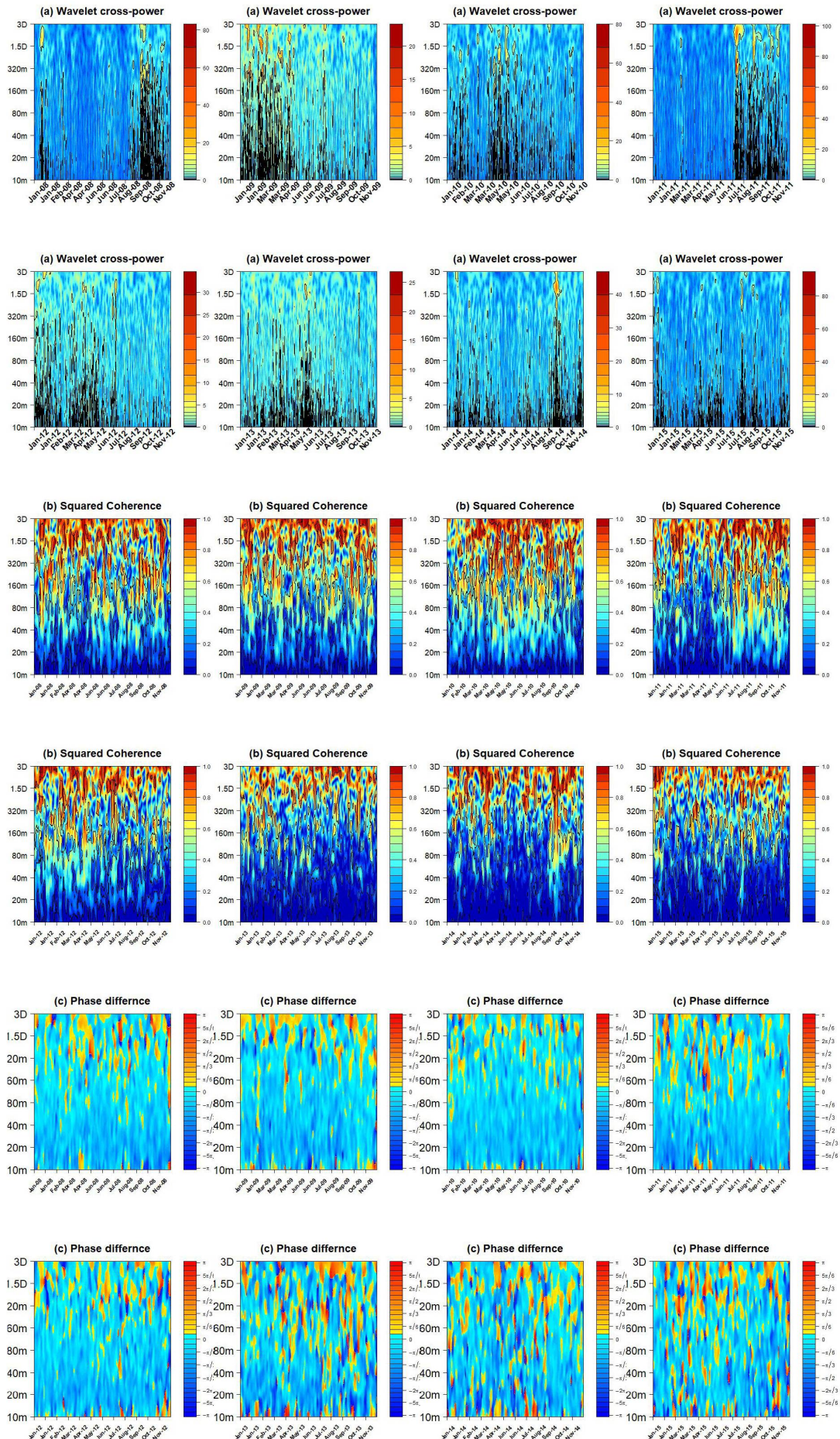
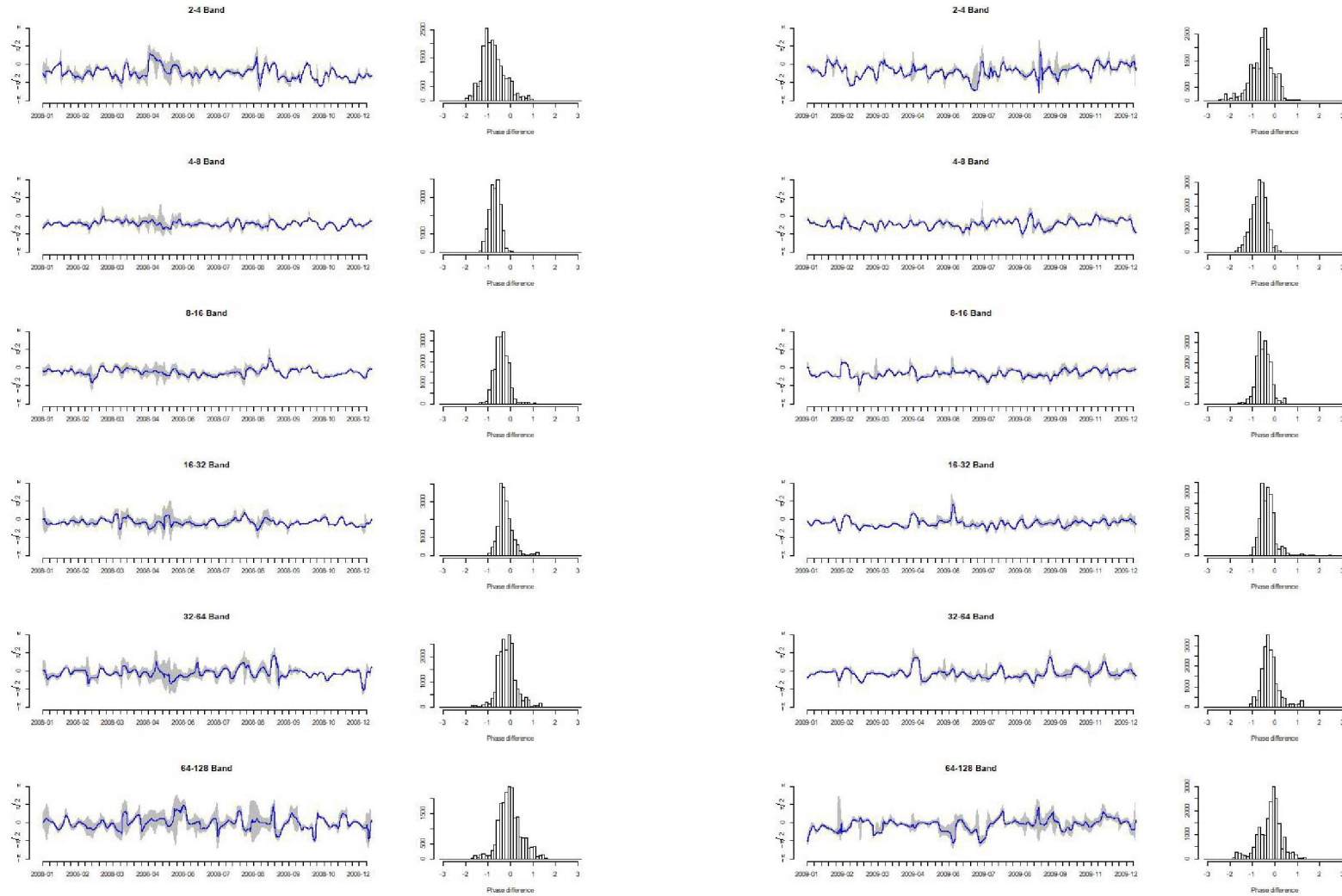


Figure A.3: Images of CWT analysis on PX and DAX

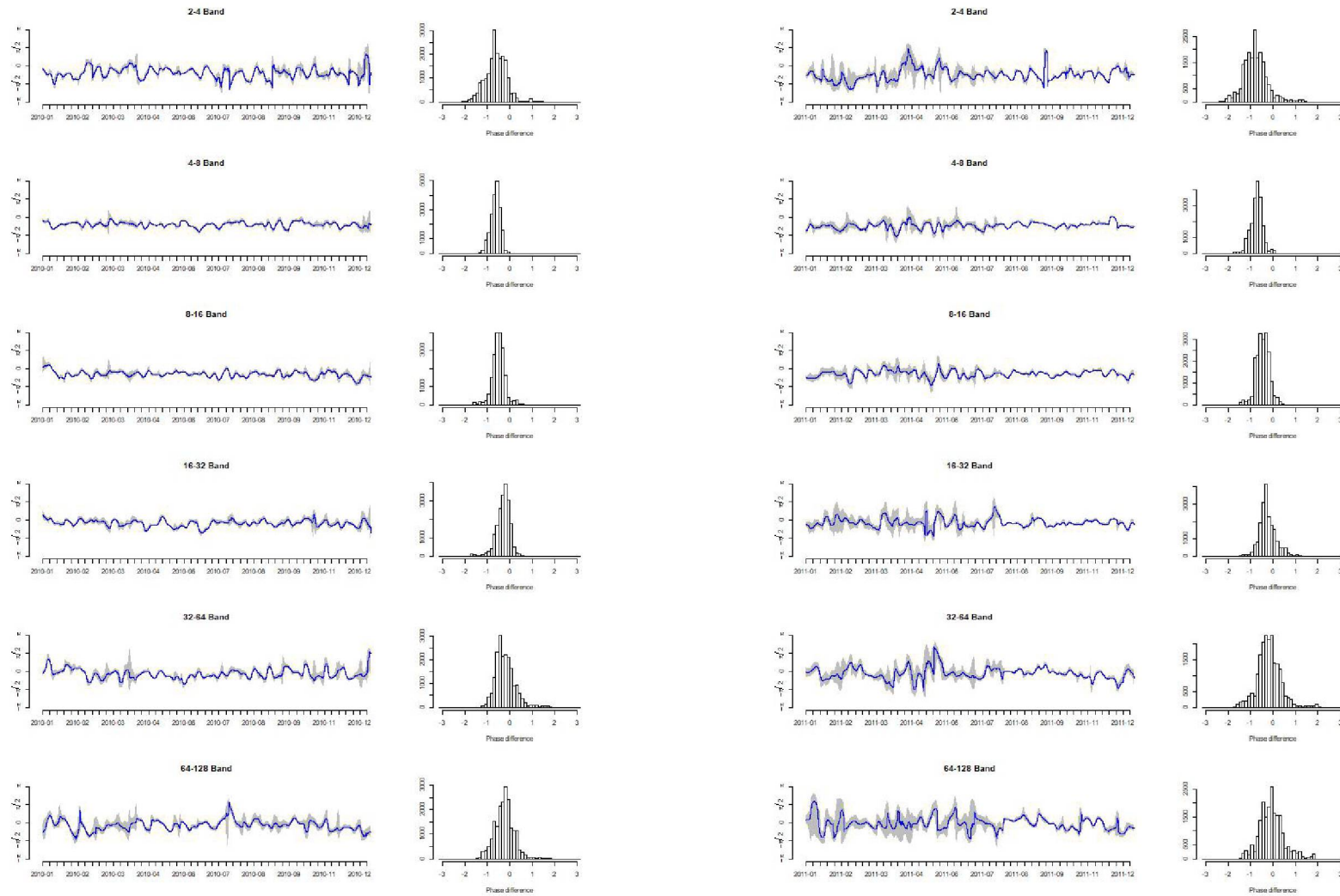
Figure A.4: Evolution of phase difference of PX and DAX



(a) year 2008

(b) year 2009

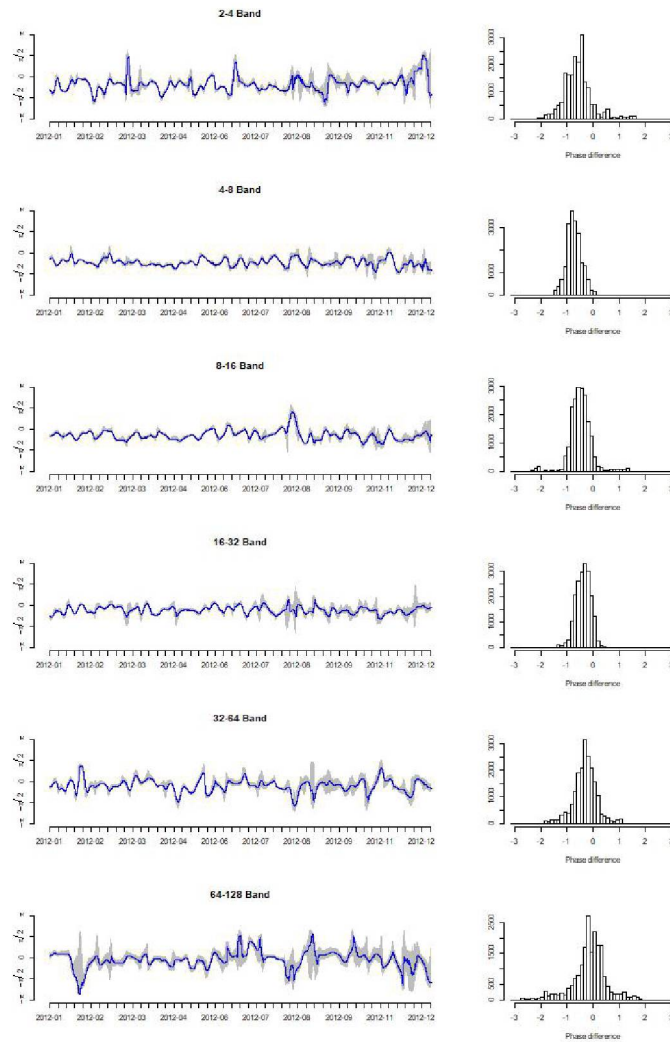
Figure A.4: Evolution of phase difference of PX and DAX



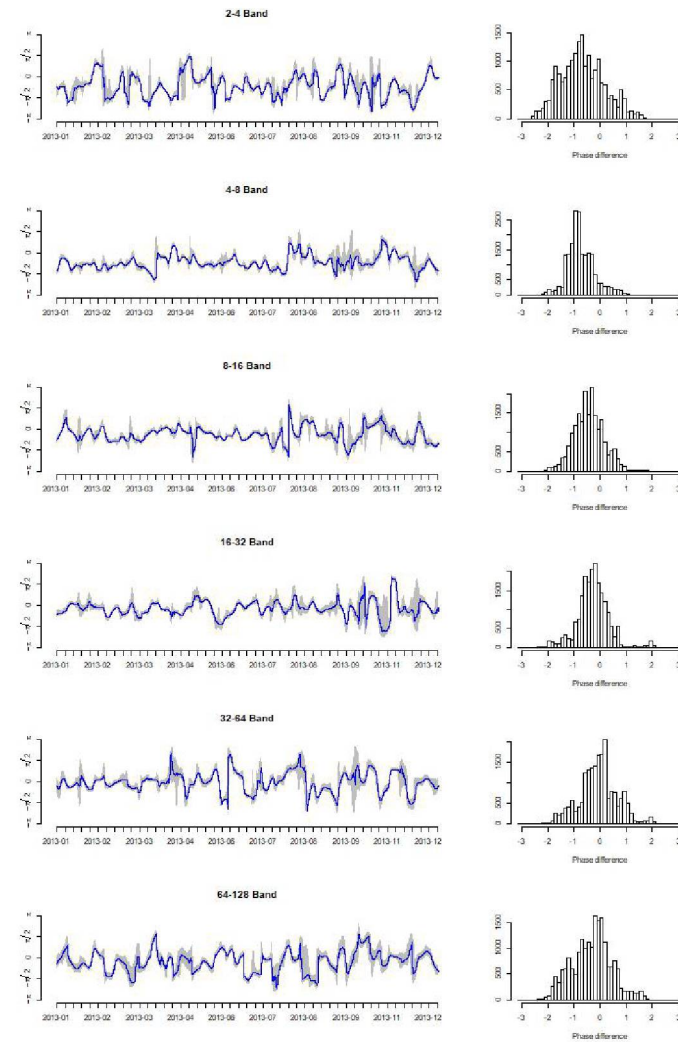
(c) year 2010

(d) year 2011

Figure A.4: Evolution of phase difference of PX and DAX

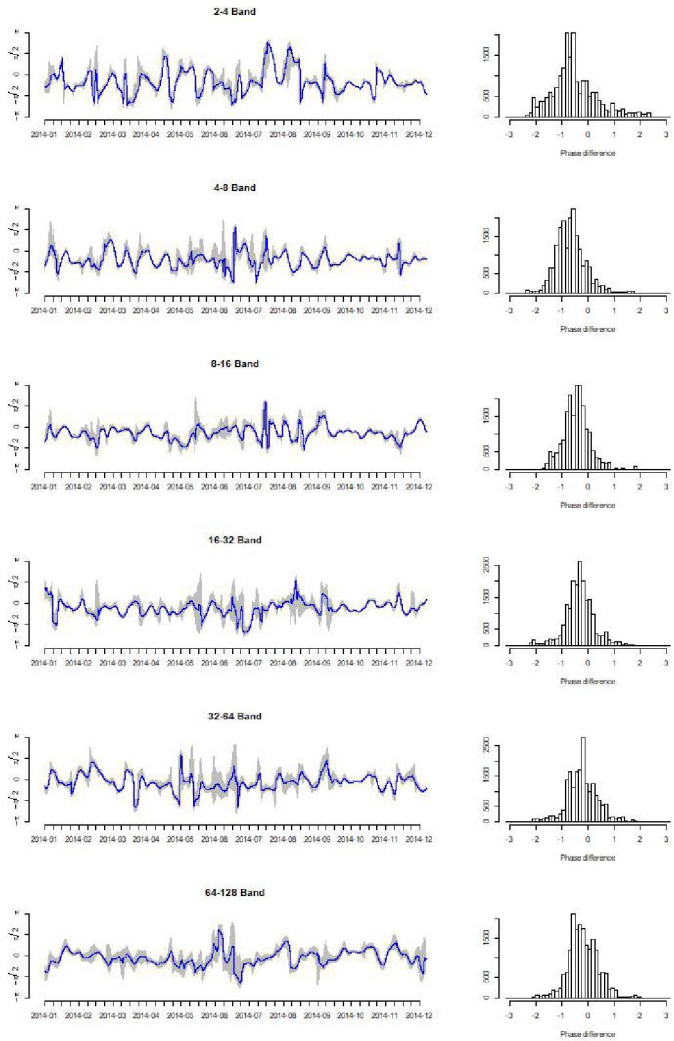


(e) year 2012



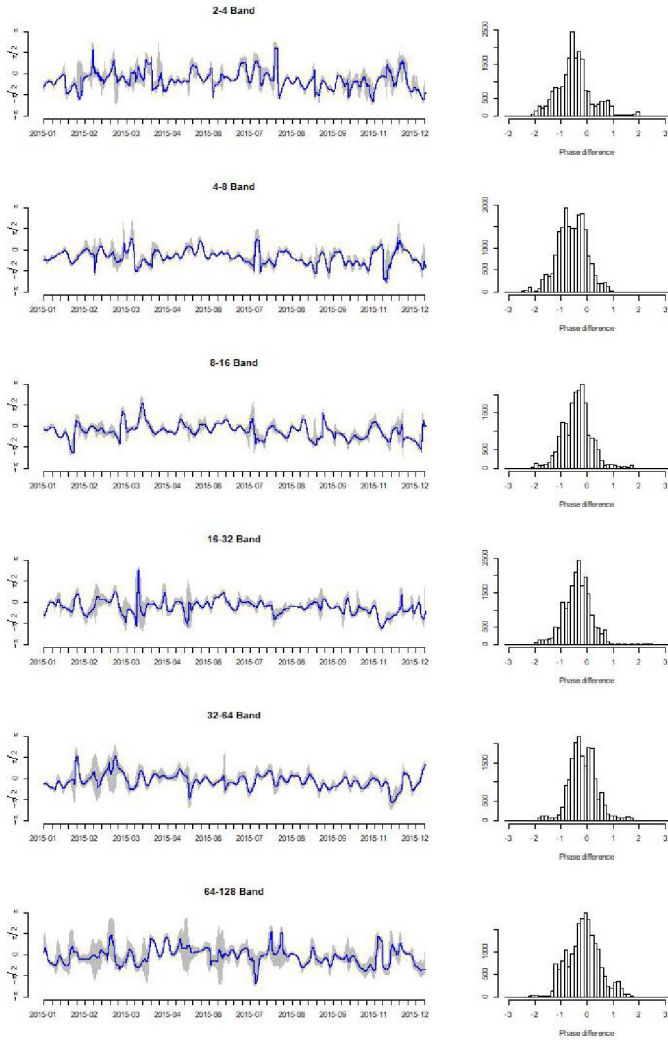
(f) Evolution of phase differences, 2013

Figure A.4: Evolution of phase



(g) year 2014

the difference of PX and DAX



(h) year 2015

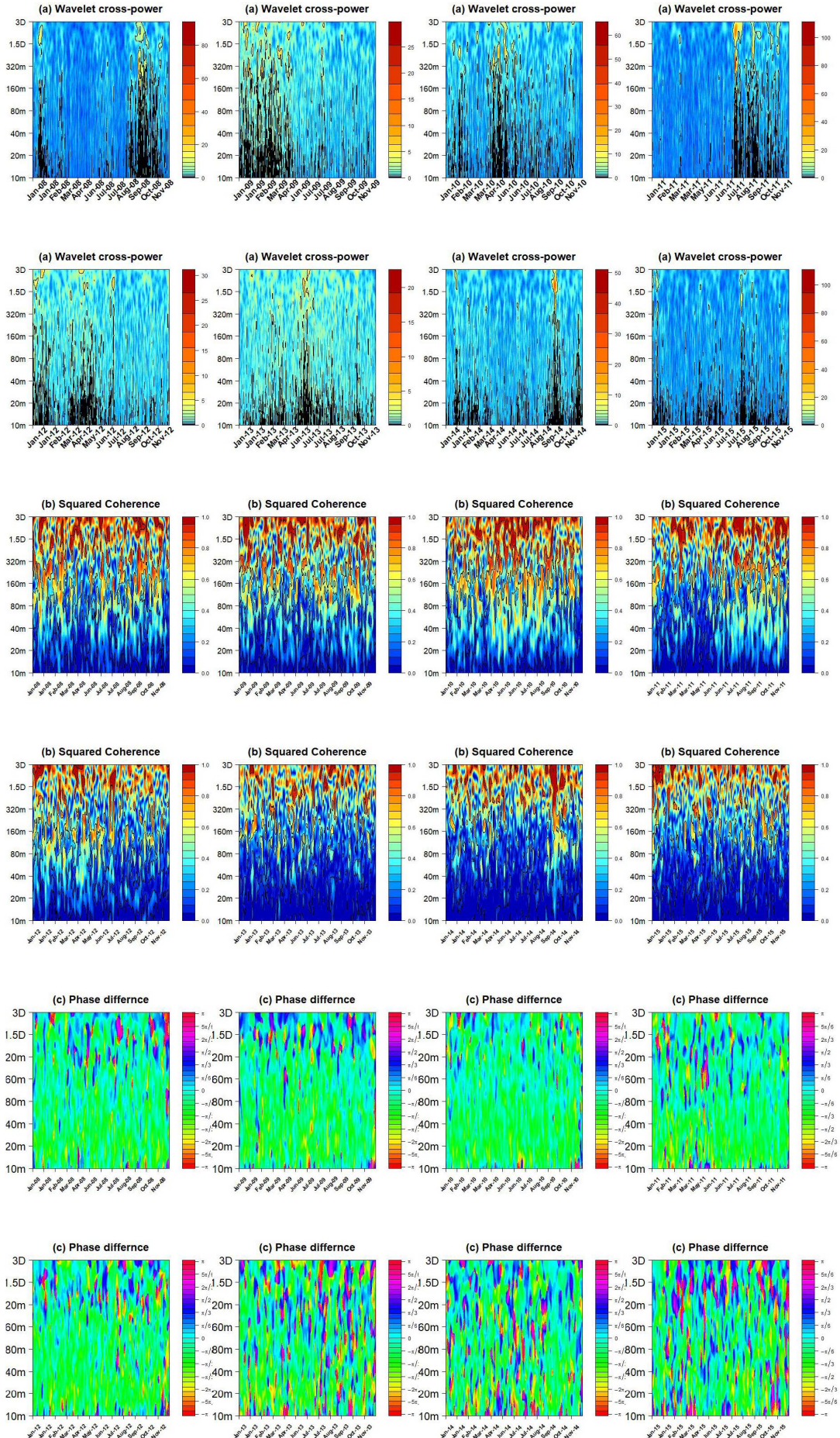
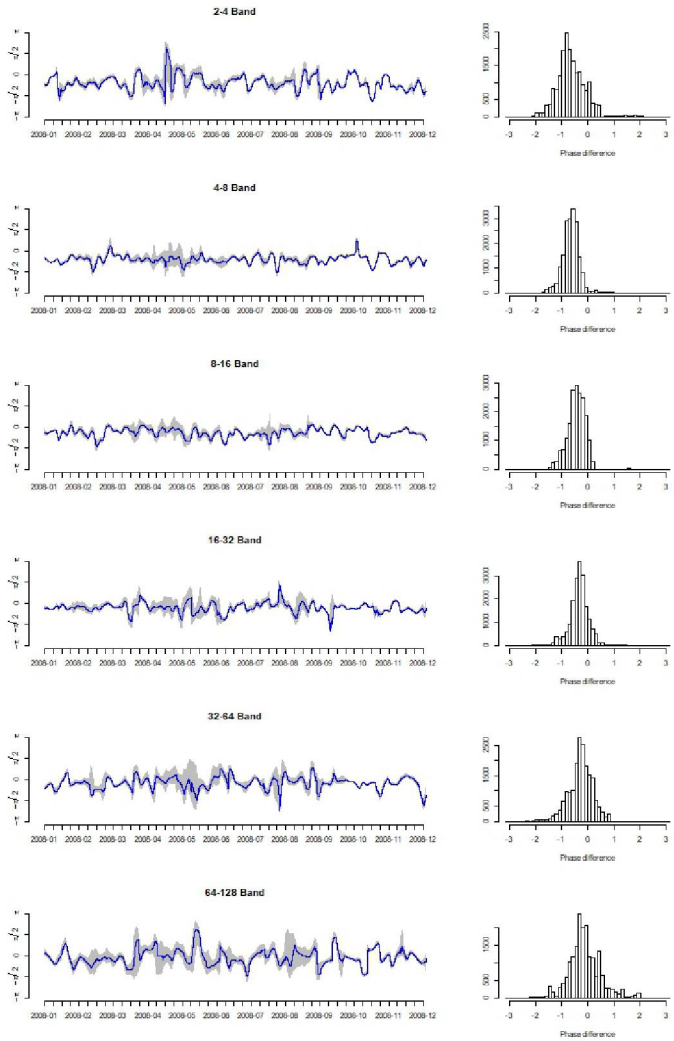


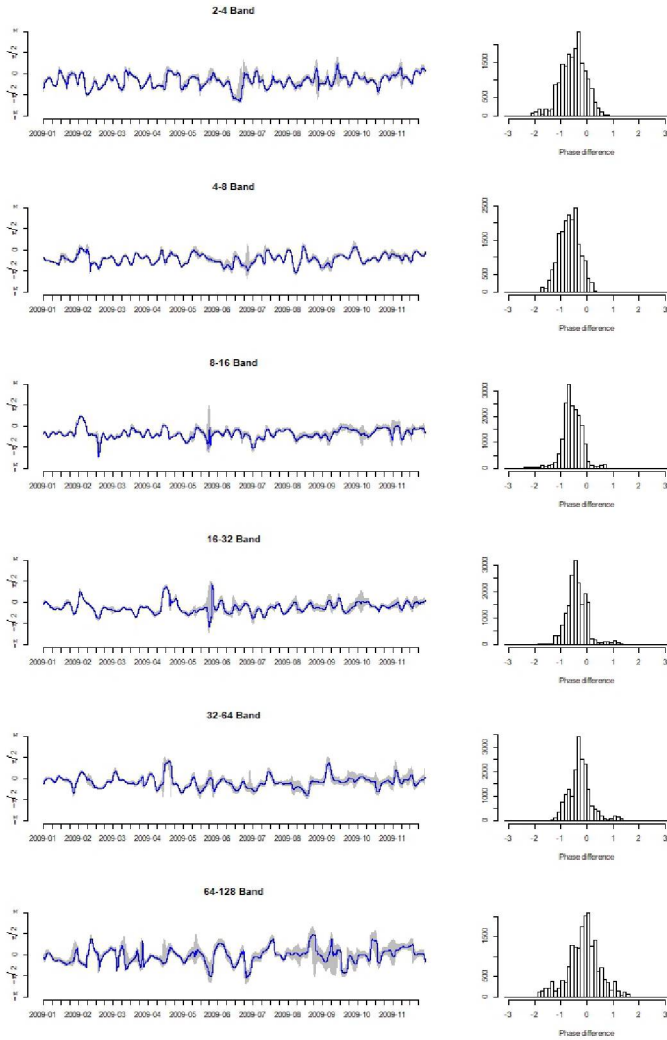
Figure A.5: Images of CWT analysis on PX and FTSE 100

Figure A.6: Evolution of phase ϕ



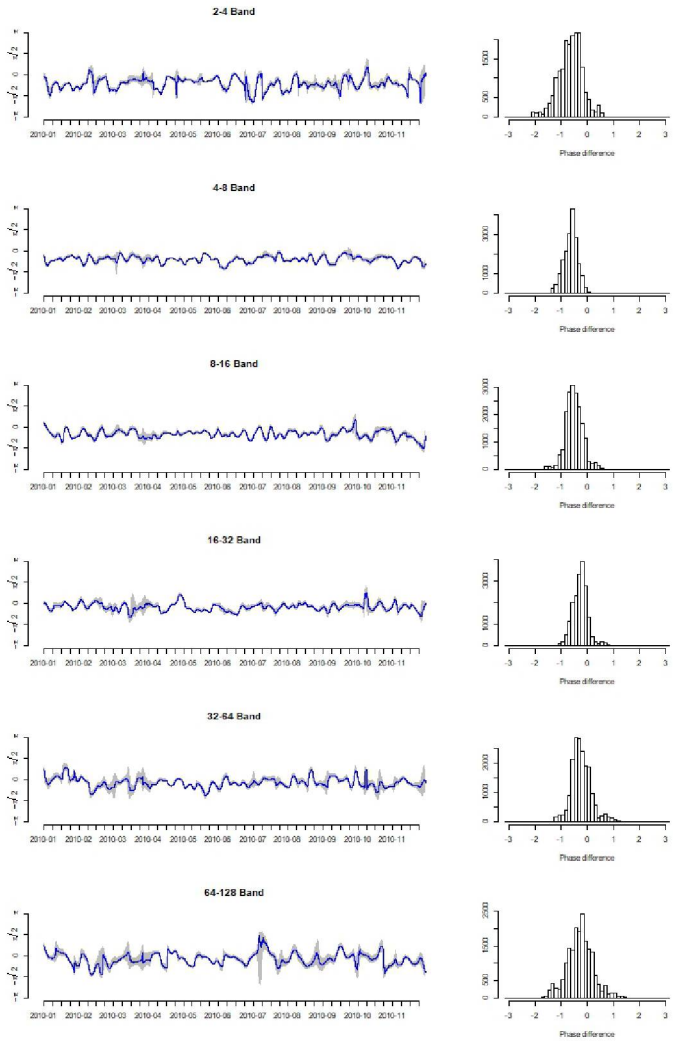
(a) year 2008

difference of PX and FTSE500



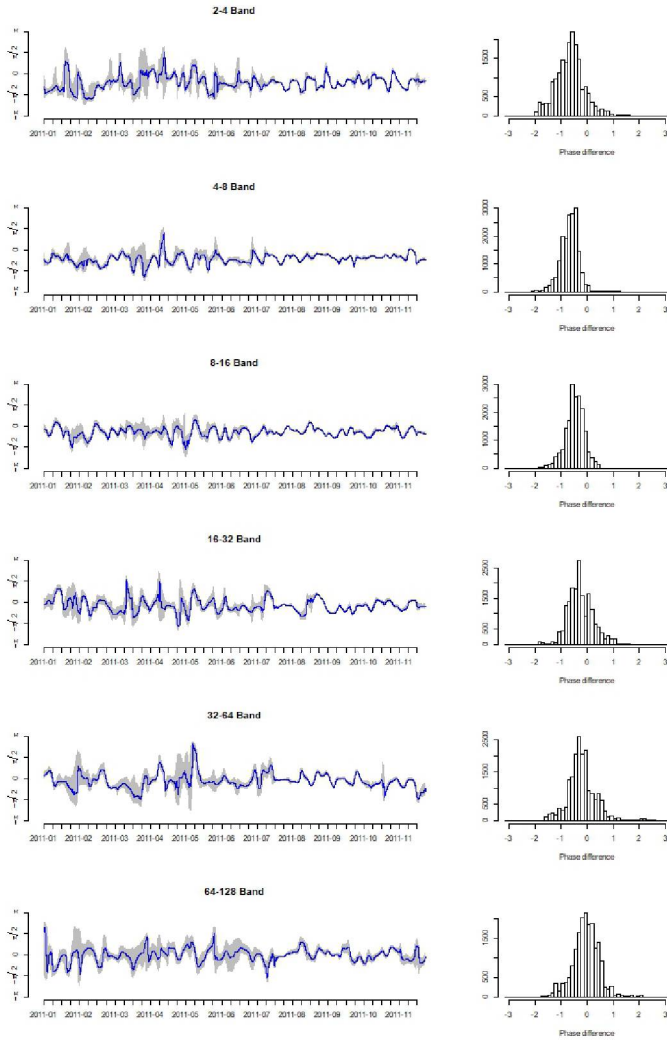
(b) year 2009

Figure A.6: Evolution of phase ϕ



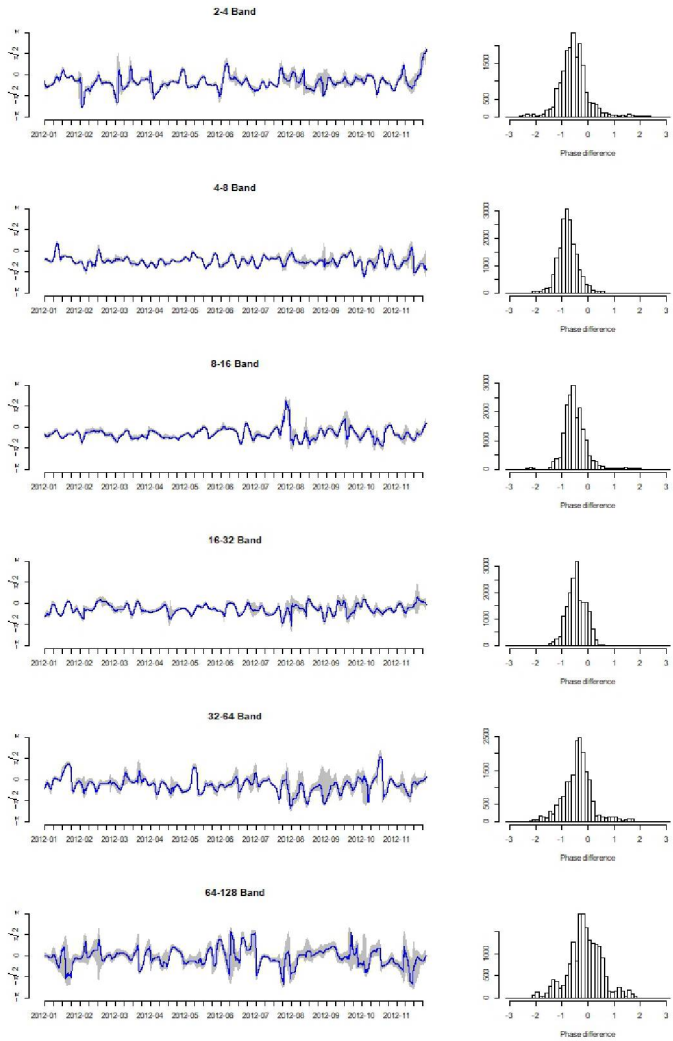
(c) year 2010

difference of PX and FTSE500



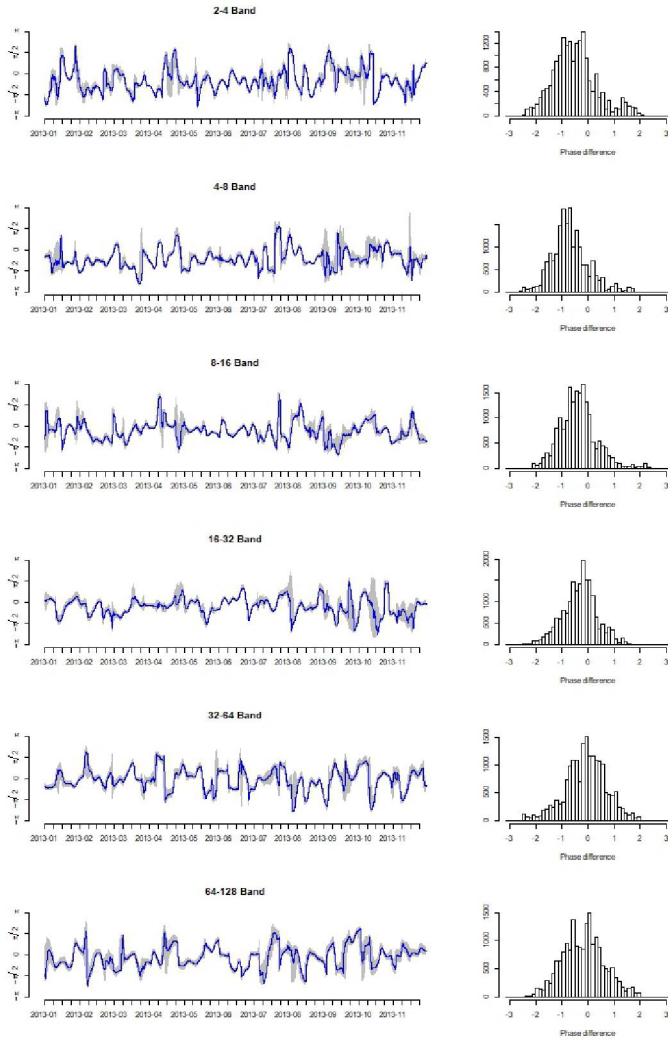
(d) year 2011

Figure A.6: Evolution of phase c



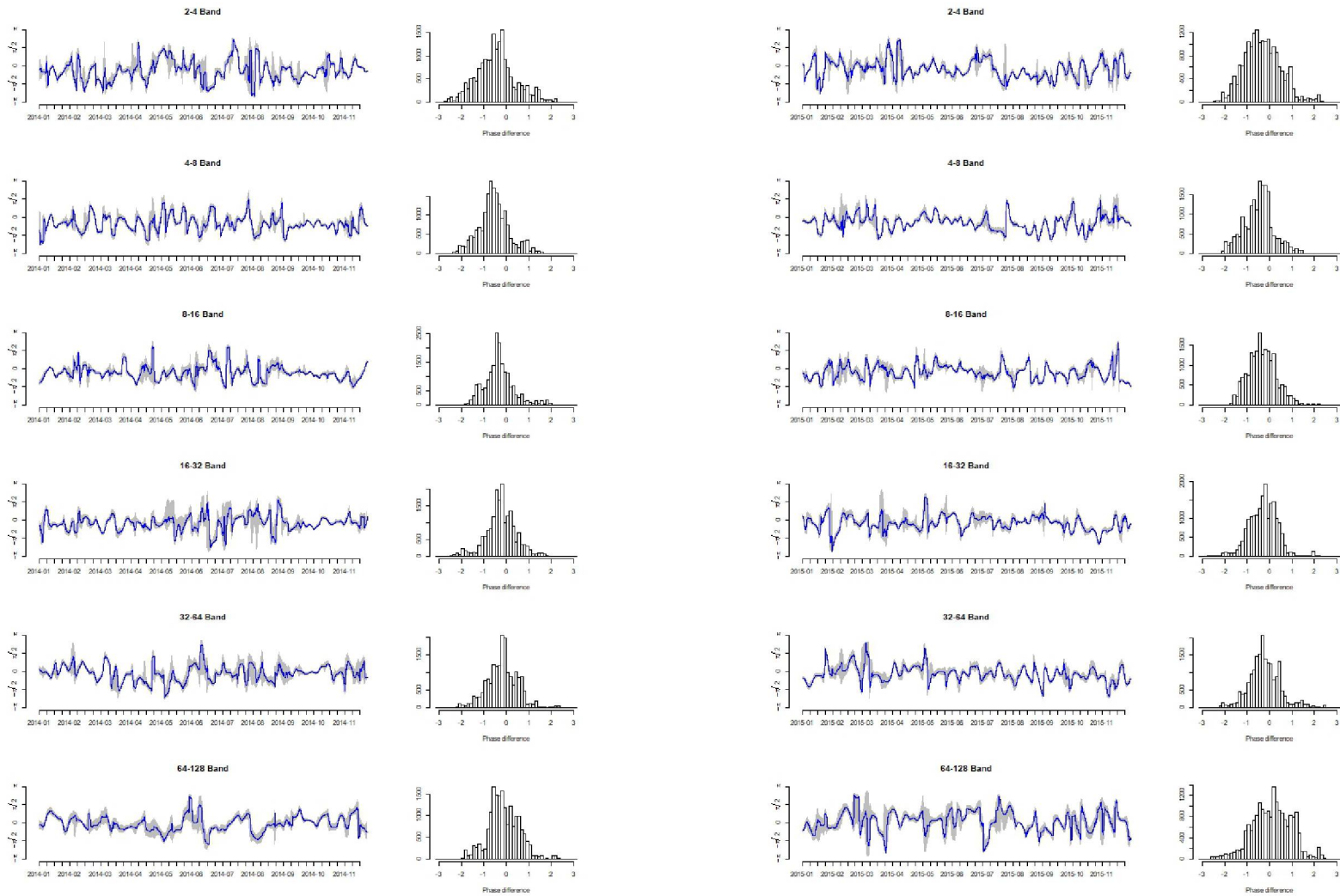
(e) year 2012

Difference of PX and FTSE500



(f) Evolution of phase differences, 2013

Figure A.6: Evolution of phase difference of PX and FTSE500



(g) year 2014

(h) year 2015

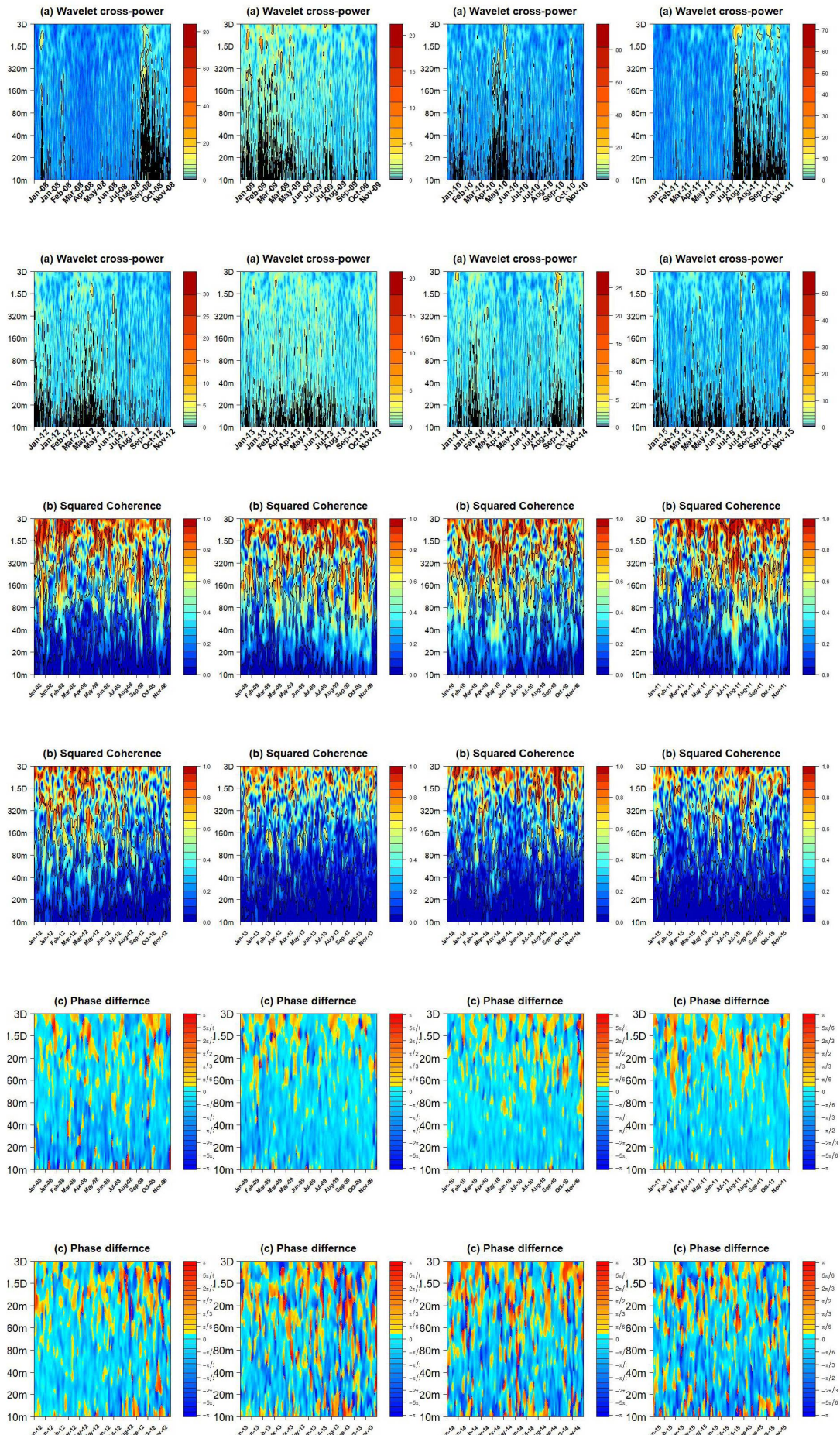


Figure A.7: Images of CWT analysis on BUX and DAX

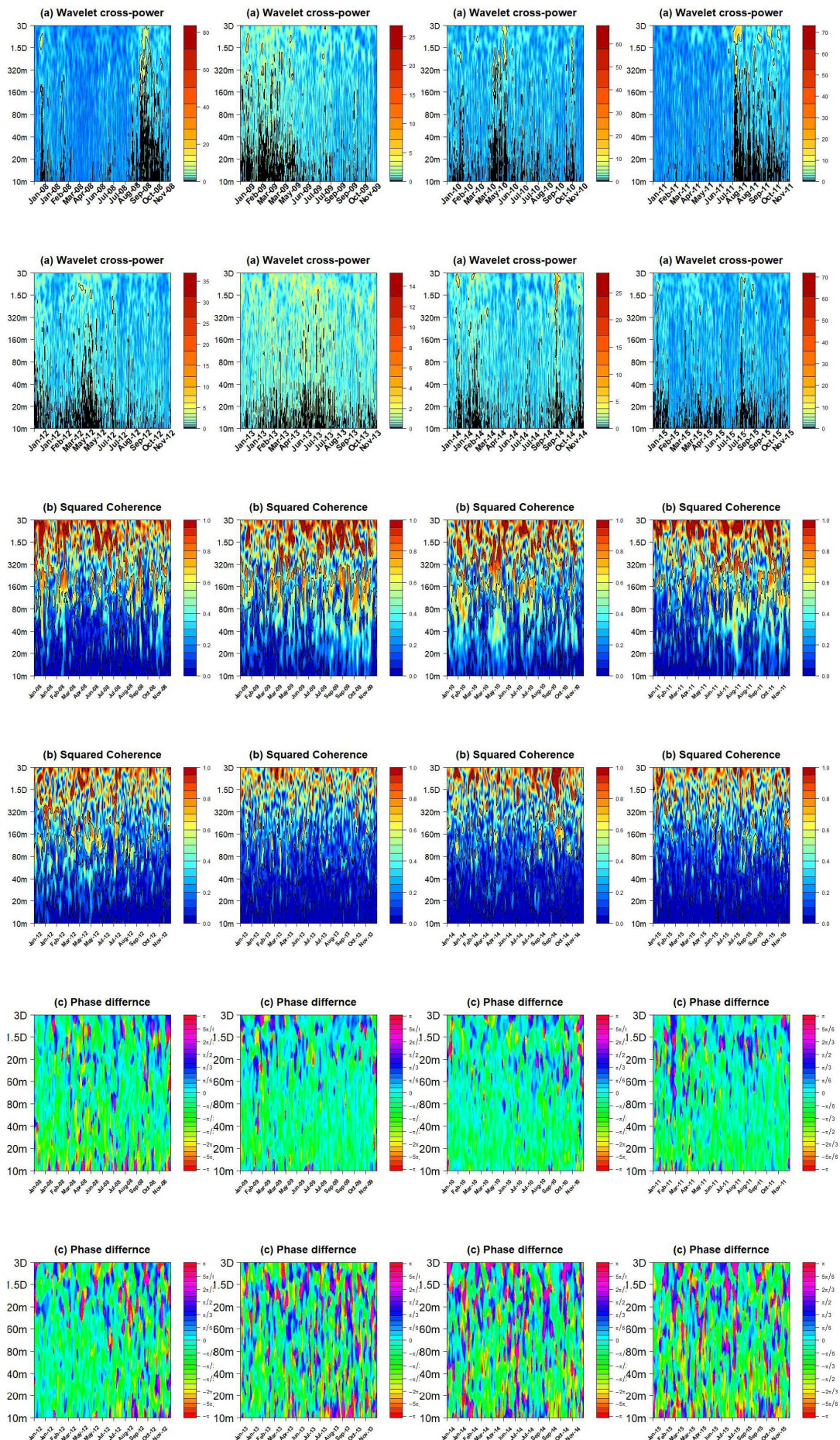
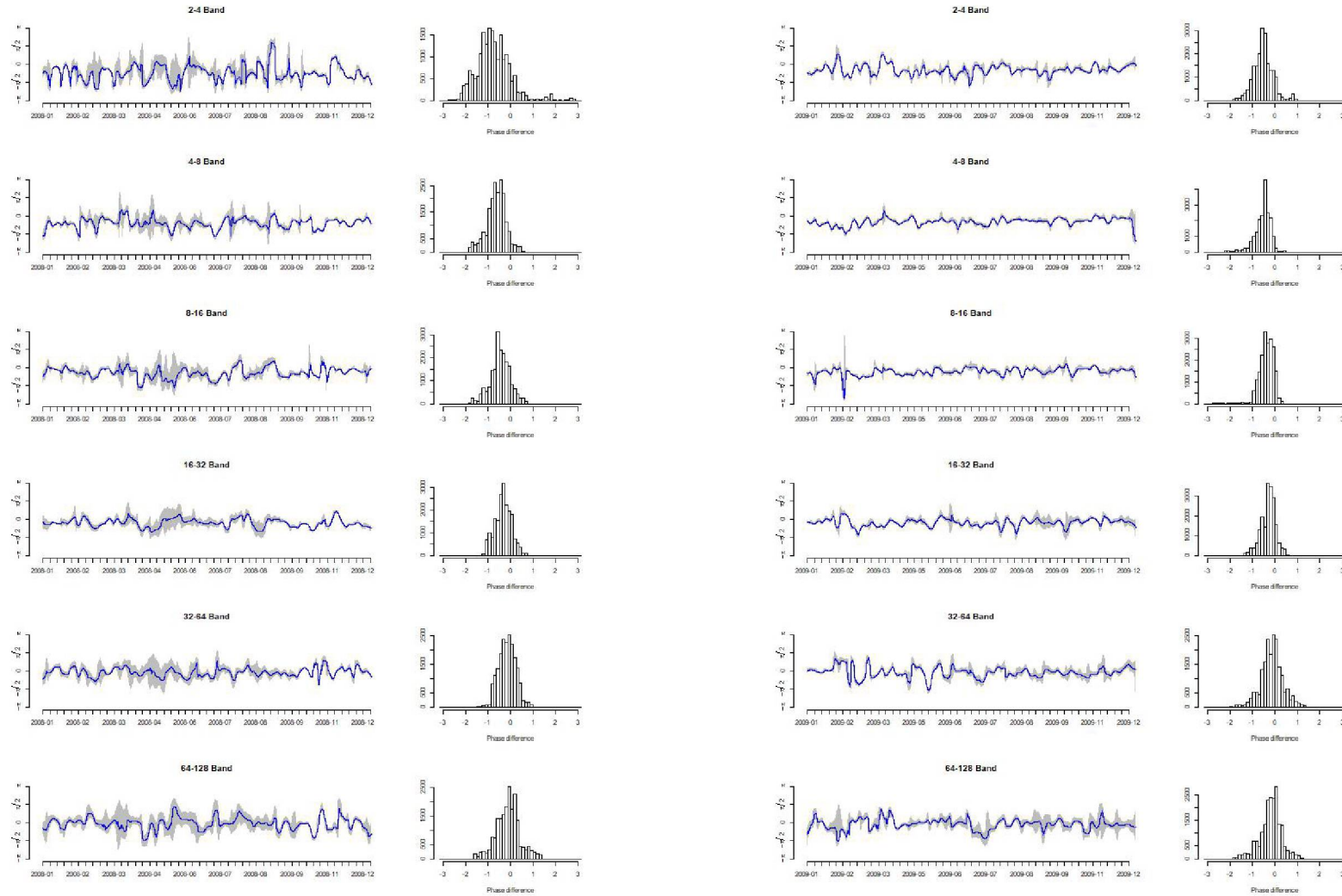


Figure A.8: Images of CWT analysis on BUX and FTSE 100

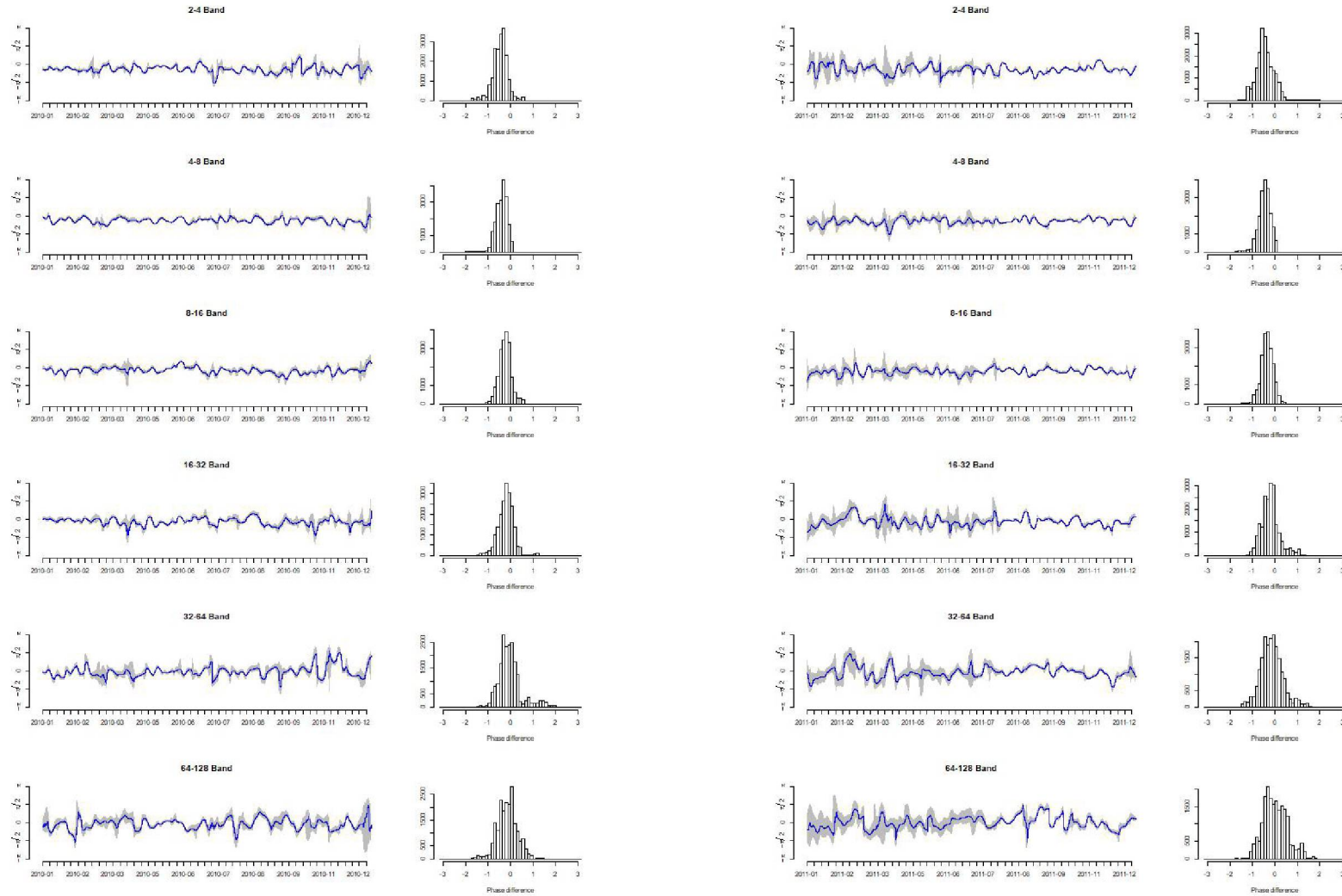
Figure A.9: Evolution of phase difference of BUX and DAX



(a) year 2008

(b) year 2009

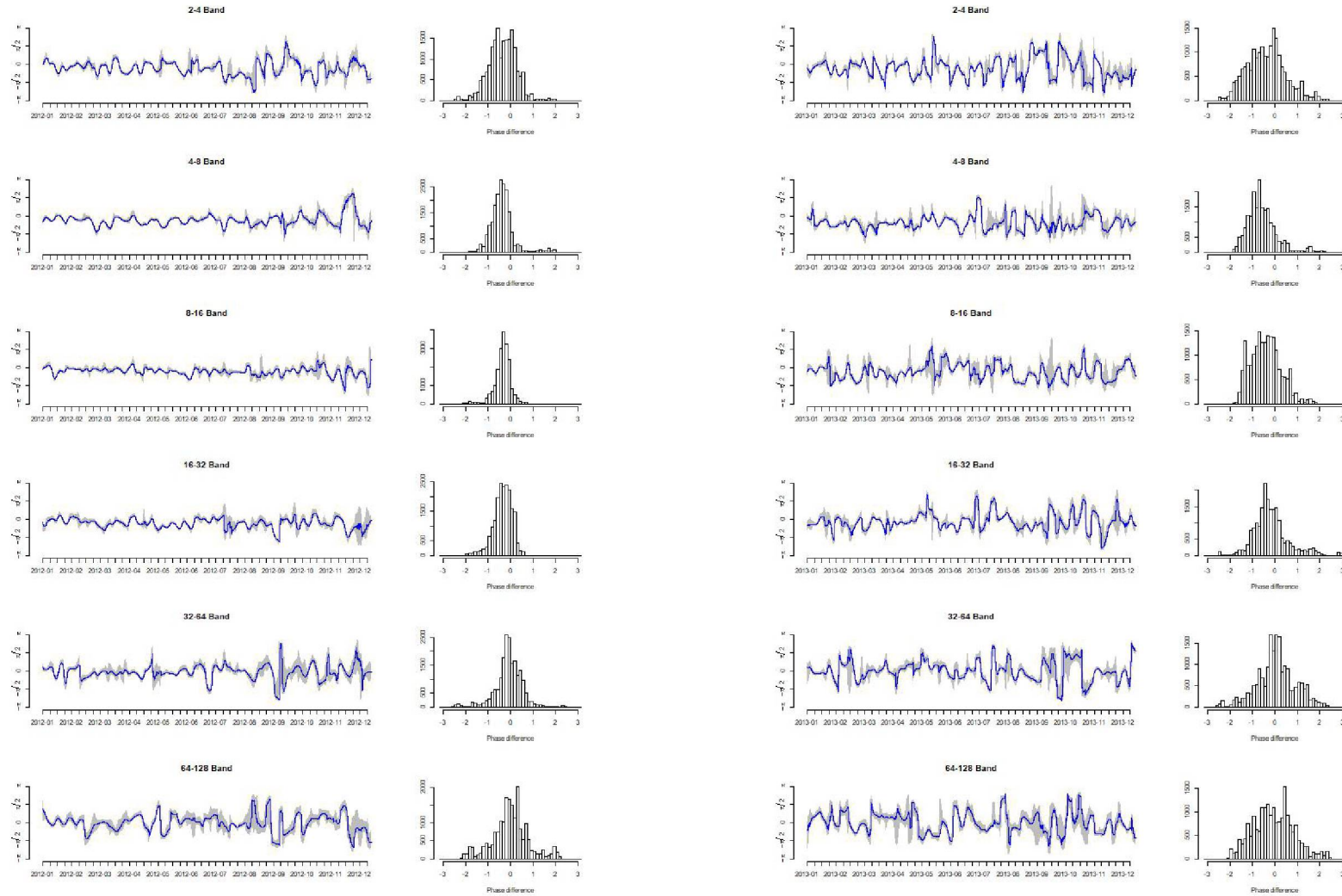
Figure A.9: Evolution of phase difference of BUX and DAX



(c) year 2010

(d) year 2011

Figure A.9: Evolution of phase difference of BUX and DAX



(e) year 2012

(f) year 2013

Figure A.9: Evolution of phase difference of BUX and DAX

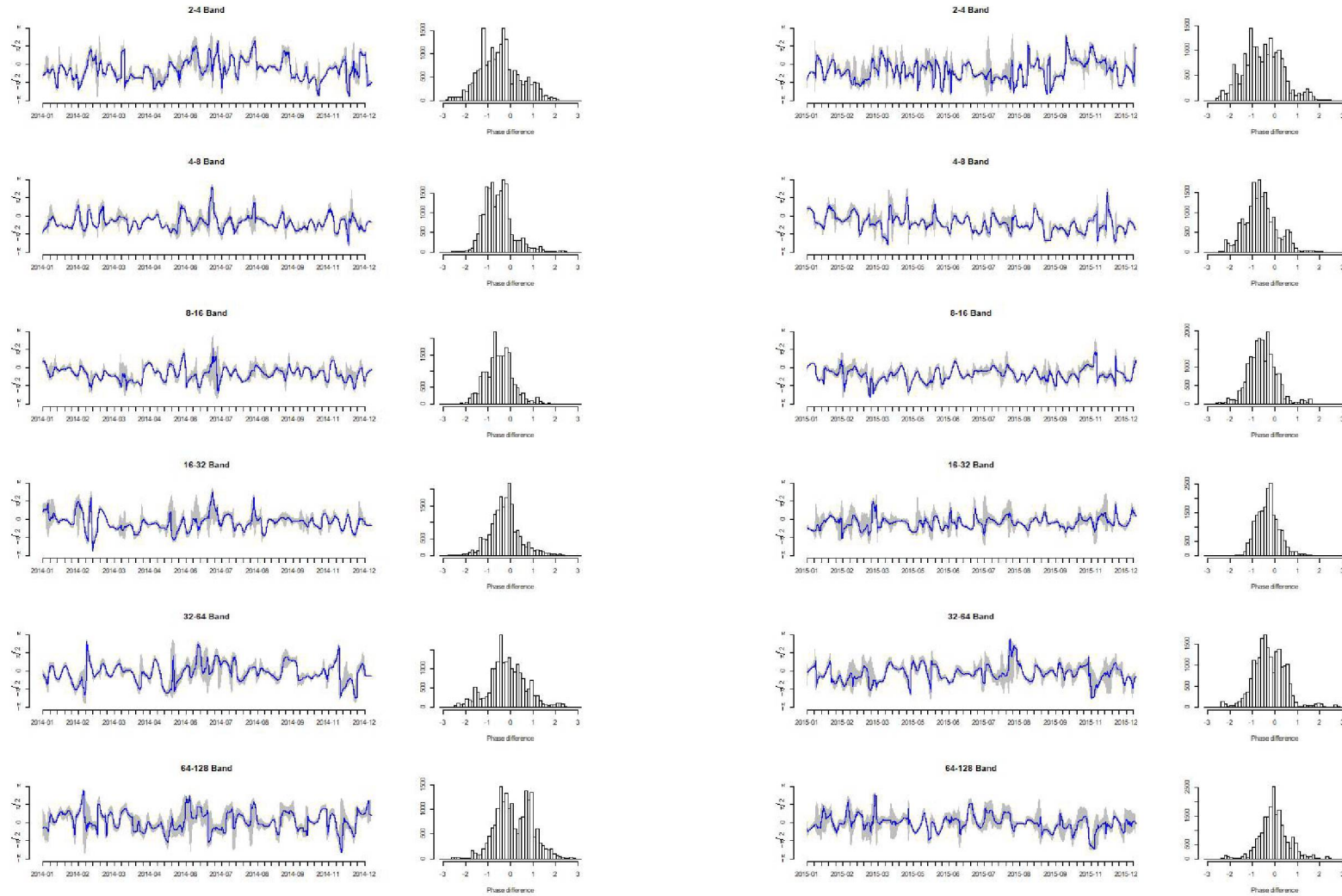


Figure A.10: Evolution of phase difference of BUX and FTSE500

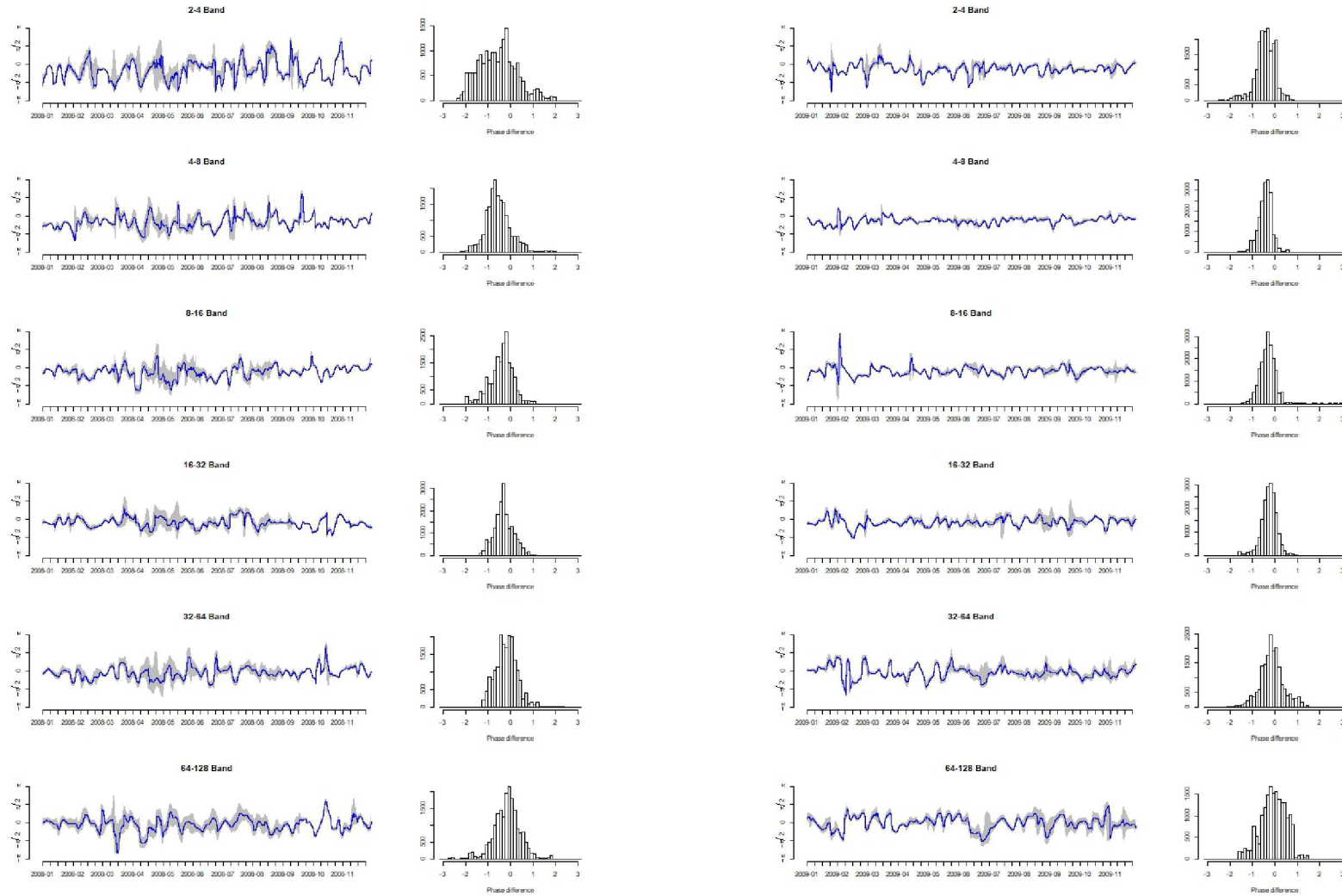
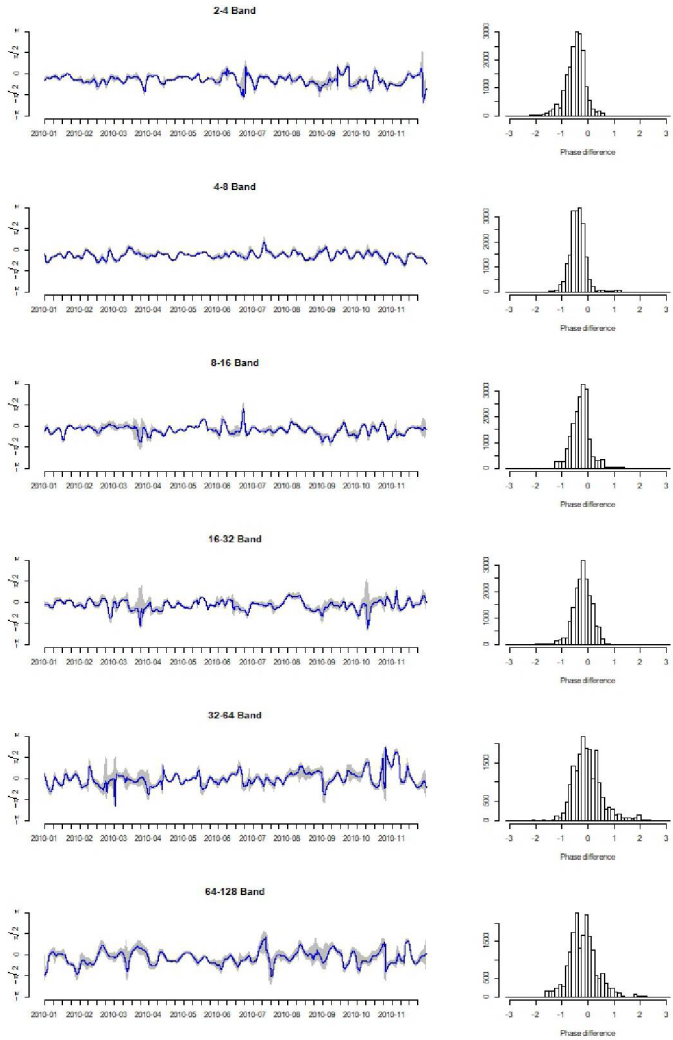
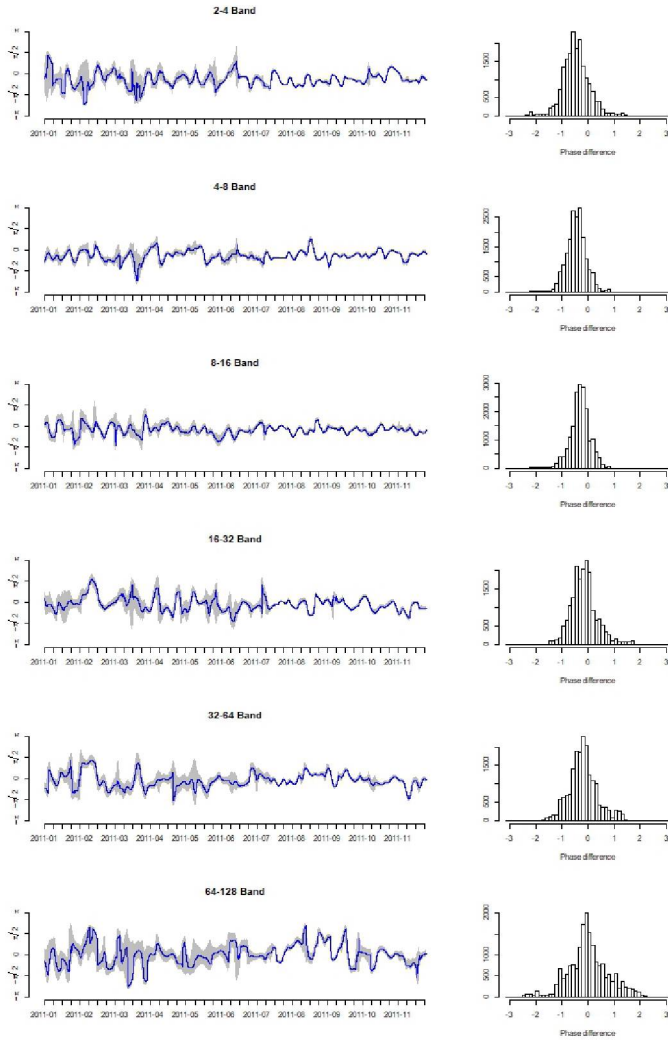


Figure A.10: Evolution of phase d



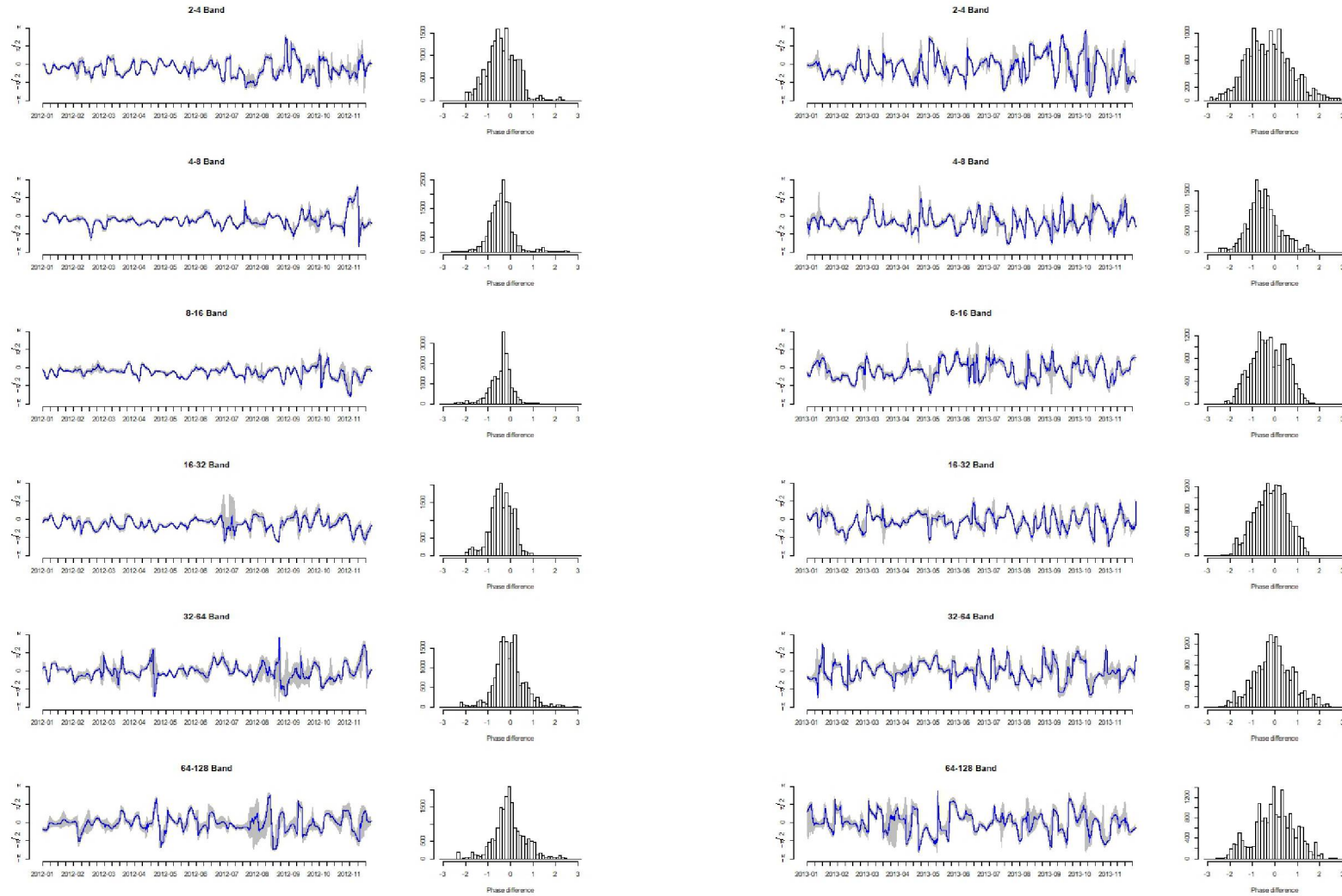
(c) year 2010

ifference of BUX and FTSE500



(d) year 2011

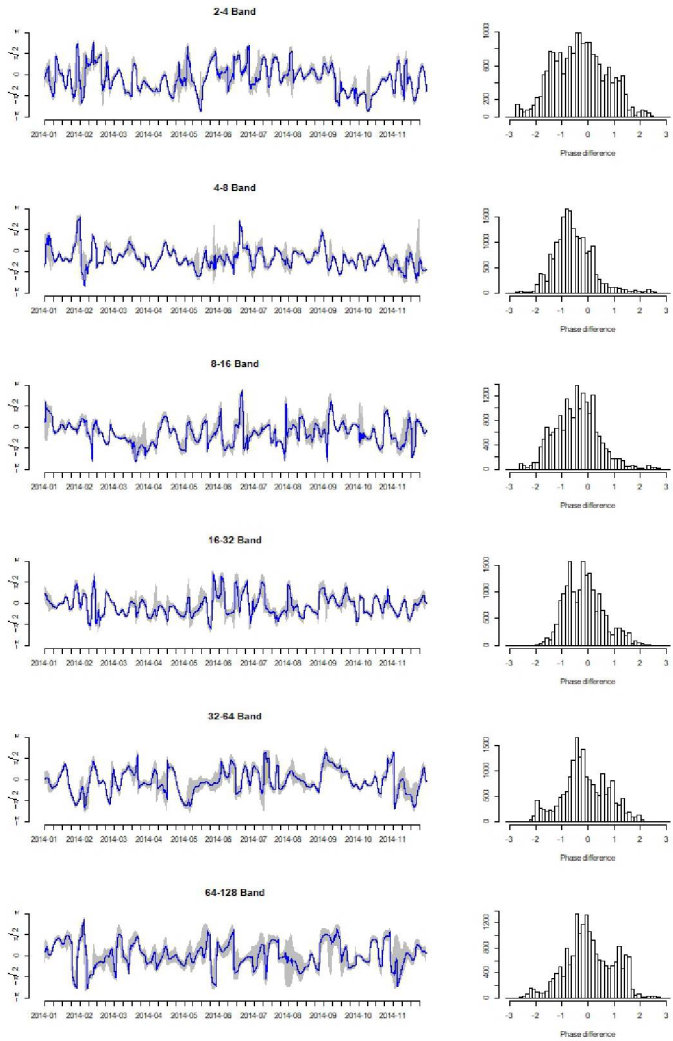
Figure A.10: Evolution of phase difference of BUX and FTSE500



(e) year 2012

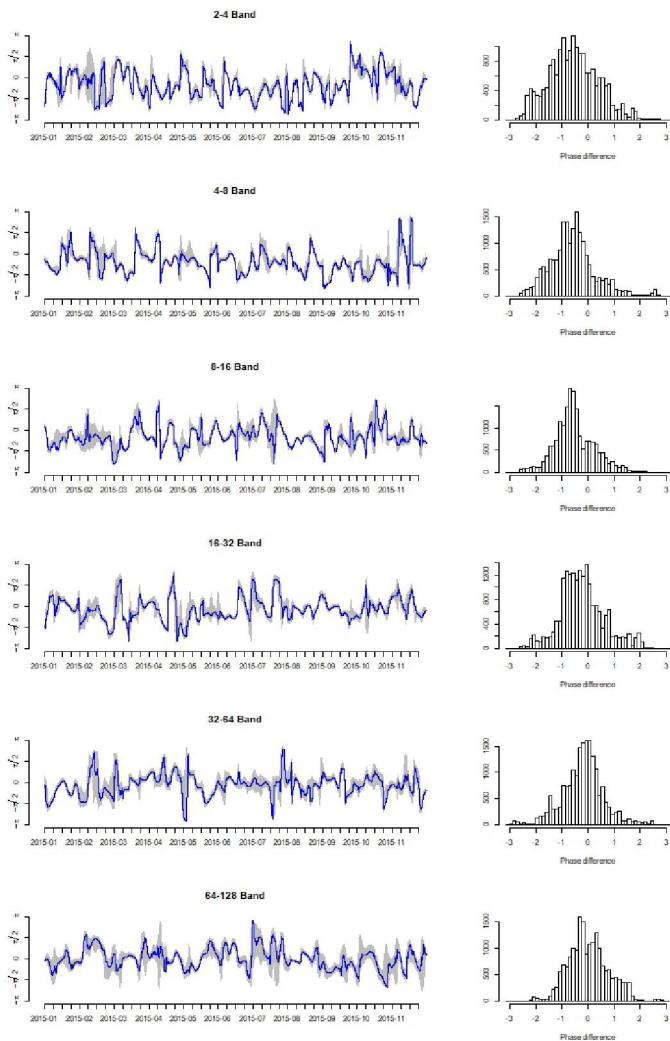
(f) Evolution of phase differences, 2013

Figure A.10: Evolution of phase d



(g) year 2014

ifference of BUX and FTSE500



(h) year 2015

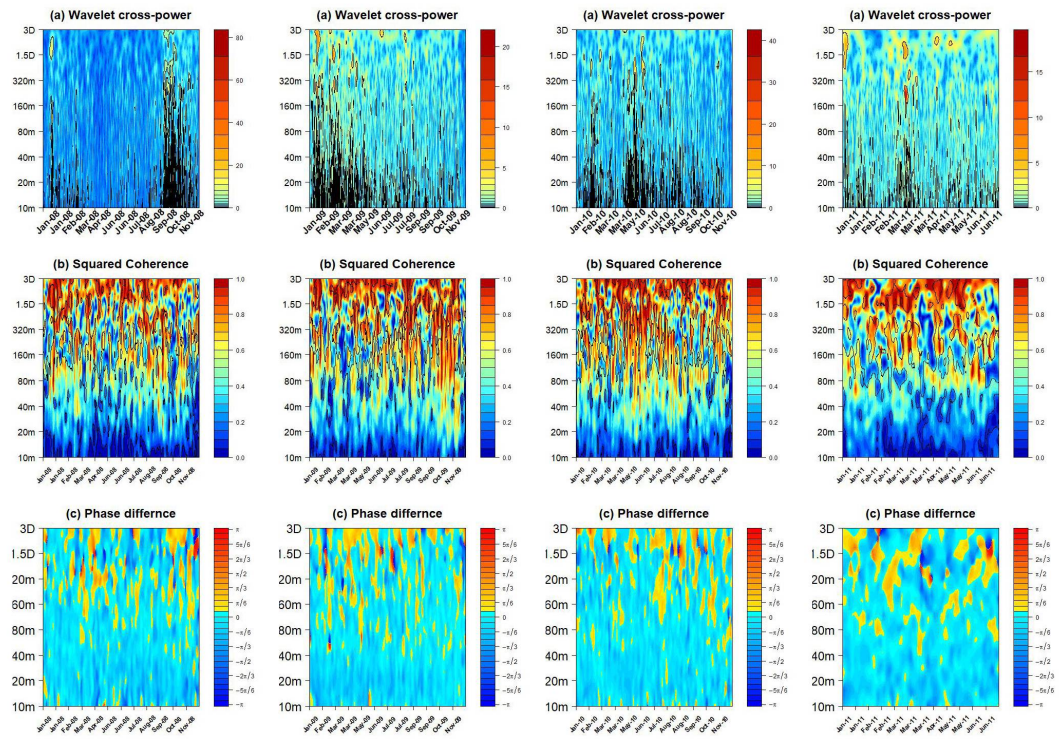


Figure A.11: Images of CWT analysis on WIG and DAX

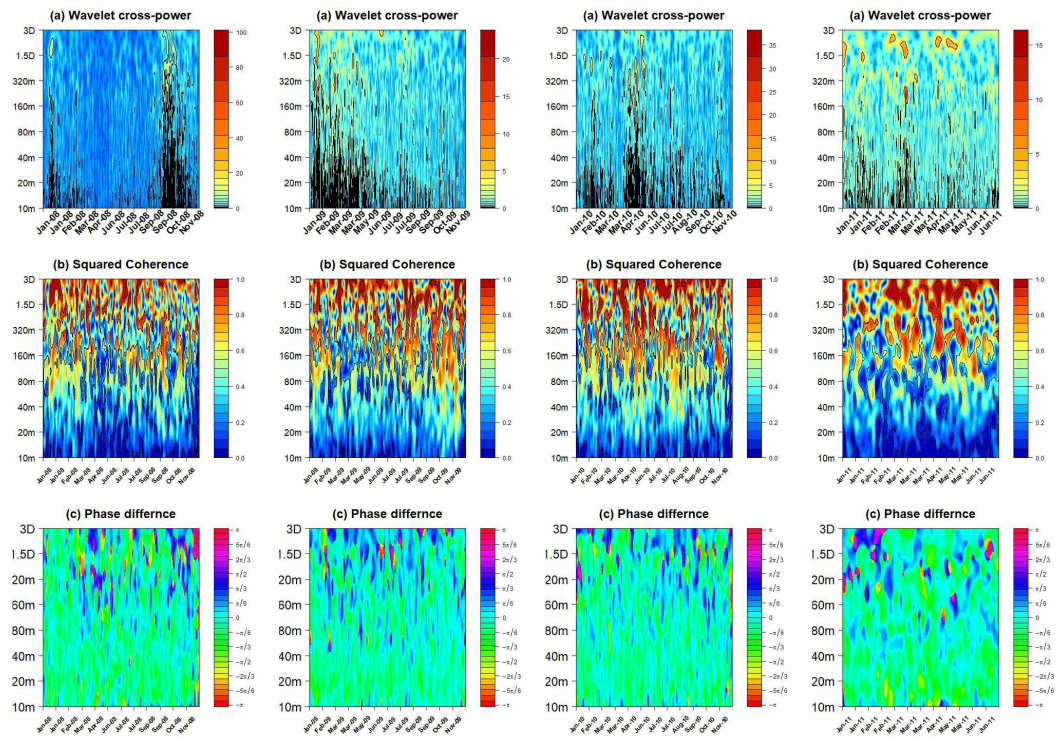
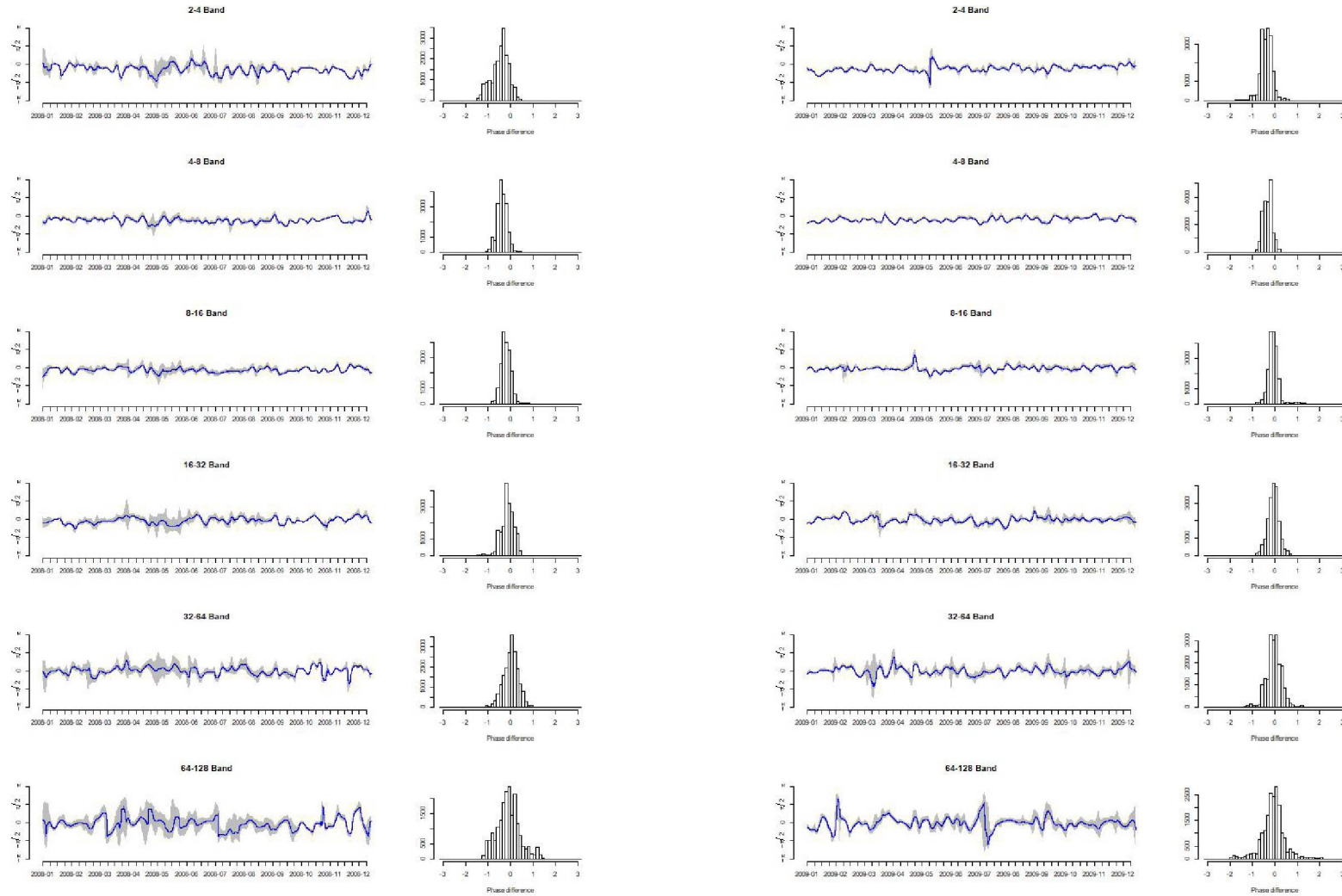


Figure A.12: Images of CWT analysis on WIG and FTSE 100

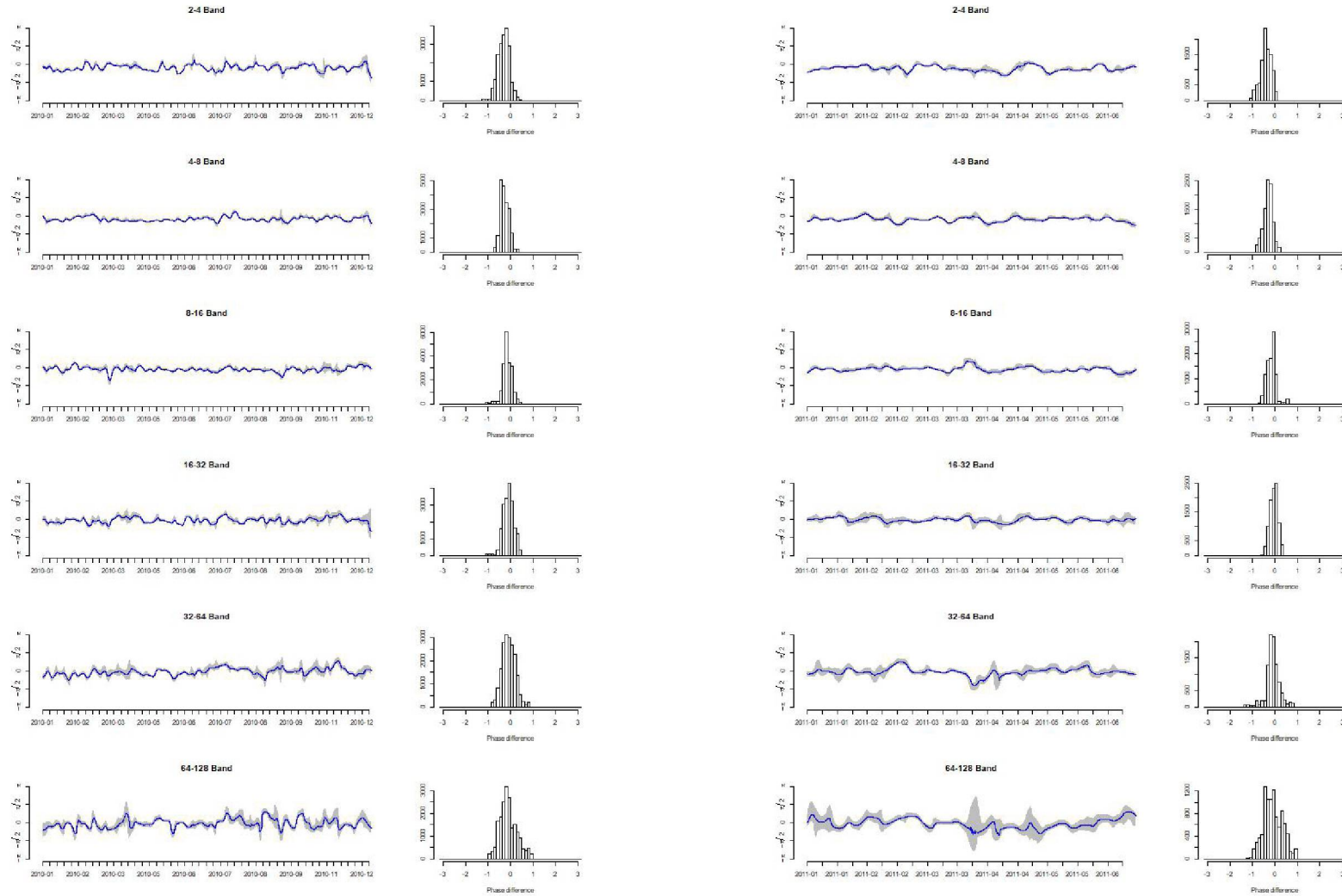
Figure A.13: Evolution of phase difference of WIG and DAX



(a) year 2008

(b) year 2009

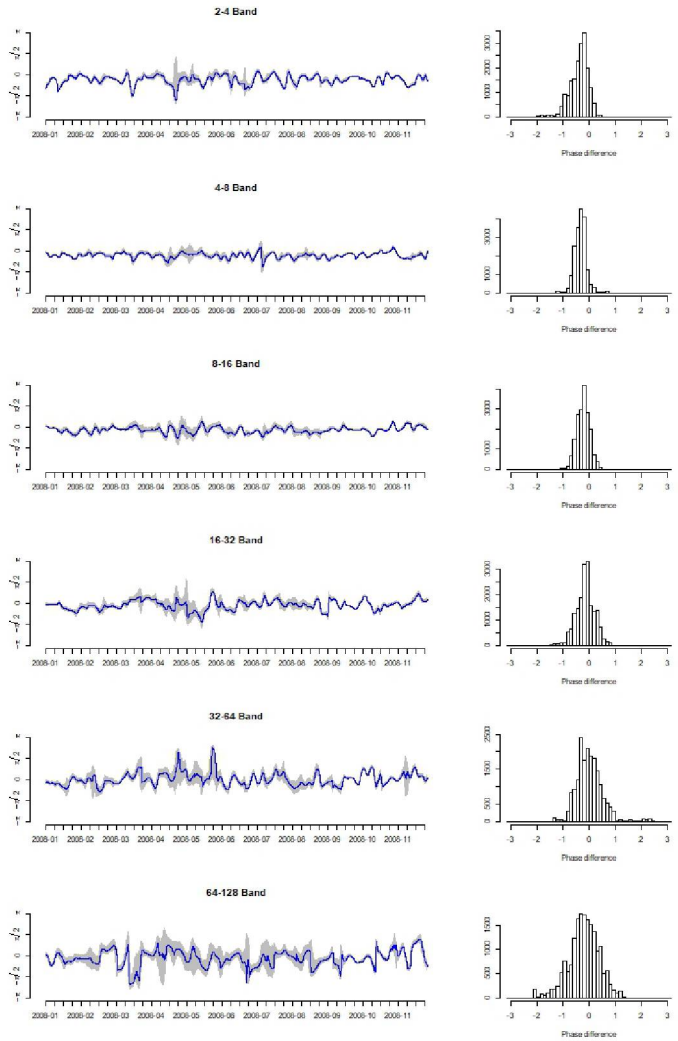
Figure A.13: Evolution of phase difference of WIG and DAX



(c) year 2010

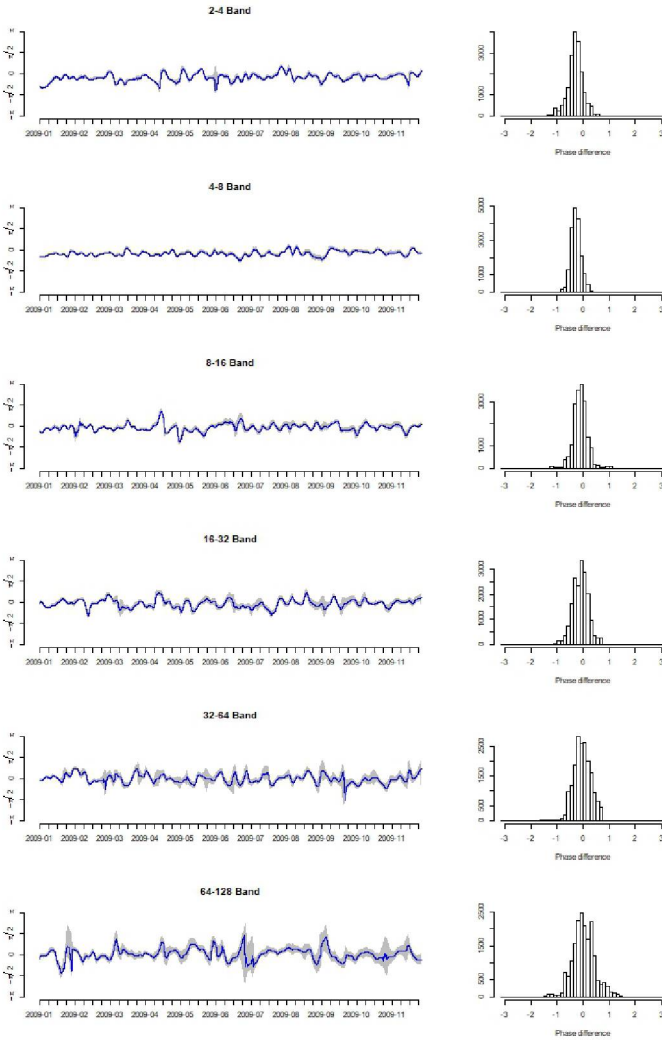
(d) year 2011

Figure A.14: Evolution of phase c



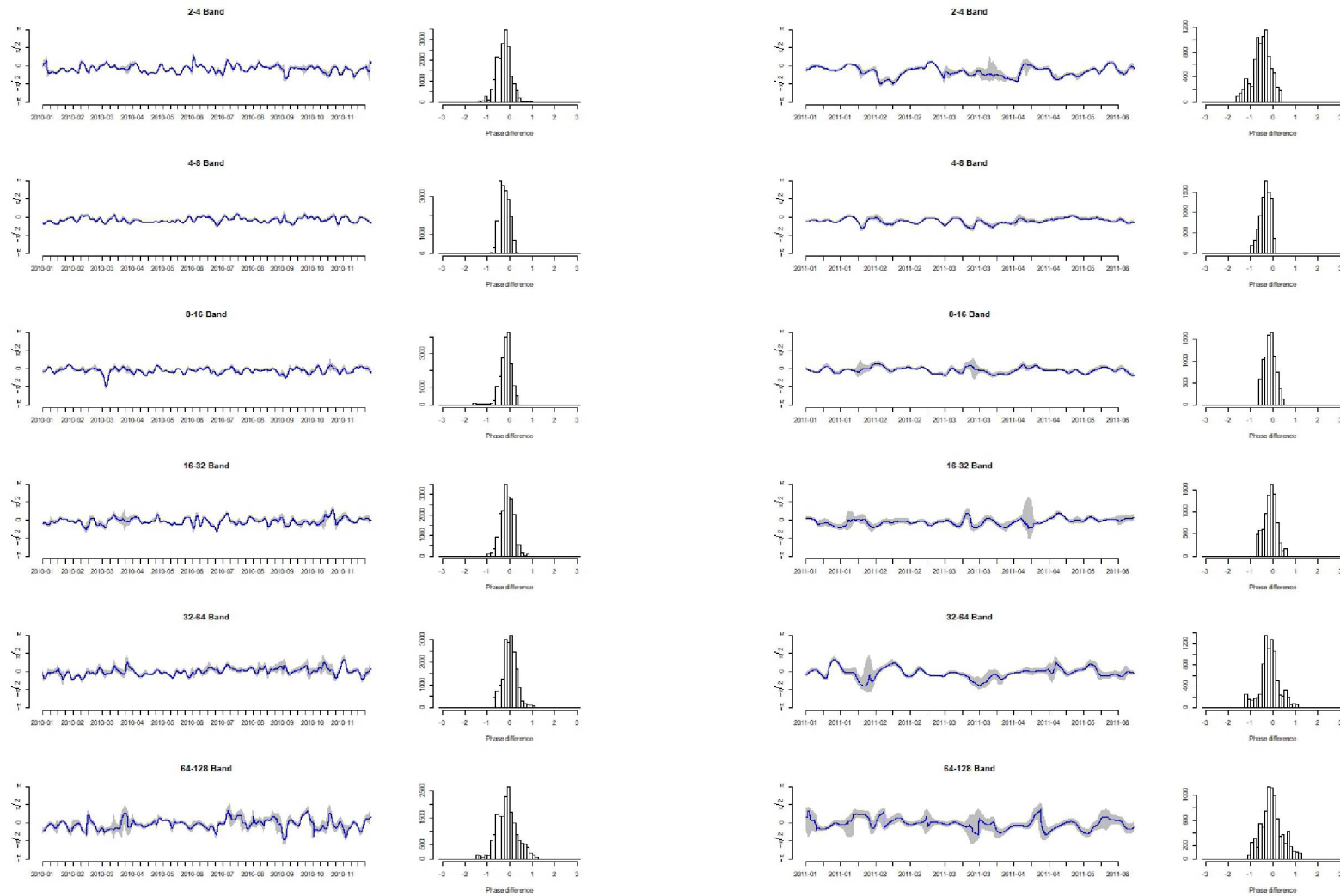
(a) year 2008

Difference of WIG and FTSE500



(b) year 2009

Figure A.14: Evolution of phase difference of WIG and FTSE500



(c) year 2010

(d) year 2011